THE OXIDATION OF CARBON AT HIGH TEMPERATURES.

A Thesis submitted for the
DEGREE OF DOCTOR OF PHILOSOPHY
in the University of London
by

John Raymond Walls, B.Sc.(Eng.).

Department of Chemical Engineering,
Imperial College of Science and Technology,
London, S.W.7.

September, 1964.

ABSTRACT.

The oxidation of carbon has been studied at high temperatures (1000 - 2000 °C) with pyrolytic graphite: the oxygen pressure was 0.21 atmospheres. This graphite has a very small porosity and is very pure. Therefore catalysis of the reaction was unlikely and it was shown that rates of mass transfer did not limit the reaction rate at any temperature in the experiments.

A maximum rate of reaction was obtained at 1900 °C and above this temperature the rate decreased. This unusual phenomenon was explained using the Nagle and Strickland-Constable theory and the overall rate equation was fitted to the experimental rate - temperature curve. Reaction rates could be calculated from the equation at all temperatures and pressures and were found to be in good agreement with the experimental results and with those reported by Strickland-Constable (obtained on carbon filaments at very low pressures). Moreover the order of the reaction has been measured at 1900 °C and was found to be in accordance with the same theory.

The maximum phenomenon had been observed

previously at normal pressures by Nagle with reactor grade graphite; but rates measured on this material in the present work appeared to be at least partly mass transfer controlled. However in the much slower reaction between carbon dioxide and reactor graphite a maximum rate was observed at 1700 °C. Therefore it is possible that the maximum rate phenomenon is a characteristic feature for gaseous reactions with all carbons at high temperatures.

With graphites, other than pyrolytic, it was shown that the porosity of the material strongly influenced its reactivity when boundary layer mass transfer control had been removed. The experimental results were interpreted using a pore diffusion theory.

No conclusive evidence of catalysis was obtained for temperatures above 1200 °C. In fact a sample of spectroscopically pure graphite was found to have a higher reactivity than the less pure reactor graphite; but this apparent anomaly was attributed to the higher porosity of the spectroscopic graphite.

ACKNOWLEDGEMENTS.

The author would like to acknowledge the most helpful supervision of Dr. R.F. Strickland-Constable at all stages of this work, and to express his thanks to Professor K.G. Denbigh in whose department the work was conducted.

In addition the author gratefully acknowledges the provision of a maintenance grant by the D.S.I.R. authorities, the financial support of the research work by the U.K.A.E.A., Harwell, and the gift of a sample of pyrolytic graphite from Dr. R.J. Diefendorf of the G.E.C. Research Laboratory, Schenectady, U.S.A.

The author is also indebted to his colleagues for their continued interest and useful discussion throughout the investigation and to Ajoi Dey, the Departmental Photographer, for his help and advice.

CONTENTS

Section 2. A STUDY OF THE EXPERIMENTAL SCATTER USING THE MICROSCOPE TECHNIQUE.

Section 3. IMPROVEMENTS TO NAGLE'S METHODS OF MEASUREMENT AND EVALUATION OF THE JET-FLOW TECHNIQUE.

Section 4. THE REACTION BETWEEN PYROLYTIC GRAPHITE AND OXYGEN.

Section 5. REACTION RATES OF CARBON IN THE PRESENCE OF CATALYTIC MATERIALS

Section 6. THE REACTION OF REACTOR GRAPHITE WITH CARBON DIOXIDE AT HIGH TEMPERATURES.

Section 7. DISCUSSION

APPENDIX

FIGURES

NOMENCLATURE

A . . .	frequency factor
B . . .	$2K_s \cdot C_o^m / D \cdot r_o$
D . . .	coefficient of diffusion
J . . .	mass flux per unit area
K_a . . .	reaction constant for A - sites
K_b . . .	reaction constant for B - sites
K_c . . .	rate constant for adsorption of oxygen
K_e . . .	rate constant for desorption of product
K_g . . .	gas phase mass transfer coefficient
K_s . . .	intrinsic activity constant
K_t . . .	rate constant for annealing of A - sites to B - sites
K_v . . .	activity constant per unit volume of solid
K_z . . .	ratio of K_c to K_e
L . . .	thickness of surface boundary layer for mass transfer
M . . .	magnification of optical system
P . . .	gas pressure (atmospheres)
Q . . .	apparent activation energy
Q_o . . .	activation energy
R_g . . .	gas constant ($Kcal.gm.mole^{-1} \cdot {}^oK^{-1} \cdot$)
R . . .	rate of reaction ($gm.at.cm^{-2} \cdot sec^{-1}$)
$\overline{R}$ . . .	mean rate of reaction
Re . . .	Reynold's number
S . . .	interfacial area between the gas and the solid

S_v . . . specific surface per unit volume of solid

Sh . . . Sherwood number

Sc . . . Schmidt number

St . . . Stanton number

T . . . temperature

a . . . area of pore mouth

c . . . concentration of gas

c_i . . . concentration of gas at the solid - gas interface

c_o . . . concentration in the bulk of the gas phase

d . . . characteristic dimension of body

d_o . . . distance between the tip of the jet and the sample surface

h . . . surface retreat of sample beneath jet

m . . . assumed constant order of chemical reaction

n . . . number of moles reacting

q . . . carbon monoxide/ carbon dioxide ratio

r . . . pore radius

r_o . . . pore radius at pore entrance

t . . . time (secs)

t_i . . . desorbed gas temperature

t_r . . . filament temperature

t_o . . . gas temperature

v . . . gas velocity

x . . . distance from pore bottom

z . . . total depth of pore

z_g . . . thickness of gas film

z_s . . . thickness of the reaction zone in the solid

β . . . effective diffusion coefficient

δ . . . boundary layer thickness

η . . . effectiveness factor : ratio of observed reaction rate to the maximum rate in the absence of diffusion

ρ . . . graphite density

θ . . . fraction of A - sites covered by oxygen

x . . . $2 K_s / r D$

x . . . fraction of A - sites as opposed to B - sites

μ . . . gas viscosity

α . . . thermal accommodation coefficient

1. INTRODUCTION.

Recent developments in high temperature engineering show that graphite is a useful construction material as it is one of the few solids which retains its mechanical strength above 2000°C. A serious limitation to its use at these temperatures is the reaction of the solid with oxidising gases.

Apart from the technical importance the oxidation of carbon is scientifically of an unusual type in that a gas reacts with a covalent solid to produce a gaseous product, whereas in most gas-solid reactions the product is also solid.

In certain respects the reaction is very similar to a gaseous reaction on a porous solid catalyst where it is normally possible to distinguish three characteristic temperature ranges of reaction.

At low temperatures where the surface rate is very slow the whole internal surface of the solid participates fully in the reaction. At higher temperatures the rate of diffusion of the reactants through the pores limits the increased reaction rate and consequently the internal surface is only partially utilised. At higher temperatures still the reaction rate is so rapid

that the reaction takes place mainly with the external surface of the solid: moreover the reaction is then usually limited by the rate of diffusion of the reactants through a stagnant boundary layer. This is formed from the reaction products at the surface of the solid.

1.1. Mathematical theories of chemical reaction on porous solids.

A quantitative theory of reaction rates in porous catalysts was first given by Thiele[b7] and later applied by others[b1-10] to the oxidation of carbon. A discussion of the three regimes of reaction will now be presented on the basis of these theories.

1.1.1. Temperatures below 650°C: In general the rate of reaction of a gas with a solid surface (dn/dt) is expressed as a product of the external surface area of the solid (S), of some function of the concentration of the species (ci), and of the reaction constant (Ks), the latter being related to temperature by a simple Arrhenius law:-

$$Ks = A\, e^{-Qo/R_G T} \quad \ldots\ldots\ldots\ldots 1.1$$

where (Qo) is termed the activation energy, (R_G) is the gas constant, (T) the absolute temperature and (A) is

the frequency factor. For porous solids it is more precise to consider the internal surface area of the solid in addition to the geometrical area so that the intrinsic rate of reaction can be determined. However the rate equation (1.1) is then further complicated by the finite rate of diffusion of the reactant into the pores. The reactant concentration is depleted along a pore and consequently varies over the reactive surface. Therefore it is necessary to integrate the reaction rate over small areas (ds) to give the overall rate (see e.g. 1.2):-

$$\frac{dn}{dt} = \int_0^S Ks.f(ci).dS \qquad \ldots\ldots\ldots \quad 1.2$$

The function of concentration is often assumed to be a simple power of the concentration but this is usually an approximation (only applicable to a limited range of the experimental variables). The reason for this is that a heterogeneous reaction may take place through a series of consecutive processes e.g.:-

1. Adsorption on the surface.
2. Dissociation of the species.
3. Chemisorption of the free radicals or atoms to form intermediate complex compounds.

4. Re-organisation of the surface structure of the solid.

5. Desorption of the reaction products.

Under certain conditions of reaction a step of the mechanism can be so slow that it determines the overall reaction rate; but in general a complex rate expression is required to define the overall chemical reaction rate completely. In such a case the reaction order cannot be satisfactorily denoted by a simple power of the concentration.

When the reaction rate is very low as in the range below 650°C, the concentration of the species at the surface (ci) is equal to the bulk concentration (co) and is virtually constant throughout the pores of the solid. The 'apparent activation energy' (Q) is therefore equal to that of the true surface reaction:-

$$-\frac{Q}{R_G} = \frac{d \ln \frac{dn}{dt}}{d \frac{1}{T}} = \frac{d \ln Ks}{d \frac{1}{T}} = -\frac{Qo}{R_G} \quad \ldots \quad 1.3$$

1.1.2. Temperatures above 1000°C: The rate of steady-state transfer of the reactants to the solid surface is given by Fick's law:-

$$\frac{dn}{dt} = -D.S. \frac{dc}{dx} \quad \ldots \ldots \ldots \quad 1.4$$

where D is the coefficient of diffusion.

When the gas phase is in turbulent motion the concentration gradient ($^{dc}/_{dx}$) can be considered to be confined to a thin film of fluid at the phase boundary. If (L) is the apparent thickness of the film and a constant concentration gradient is assumed, then the rate of mass transfer ($\frac{dn}{dt}$) is directly proportional to the concentration difference across this film (ΔC), see equation 1.5. The constant of proportionality ($K_G = {}^{D}/_{L}$) is termed the mass transfer coefficient.

$$\frac{dn}{dt} = \frac{D.S(co-ci)}{L} = K_G S \Delta C \quad \ldots\ldots\ldots 1.5$$

$$\therefore \quad Ci = Co - \frac{L}{S.D} \cdot \frac{dn}{dt}$$

The rate of mass transfer equals the rate of reaction, therefore:-

$$\frac{dn}{dt} = K_S.S.f(Co - \frac{L}{S.D}\frac{dn}{dt}) \quad \ldots\ldots 1.6$$

This equation can be solved if an explicit form of f (ci) is known. For instance a first order law gives:-

$$\frac{dn}{dt} = \frac{K_S.S.co}{1 + K_S L/D} = K_S.S.Co.\zeta \quad \ldots\ldots 1.7$$

The additional factor (ζ) in the rate equation accounts for the boundary layer diffusion, and is the ratio of the observed reaction rate to the maximum possible rate in

the absence of diffusion. The two factors (K_S) and (η) can be combined into a single reaction constant (Ko) for a first order reaction. In which case:-

$$K_s \cdot \eta = K_o = \frac{K_S K_G}{K_S + K_G}$$

$$\text{i.e.} \quad \frac{1}{K_O} = \frac{1}{K_S} + \frac{1}{K_G} \qquad \ldots\ldots\ldots\ldots\ldots 1.8$$

However for any other value of the reaction order the relationship is much more complicated.

For mass transfer effects to be small:-

$$\eta \longrightarrow 1$$

$$\text{i.e.} \quad \frac{K_S L}{D} \longrightarrow 0 \qquad \text{(from equation 1.7)}$$

Therefore studies of the reaction kinetics where transport phenomena does not interfere with the rate of reaction have been conducted in three separate systems:-

a) K_S small ..... low temperature studies below 650°C.

b) L small ..... oxidation in high speed gas streams which reduce the boundary layer thickness.

c) D large ..... low pressure studies such that the mean free path of the molecules is very large.

Otherwise, when (ci) is reduced to a small value the mass transfer of oxygen to the surface can

determine the overall reaction rate. The small apparent activation energy in this case reflects the small temperature coefficient for mass transfer.

1.1.3. Interpretation of reaction rates which are partly controlled by the rate of pore diffusion.

In the intermediate temperature range the concentration of the reactant is depleted along the pore. For such a case a complete solution of the rate equation is extremely complex, but Thiele[b.7] suggested an analytical treatment of the situation and several important results were achieved.

The theory was developed later by Wheeler[b9] and others[b8] but was mainly concerned with catalytic reactions taking place in the pores of a solid catalyst. In the case of oxygen and carbon the situation is rather different because the carbon is consumed and the pores are continually changing in shape; nor are they parallel sided, which is what Thiele assumed to obtain an analytical solution. Although rates were measured at very high temperatures, when boundary layer diffusion normally controls the reaction rate, it is proposed to develop the theory to cover this case, because under high speed flow conditions the reaction rate becomes

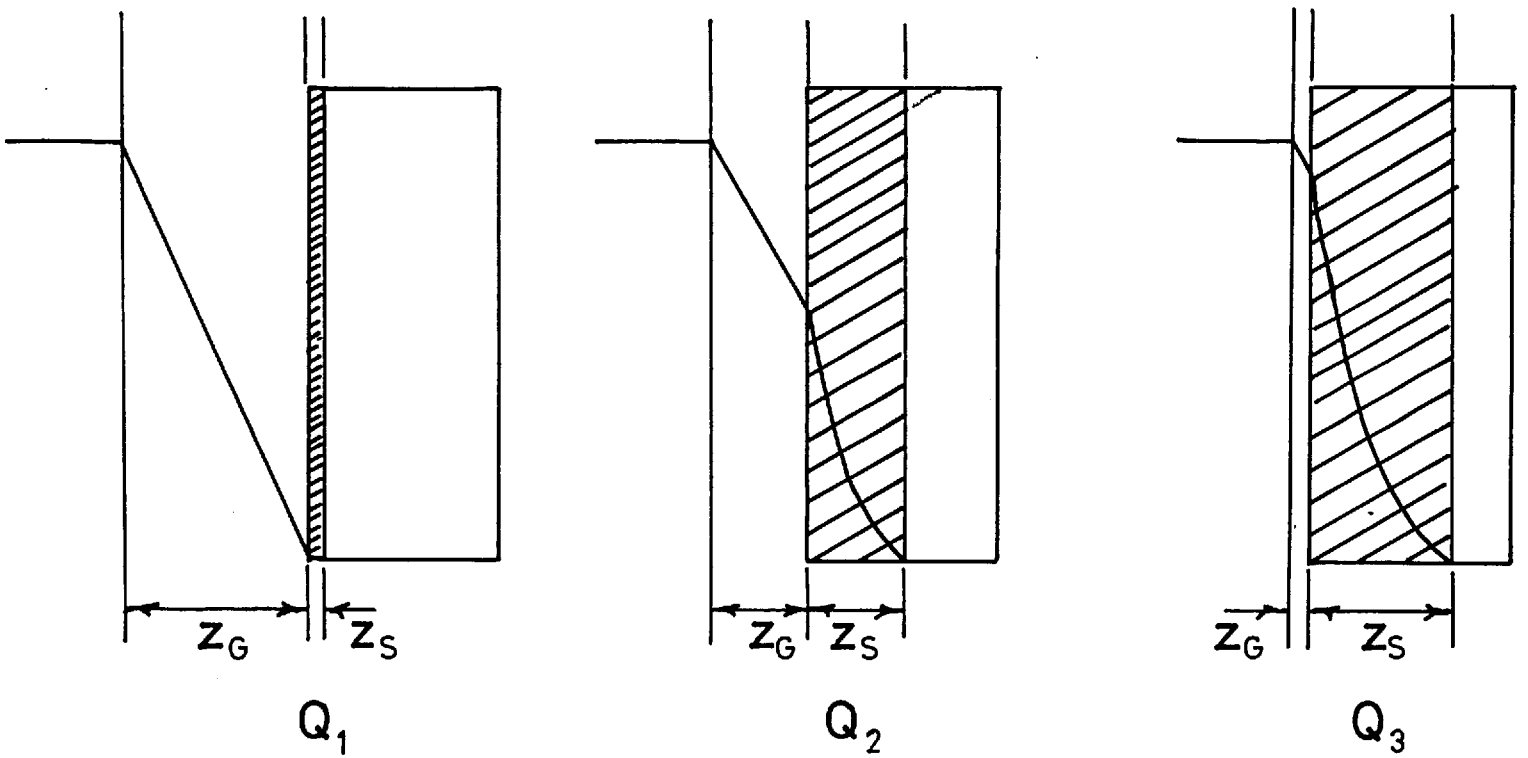

Fig.1.1 THREE STAGES OF REACTION CONTROL
(Rossberg and Wicke Model)

independent of the gas velocity and can be controlled by the rate of in-pore diffusion.

The three stages of mass transfer are illustrated in fig. 1.1 on the Rossberg and Wicke[b.6] scheme at different velocities (Q). At low gas velocities (Q.1) the gas film thickness (Z_G) is large and the reaction zone in the solid surface (Z_S) is very thin. However when the rates are independent of the velocity (Q.3) the reverse is true; (Z_G) is very small in comparison with (Z_S) and this is normally the case with the present experimental technique.

In the following analysis a steady-state pore profile is considered to develop by reaction, see fig. 1.2, where (r) is the pore radius and (x) the distance along the pore measured from the pore bottom. In the steady state the concentration (c) will be some function of (x), and independent of time.

i.e. $c = f(x)$

Also the rate of reaction $(\frac{dr}{dt})$ may perhaps be written:-

$$\frac{dr}{dt} = K_S . c^m$$

where K_S is a constant and (m) is an assumed constant order of reaction, and therefore:-

$$\frac{dr}{dt} = K_S \, f(x)^m$$

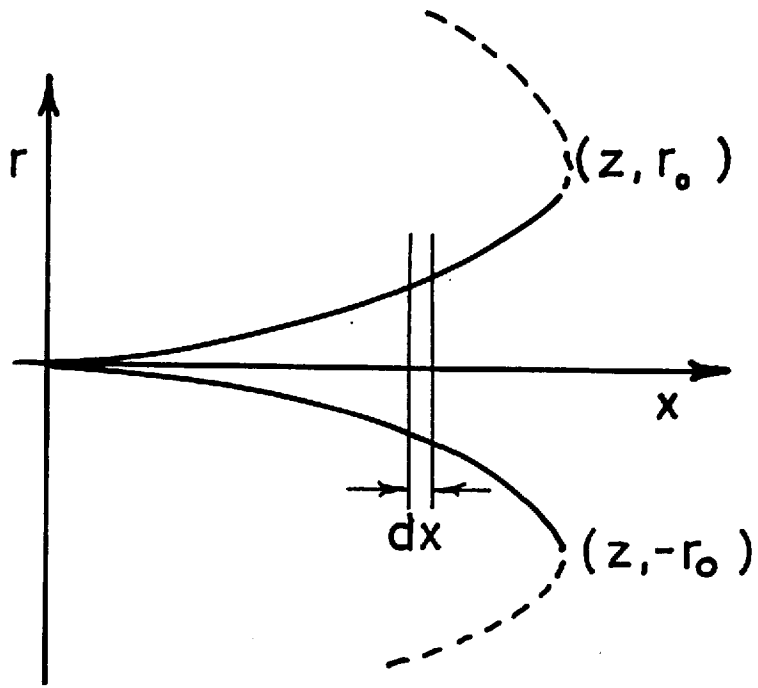

Fig.1.2 PORE PROFILE DURING REACTION

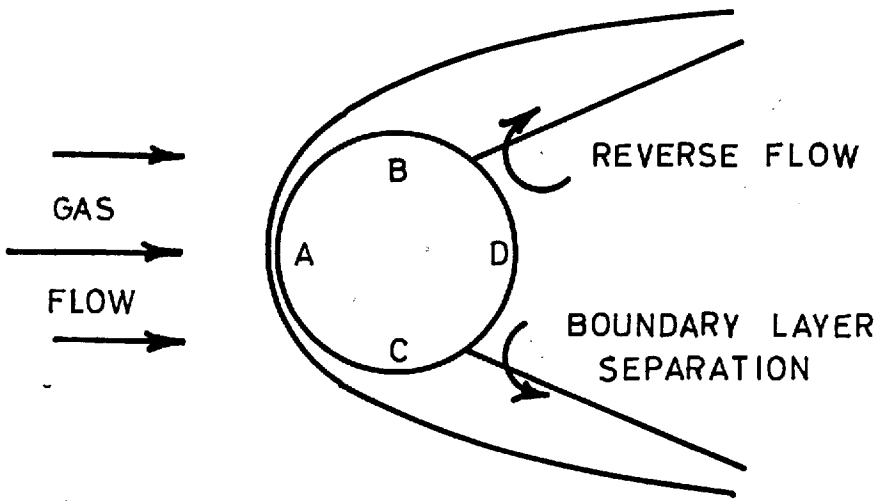

Fig.1.3 AERODYNAMIC FLOW AROUND A CYLINDER

This means that $(\frac{dr}{dt})$ is some function of (Z) but this function is not easy to know. Therefore it is assumed in the present analysis that the pore radius (r) is proportional to the m^{th} power of the concentration (C) in that section of the pore. In fact this means that the shape of the pore side is parabolic.

i.e. $r \propto c^m$

$$\therefore \quad \frac{r}{r_o} = \left(\frac{c}{C_o}\right)^m \qquad \ldots\ldots\ldots\ldots\ldots\ldots\ldots\ldots 1.9$$

Other assumptions in the analysis:-

1. The temperature is constant throughout the solid.
2. The external surface reaction is negligible i.e. the surface is completely filled with the pore entrances.
3. Diffusion through the external boundary layer is rapid compared with diffusion in the pores.
4. No volume changes take place in the reaction.
5. Secondary reactions are negligible.

Consider a section of the pore dx: the depletion of the concentration across the section results from reaction at the section periphery, but radial diffusion is neglected. (Poiseuillian flow and bulk flow are also neglected).

$$\therefore \quad d\left(D.\pi r^2.\frac{dc}{dx}\right) = K_S.C^m.2\pi r.dx$$

$$\therefore \quad 2r.\frac{dr}{dx}.\frac{dc}{dx} + r^2.\frac{d^2c}{dx^2} = \frac{2K_S}{D}.C^m$$

From equation 1.9:-

$$\frac{Co^m}{ro} \cdot \frac{dr}{dx} = m.c^{m-1}.\frac{dc}{dx}$$

$$\therefore \quad \frac{2ro}{Co^m}.m.\left(\frac{dc}{dx}\right)^2.C^{m-1} + \frac{ro}{Co^m}.C^m\frac{d^2c}{dx^2} = \frac{2K_S}{D}C^m$$

$$\therefore \quad \frac{d^2c}{dx^2} + \frac{2m}{C}.\left(\frac{dc}{dx}\right)^2 = \frac{2K_S}{D}.\frac{Co^m}{r_o} = B \qquad 1.10$$

Put $p = \frac{dc}{dx}$ $\quad \frac{d^2c}{dx^2} = \frac{dp}{dx} = \frac{dp}{dc}.\frac{dc}{dx} = p\frac{dp}{dc}$

$$\therefore \quad p\frac{dp}{dc} + \frac{2m}{C}.p^2 = B$$

Put $p^2 = u$ $\quad \therefore \quad \frac{1}{2}.\frac{du}{dc} + \frac{2m}{c}.U = B$

$$\therefore \quad \frac{du}{dc} + \frac{4m}{c}.u = 2B$$

$$I.F = C^{\int \frac{4m}{c}.dc} = C^{4m\ln c} = C^{4m}$$

$$\therefore \quad C^{4m}\frac{du}{dc} + 4mc^{4m-1}.u = 2B.C^{4m}$$

$$\text{i.e.} \quad (u.c^{4m}) = 2B\int c^{4m}.dc$$

$$\therefore \quad u.c^{4m} = \frac{2B}{4m+1}.c^{4m+1} + K.$$

$$\text{i.e. } \left(\frac{dc}{dx}\right)^2 = \frac{2B}{4m+1} c + \frac{K_1}{c^{4m}} \quad \therefore \quad 0$$

Boundary conditions: Let $c = o$ Let $c = co$

When $x = o$ $x = z$

and $dc/dx = o$ $\therefore$ $K_1 = 0$

$$\therefore \quad c^{-\frac{1}{2}} . dc = \sqrt{\frac{2B}{4m+1}} . dx$$

$$2c^{\frac{1}{2}} = \sqrt{\frac{2B}{4m+1}} . x + K_2 \quad \therefore \quad 0$$

$$c = \frac{B}{4m+1} . \frac{x^2}{2} \qquad \ldots\ldots\ldots\ldots \quad 1.11$$

Let all the pores fill the external surface area.

Therefore the total rate (R) per unit external area:-

$$R = D . \left.\frac{dc}{dx}\right|_z$$

$$= D . \frac{B}{4m+1} . z$$

$$= D \frac{B}{4m+1} . \sqrt{\frac{4m+1}{B} . 2co} = D \sqrt{\frac{B}{4m+1} . 2co}$$

$$= D \sqrt{\frac{2Ks}{D} . \frac{co^m}{r_o} . \frac{2co}{4m+1}}$$

$$\therefore \quad R = \sqrt{\frac{4}{4m+1} . \frac{1}{r_o} . K_s D . Co^{m+1}} \qquad \ldots \quad 1.12$$

From the above equation the apparent activation energy (Q) and apparent order of the chemical reaction can be determined as they were in the Thiele-

Wheeler theory. In the present circumstances pore diffusion was fully developed, consequently the assumptions which were necessary to derive the Thiele equations are different: but the variation of the reaction rate (R) with (D),(K_S) and (Co) are identical for both derivations. Only the constants of proportionality are different.

1. Apparent activation energy: i.e. comparison of rates at constant partial pressure (P_{O_2}) and total pressure (P_T). From equation 1.12:-

$$R \propto K_S^{\frac{1}{2}} \qquad D \simeq \text{constant}$$

$$e^{-Q_o/2R_GT} \qquad Cc \simeq \text{constant}$$

$$\therefore \quad -\frac{Q}{R_G} = \frac{\log R}{1/T} = -\frac{Q_o}{2R_G} \qquad 1.13$$

Therefore half the true activation energy (Q_o) would be measured by experiment.

2. Apparent reaction order: i.e. comparison of rates at constant temperature and different oxygen pressures. From equation 4.7:-

$$R \propto \sqrt{D\ Co^{m+1}} \qquad K_S \text{ is constant}$$

$$D \propto Co^{-1}$$

$$\therefore \quad R \propto Co^{m/2}$$

Therefore half the true reaction order is measured by experiment.

3. Effect of total pressure (P_T) at constant temperature with the partial pressure of oxygen a constant value; from equation 1.12:-

$$R \propto D^{\frac{1}{2}} \qquad K_S \text{ is constant}$$

$$\propto P_T^{-\frac{1}{2}} \qquad c_o \text{ is constant}$$

$$D \propto P_T^{-1}$$

Therefore the reaction rate is inversely proportional to the square root of the total gas pressure.

Some apparently successful comparisons with the Thiele-Wheeler theory have been made with experiments. For instance rates of reaction have been shown to depend upon the size of the carbon specimen (Wicke[b10] and others[b9.6, b4]. Also for large particles the apparent activation energy was half that observed when using thin carbon deposits (Eyring)[b9.1]

1.2. Effect of porosity on the observed reaction rates.

From the above discussion it is apparent that the interpretation of the kinetics of carbon oxidation in porous graphite samples is often difficult because of the assumptions that have to be made to account for

the effects of diffusion.

If graphites of low porosity are used the reaction is mainly with the external surface. Therefore a more accurate understanding of the kinetics involved can be obtained. Such graphites have a high bulk density comparable with that of the perfect crystal structure which has a density of 2.265 $g.cm^{-3}$. Natural graphites and graphites produced by the pyrolysis of hydrocarbon vapours have densities approaching this figure (1.9 to 2.2 $g.cm^{-3}$). Commercial graphites, apart from pyrolytic graphite, are usually manufactured by the pyrolysis of a mixture of ground coke and pitch. As a result the solid has a high porosity with resulting bulk densities between 1.4 and 1.76 $g.cm^{-3}$.

1.3. Review of carbon oxidation studies at high temperatures.

At high temperatures the reaction has often been studied at very low pressures.[a1-8] Under these conditions the rates of gaseous diffusion are so rapid that the overall reaction is no longer limited by the diffusion process.

Amongst others Duval[a3,4] and Strickland-Constable[a7] studied the oxidation of graphitised carbon

filaments which were heated electrically. The interesting common feature of their results was the observation of a maximum rate of reaction at about 1400°C. A decrease of the rate then occurred as the temperature was increased up to 1900°C.

Somewhat similar results were reported by Strickland-Constable[a7] with carbon dioxide, steam and nitrous oxide, although in the latter reaction the rate again showed a positive temperature coefficient after the maximum. Yates[a8] has reported that even in some experiments with nitrogen, the rate-temperature curve appeared to suggest a maximum. The similarity of these results with very different gases suggests a common mechanism for the reaction dependent mainly on the reactivity of the graphite.

1.4. Experimental methods for measuring gas-solid kinetics at high gas pressures.

As explained earlier, at normal pressures the overall reaction is limited by the rate of mass transfer through the bulk gas phase, so the unusual kinetics observed at very low pressures are not observed. Moreover the rate of mass transfer depends on the turbulence of the gas phase, so that in a flow system

the overall reaction rate depends upon the velocity of the gas stream.

1.4.1. Aerodynamic flow around a cylinder.

In a real fluid flowing over a solid body the gas velocity at the solid surface is zero (except at low gas pressures). Viscous drag produces this effect and establishes a velocity gradient at the wall called the boundary layer. The drag can only be transmitted to the fluid at a finite rate so that at the leading edge of the surface the boundary layer thickness is very small. It will increase in thickness away from the leading edge but will become thinner in a decreasing pressure gradient. In an increasing pressure gradient as from B to D and C to D (fig.13) the boundary layer will thicken until reverse flow takes place when the boundary layer separates from the surface. Energy will then be dissipated by eddies in the wake giving form drag in addition to skin drag on the front surface of the cylinder CAB.

1.4.2. Mass transfer analogy to momentum transfer.

The Reynold's analogy for heat, mass and momentum transfer is only valid when each transport mechanism is by an analagous process: there is no mass

transfer analogy for form drag. However, before flow separation occurs, the mass transfer resistance can be considered as confined in the region of the velocity gradient i.e. in the surface boundary layer.

If (J) is the mass transfer rate per unit area, Δc the concentration difference across the boundary layer of thickness (δ), and (β) is the effective diffusion coefficient then from equation 1.5:-

$$J = \frac{\beta}{\delta} \Delta C = K_G . \Delta C \qquad 1.13$$

It is usual to consider the boundary layer at the leading edge to be in laminar flow so that the gas velocity is parallel to the surface. Mass transport across the laminar film is then purely by molecular diffusion so $\beta = D$. Away from the leading edge the boundary layer develops into turbulent flow, the onset of which is dependent upon the gas velocity and the roughness of the solid surface. In laminar flow the boundary layer thickness (δ) can be shown to be proportional to $(Re)^{-\frac{1}{2}}$; in turbulent boundary layers (δ) is proportional to $(Re)^{-1/5}$. The change in (K_G) can therefore be estimated as a function of the flow conditions.

In general, however, the mass transfer coefficient (K_G) can only be found experimentally and

one has to use dimensionless groups to generalise the data. Such a correlation is:-

$$Sh = f(Re \cdot Sc) \quad \ldots\ldots\ldots\ldots 1.14$$

where the Sherwood number ($Sh = K_G L/D$) is characteristic of the mass transfer conditions, the Reynold's number ($Re = \frac{\rho d v}{\mu}$) is characteristic of the flow conditions and the Schmidt number ($Sc = \mu/\rho D$) is characteristic of the fluid properties. In external flow over a solid body the correlation can be expressed as $Sh = K.Re^{m}.Sc^{n}$ and several values for (m) and (n) have been given in the literature, for instance:-

$$0.4 < m < 0.67$$

$$0.3 < n < 0.4$$

For the flow of gases, (Sc) is close to unity therefore the main change in (Sh) is caused by changes in (Re).

At very high gas velocities a turbulent boundary layer is quickly formed at the leading edge of the cylinder especially if the solid surface is rough and is reacting with the gas. Under these highly turbulent conditions mass transfer rates can often be very much faster than chemical reaction rates.[K2] Consequently the latter rates are measured directly in the experimental observations.

This situation was used by Nagle to measure the reaction kinetics of carbon oxidation at normal pressures. Graphite rods were heated electrically and the reactant gas directed across the rod surface from a jet. The rates were calculated from the linear retreat of the carbon surface beneath the jet over a measured time interval.

Nagle observed similar rate-temperature curves to those found in the low-pressure studies; however Nagle's maximum rate occurred at 1700°C as opposed to 1400°C in the case of filaments. A theory was proposed to account for these results.

1.5. Theory of the reaction kinetics of graphite oxidation.

The theory of Nagle and Strickland-Constable[e.1] is based on the presence of two different reactive sites on the carbon surface. In this respect it follows a theory proposed by Eyring[e.3] but the concept of the nature of the sites is different. An A site, the more reactive, is associated with loosely bound atoms in the graphite lattice. The B sites are in a more stable configuration but reactions on B sites produce reactive A sites. A third activated process is considered to be

the thermal annealing of the surface by the migration of carbon atoms: in this process A sites are converted into B sites. The overall reaction kinetics can then be developed as follows:-

Let the fraction of the surface occupied by A sites be x. Of these a fraction (θ) is occupied by adsorbed oxygen.

Rate of oxygen adsorption on A sites = $K_C(1-\theta)P$

Rate of desorption of product from A sites = $K_E.\theta$

Under steady-state conditions (θ) is constant

$$\therefore \quad K_C(1-\theta)P = K_E.\theta$$

$$\theta = \frac{K_C.P}{K_E+K_C.P} \qquad \ldots\ldots\ldots\ldots \quad 1.15$$

$\therefore$ Rate of reaction on A sites = $K_A.\theta.x$

$$= \frac{K_A.K_C.P.x}{K_E+K_C.P} \qquad \ldots \quad 1.16$$

B sites are considered to have a low adsorption coverage of oxygen. Therefore :-

$$\text{Rate on B sites} = K_B(1-x).P \qquad \ldots\ldots\ldots \quad 1.17$$

$$\therefore \text{ Total Rate} = \frac{K_A.K_C.Px}{K_E+K_C.P} + K_B(1-x).P \qquad \ldots \quad 1.18$$

The fraction (x) is pressure and temperature dependent.

Rate of conversion of B sites into A sites = $K_B(1-x)P$

Rate of annealing of A sites to B sites = $K_T.x$

At steady-state conditions, (x) is constant

$$\therefore \quad K_B(1-x).P = K_T.x$$

$$x = \frac{K_B.P}{K_T+K_B.P} \qquad \ldots\ldots\ldots \quad 1.19$$

1.6. Deductions from the theory.

i.) At low temperatures (x) is close to unity and therefore (K_T) is small: (x) depends very little on (P) and the overall rate is given by $R \simeq \frac{K_A.K_C.P}{K_E+K_C.P}$

However the overall reaction rate may tend to zero or first order dependent upon the relative magnitude of $K_C.P$ and K_E.

ii.) At very high temperatures (x) is close to zero and (K_T) large: (x) depends on (P) so the surface anneals most rapidly when (P) is small i.e. a maximum rate at low oxygen pressures is reached at a lower temperature than at higher pressures. The overall rate is given by

$$R \simeq K_BP$$

This is a first order reaction.

1.7. Scope and aims of the present investigation.

In the above work there was considerable scatter in the experimental results owing principally to the uncertainty of temperature, and inaccuracy in

measuring the rate of burning of the carbon surface. Nagle interpreted the data by a statistical correlation which gave the best fit to the known experimental variables. However because of the complexity of the reaction kinetics and the partial dependence of the overall rate of reaction on mass transfer effects, the information from the analysis was necessarily limited.

Nagle found that the rates of pyrolytic graphite oxidation depended very little on the gas velocity but adequate proof of the absence of the effects of mass transfer was not presented. Furthermore because of the experimental scatter, the small decrease observed in the reaction rates above 1700 ^{o}C was not very significant. In fact it was possible to consider the 'apparent' maximum to be a flattening of the rate-temperature curve caused by partial control of the kinetics by rates of mass transfer.

In the present work it was decided to improve and develop the experimental technique described above. Then the effects of mass transfer on the reaction rate at high temperatures could be investigated so that the conclusions reached by Nagle could be verified or rejected.

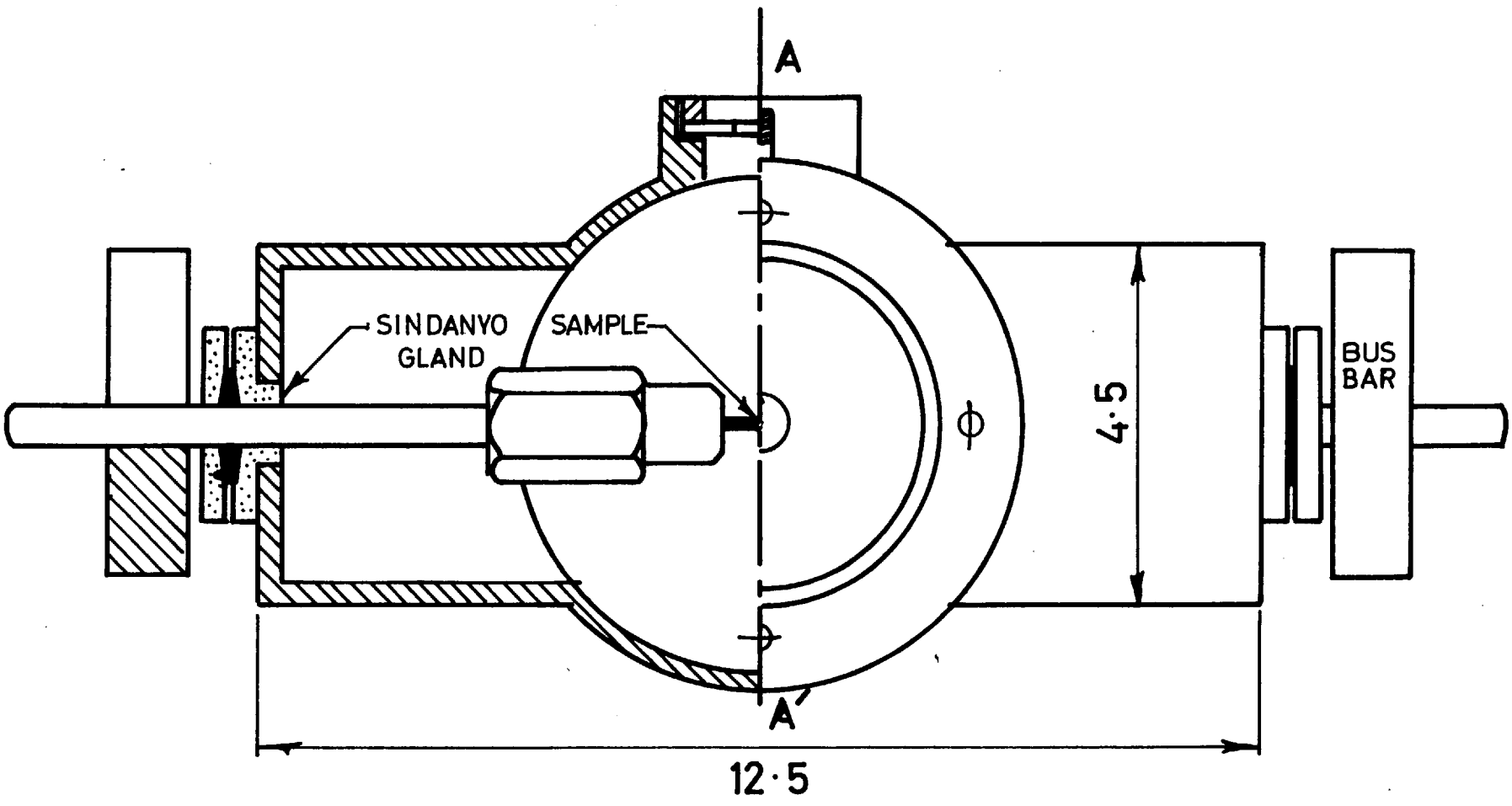

Fig.2.1 FRONT ELEVATION OF REACTION VESSEL

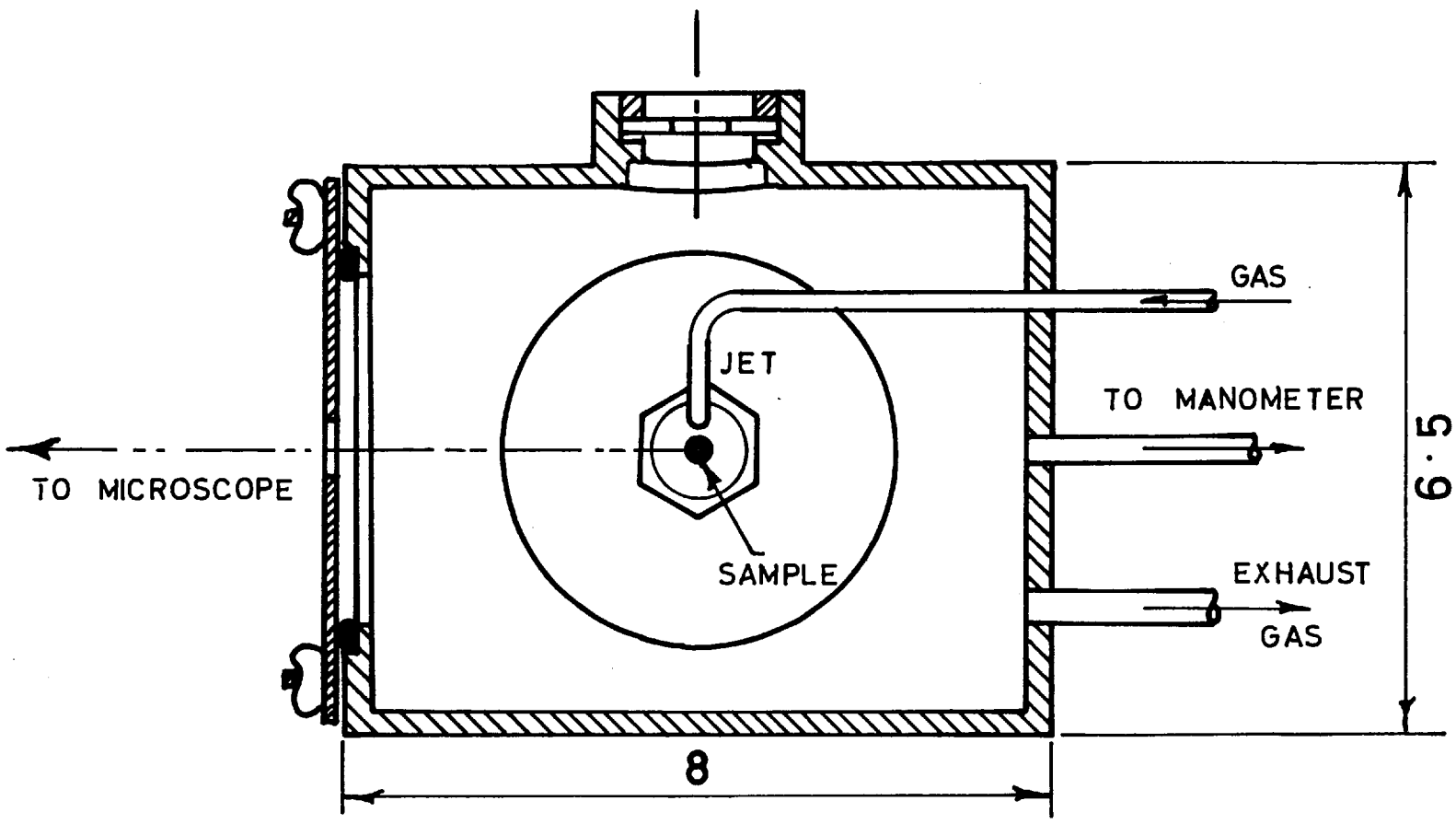

SECTION ON AA'

ALL DIMENSIONS IN INCHES

SCALE: 1/2 FULL SIZE

2. A study of the experimental scatter using the microscope technique.

2.1. Introduction: In order to study the reproducibility of the experimental results using Nagle's technique, the air-oxidation rates of reactor graphite were measured at a constant temperature of 1400°C and a constant gas velocity of 7000 cm.sec.$^{-1}$ The data was subsequently analysed by statistics to find the magnitude of the variation about the mean (this analysis is given in Appendix 2). In addition a complete reaction-temperature curve was established and compared with the results published by Nagle.

2.2. Apparatus: The apparatus used in this part of the experimental work was that set up by Nagle[C.1.] and will be briefly described. A cylindrical rod of graphite was enclosed by a metal vessel but could be viewed from outside through a small glass window, (a drawing of the reaction vessel is given in fig. 2.1.). Large currents were taken from a step-down transformer and passed through the sample, which was rapidly heated to a steady temperature. A stream of the oxidant gas was directed over the graphite to increase the rate of

mass transfer to the solid surface: rate measurements were calculated from the rate of retreat of this surface beneath the gas jet. The retreat was observed in a travelling microscope and the rod temperature measured with a disappearing filament pyrometer.

2.3. Preparation of graphite samples: The graphite samples used above were prepared as follows:-

A $\frac{1}{4}$ inch diameter brass tube was drilled into a large block of graphite. On withdrawal, the tube removed a cylindrical core from the graphite block. This was cut to 4 cms. in length and jammed between the graphite bushes immediately below the tip of the gas jet.

Square samples of the same width were found to give identical rates of reaction, and as these were easier to make, they were used in place of cylindrical rods in later experiments.

Square pyrolytic graphite samples were cut from a large sheet of the material as described later. Great care was taken to prepare the ends of each sample to make a good electrical contact with the supports.

2.4. Nagle's Method of rate measurement: The duration of each run was only about a minute so all instruments were prepared before the sample was heated; the pyrometer and microscope were focussed onto the cold graphite surface and the pyrometer set to read a temperature of about 1400°C. When the entrance to the vessel had been sealed, the pumps evacuated the air space and air was drawn in through the jet over the graphite surface. The flowrate was adjusted by constricting the rubber supply tubing to give a gas velocity of 7000 cm.sec.$^{-1}$ at the jet. A similar adjustment to the exhaust line set the vessel pressure to 0.21 atmospheres. When the gas pressure ceased to fluctuate an appropriate transformer voltage was selected to give the required temperature and the current was switched on.

The attack proceeded most quickly at the site where the jet impinged on the rod, forming a saddle depression in the surface. As soon as the graphite appeared to attain a steady temperature the position of the bite seen in silhouette on the microscope graticule was read and mentally noted:

the stopwatch was started simultaneously. Without delay the pyrometer filament was matched with the brightness of the graphite surface. Then the new position of the retreating surface was measured as the timing was stopped. The reaction temperature was read from the calibrated scale of the pyrometer and the rate was calculated from the other measurements as shown below in equation 2.1.

The magnification of the microscope (M) was

100 divs ≡ (0.250 or 0.390) cms.

All the graphite rods were cut from the same sample in which the bulk density measured in a specific gravity bottle in comparison with water was 1.76 $g.cm.^{-3}$

If the surface retreat was (h) divisions of the microscopic scale in a time of (t) secs, then the rate of reaction was given by:-

$$R_v = \frac{h}{t} \cdot \frac{1}{M} \cdot \frac{\rho}{12} \text{ g.at. cm.}^{-2}\text{. sec.}^{-1}\text{. . . . 2.1.}$$

2.5. Results of rate against temperature.

The results of the experiment are set down in table A4, which is given in Appendix 2, where the symbols are the same as described above. The full

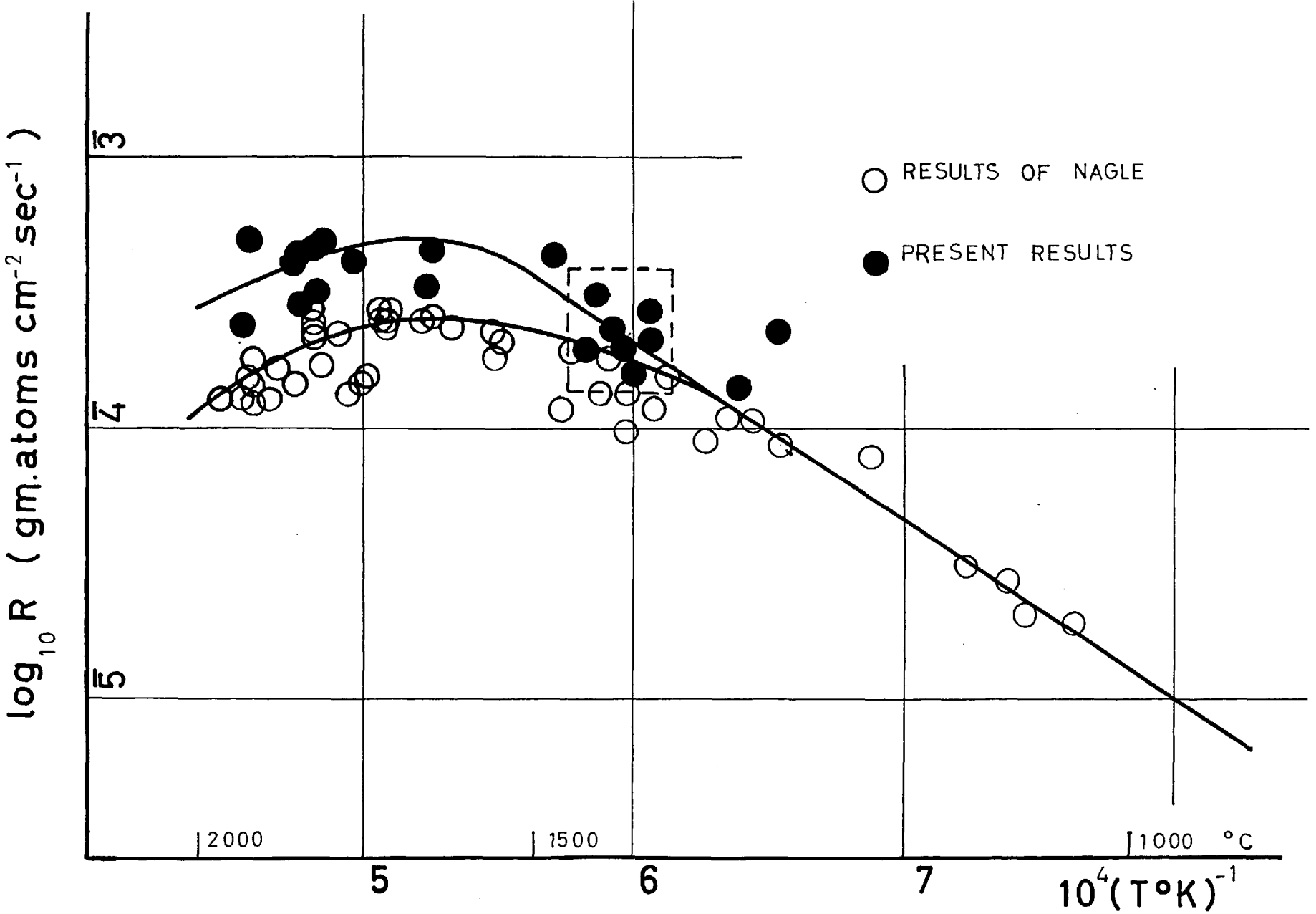

Fig.2.2 OXIDATION OF REACTOR GRAPHITE IN AIR (0·21atm.)

experimental curve was plotted in fig. 2.2 as the logarithm of the rate (R g.at.cm^{-2}.sec^{-1}) against the reciprocal of the absolute temperature. Nagle's published results are shown on the same graph: the experimental scatter is seen to be similar in both cases.

A higher gas velocity (7000 cm.$sec.^{-1}$) was used in the present experiments which probably accounts for the maximum rate being higher than Nagle's had been: this result supported the supposition of partial mass transfer control of the reaction rate.

It is also possible that once a maximum value for the results is obtained, they remain constant, instead of decreasing as suggested by Nagle.

Below 1500°C the corresponding velocity difference has no effect on the reaction rates. This appears to suggest that reaction rates below this temperature are not controlled by rates of mass transfer and from Nagle's results an apparent activation energy of 30 K.cals.$mole^{-1}$ was calculated.

2.6. Results for pyrolytic graphite: With the same

apparatus and technique as described above some rate-temperature results were obtained with pyrolytic graphite; these are described in detail in a later section (4.3). The rate-temperature curve was similar in shape to that observed with reactor graphite.

It is interesting to note that neither gas-velocity difference nor pressure difference affected the comparison with Nagle's results for pyrolytic graphite and below 1500°C an apparent activation energy of 44 K cal.mole^{-1} was found in both cases.

2.7. Conclusions:

2.7.1. From this preliminary analysis, it became clear that the large fluctuation in the temperature whilst the retreat was measured was a small but significant contribution to the experimental scatter about the rate temperature curve. An improvement would be obtained if the temperature could be brought under closer control.

2.7.2. The error in the measure of length (h) contributed most to the experimental scatter as was shown by an error analysis (see appendix 2). Therefore if this could be measured with greater precision more

accurate predictions could be made from the reaction-temperature curve.

2.7.3. The velocity of the gas stream altered the reaction rates: this required a fuller investigation preferably at a constant reaction temperature.

2.7.4. Below 1500 ^{o}C the apparent activation energy for the reaction of oxygen with pyrolytic graphite was higher than that for the reaction of air with reactor graphite.

3. Improvements to Nagle's methods of measurement and evaluation of the jet-flow technique.

The investigation of scatter in the rate measurements suggested several major improvements to the experimental methods. These were successively introduced and are described below in detail.

3.1. Measurement of the sample temperature.

The causes of temperature fluctuations during a run were as follows:-

a) The development of the bite in the graphite surface altered the electrical resistance of the sample.

b) The contact resistance between the sample and support sometimes changed during the run.

c) The reaction was exothermic, so where the reaction rate was greatest, i.e. under the jet, more heat had to be dissipated.

The following values of the temperature change were noted, in the presence and absence of a jet of gas; three different carbons were oxidised using both air and oxygen at atmospheric pressure, and a mean initial temperature of 1500 ^{o}C:-

	$\Delta T(O_2)$	ΔT (air)
carbon rod	+ 210	+ 130
reactor graphite	+ 30	+ 10
pyrolytic graphite	- 90	- 150

As might be expected the biggest temperature rise was observed with the most reactive material (carbon rod) in a stream of pure oxygen. In contrast a fall of temperature was observed with pyrolytic graphite.

In general the temperatures as measured were not corrected for glass absorption, emissivity, etc., because these were systematic errors and the absolute temperature values were not essential for interpretation of the rate-temperature curve in the present investigation.

Modifications: The pyrometer line of sight was changed by moving the sample to the centre of the vessel and fitting a window directly above it: a view of the sample could now be made mutually at right angles to the axis of the graphite rods and the line of site of the microscope. If the jet was inclined at 45° to the rod axis the temperature at the seat of

Fig. 3.1. Photograph of apparatus.

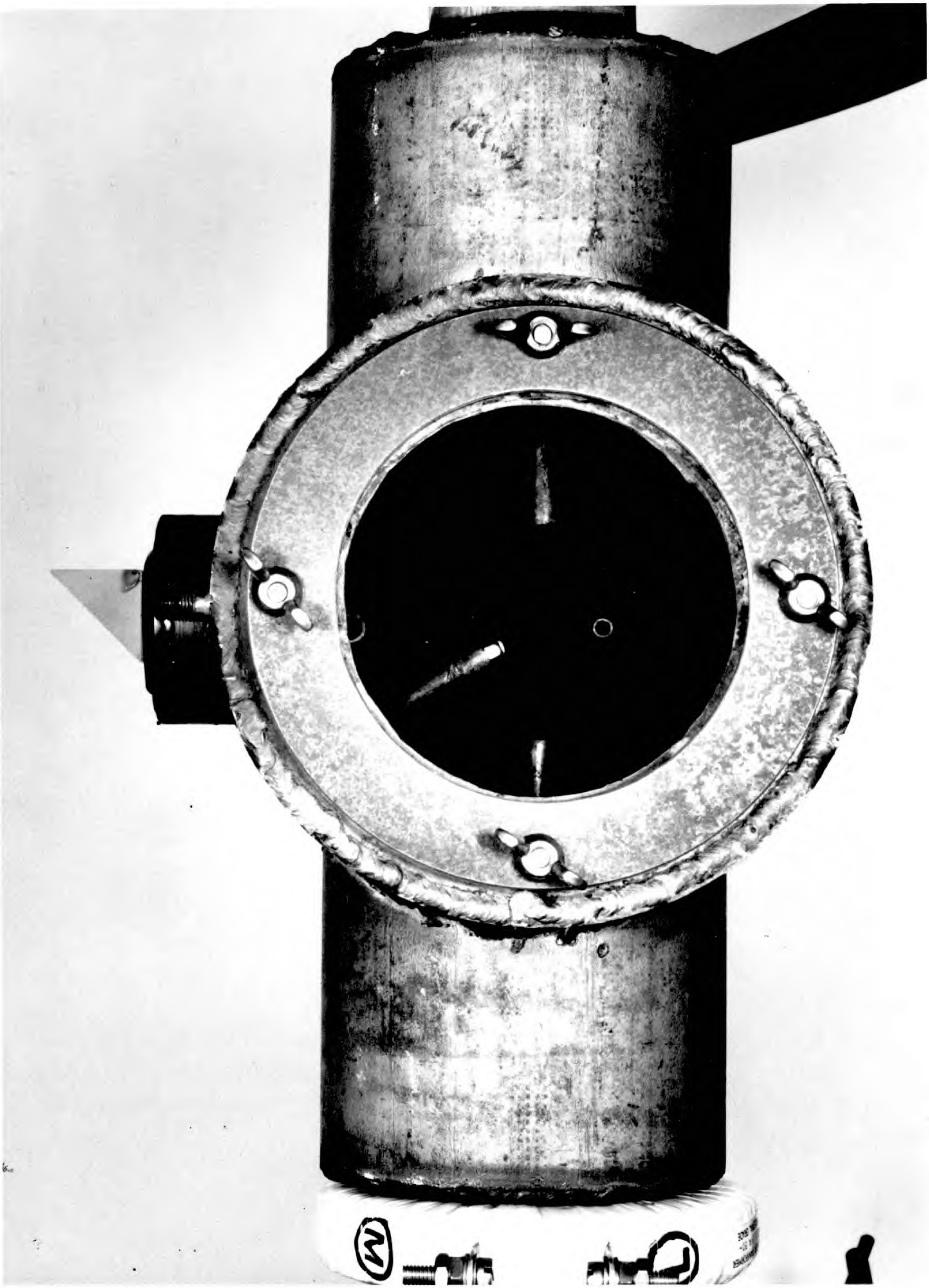

the reaction could then be viewed directly through a 45° glass prism, placed on the top window (for detail see photograph fig. 3.1).

Different supports were needed for this new arrangement and these were made from much larger pieces of graphite as described in section (4.2). These were easily removed between runs and could be machined to give two new parallel faces to support each fresh graphite sample. An additional advantage was that the supports did not become hot and burn away during a run because of their greater thermal capacity: they therefore provided a firm support for the sample during oxidation and no further experimental difficulty was experienced in this respect.

3.2. New method of temperature control.

In order to compensate for the electrical resistance changes in a sample during a run it was decided to adjust the heating current manually whilst the sample temperature was under continuous observation. The magnitude of the heating current was of the order of 600 amps, at the low-voltage side of the transformer,

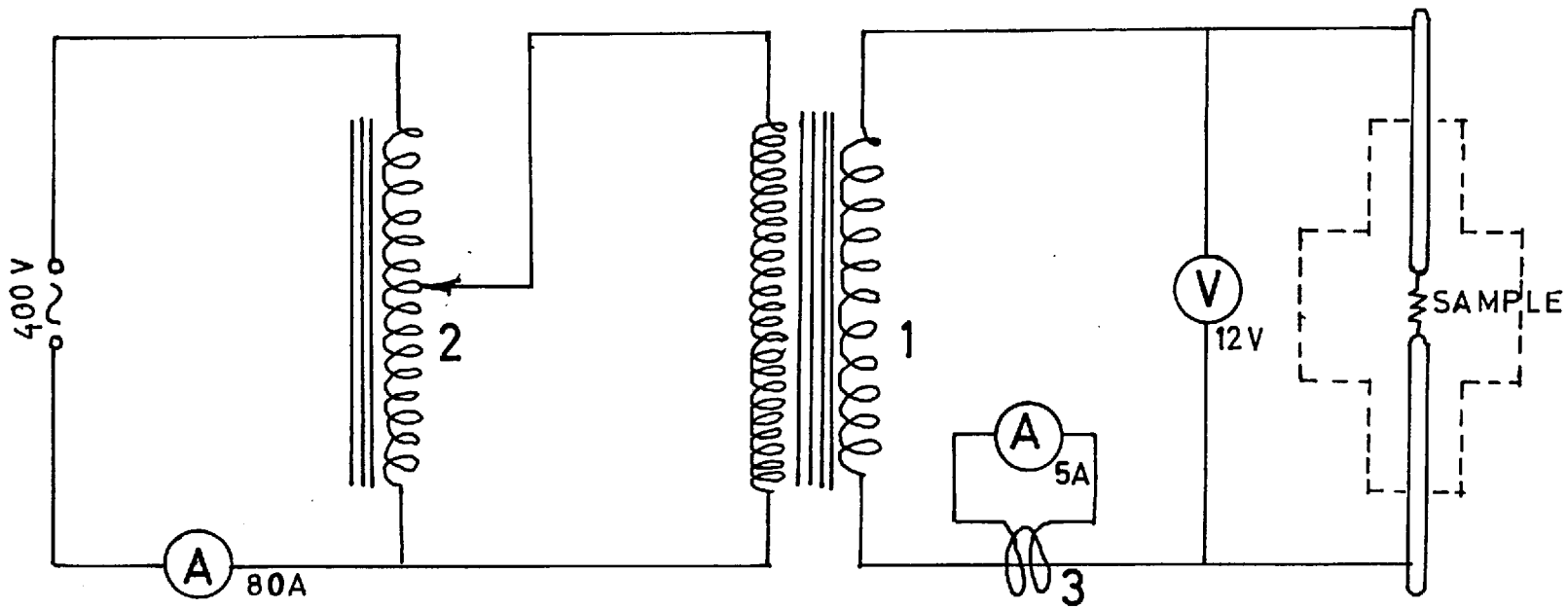

1	Hackbridge Transformer B.S.S 171 (1936)	33 KVA	82·5/3000A 400/11V
2	Auto - transformer 'VARIAC' V30H-G2	15amps	400/0-400V
3	Ammeter Transformer SMITH HOBSON LTD	600/5A	

Fig. 3.2 ELECTRICAL CIRCUIT DIAGRAM

and was now varied by controlling the input power to the high-voltage side of the transformer with an additional auto-transformer; since the input current was only 15 amps (at 400 V) a standard 'Variac' could be used.

To assist further in control, the size of the heating current was estimated by a current transformer (in the shape of a coil) placed around the electrical lead rods to the reaction vessel. The current induced in the coil was observed continuously on an 'Avo' meter (see the electrical diagram fig. 3.2, and the photograph, fig. 3.1, for the position of the coil next to the reaction vessel).

3.3. Pressure control:

A "Cartesian Manostat" was fitted into the exhaust line from the vessel in order to control the pressure in the vessel more closely. In effect the manostat controlled the rate of pumping from the vessel by means of a stainless-steel bell floating on a pool of mercury. The space beneath the bell was connected through a three-way tap to the exhaust line. When the vessel pressure was at the required level this connection

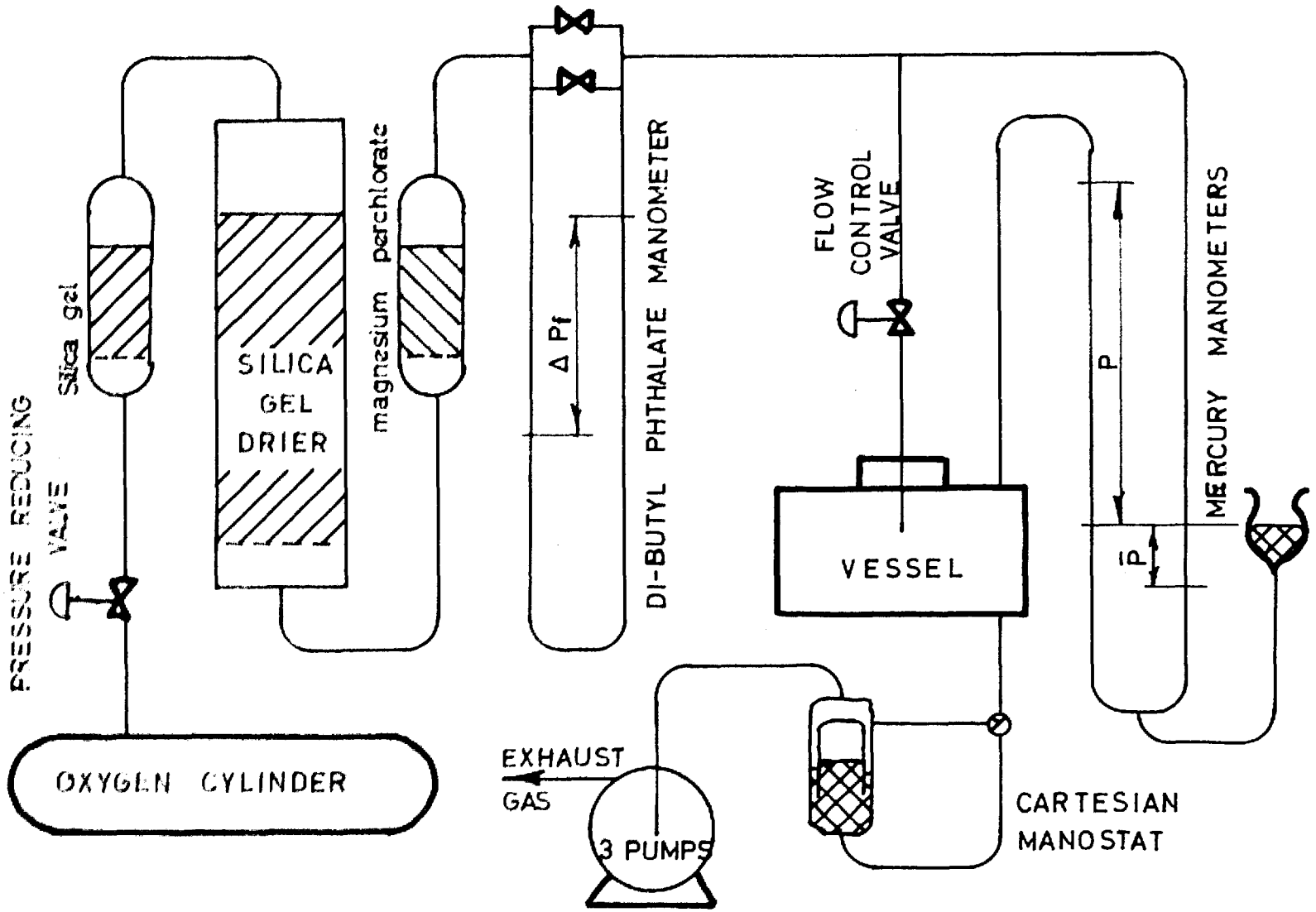

Fig.3.3 SCHEMATIC DIAGRAM OF GAS FLOW

was sealed off; further pressure reduction caused the bell to rise so that the top (covered in hard rubber) sealed the exhaust orifice (fig. 3.3). This instrument worked well except for high flow-rates (5 litres per minute) at low pressures (less than 1/5 atmosphere) when the orifice was too small to pass the volume of gas. However it was very satisfactory for rate-velocity work on pyrolytic graphite.

3.4. The Jet:

A "Bray-burner" gas jet was used to direct the gas flow. The small jet ($\frac{3}{8}$" overall height) consisted of a hexagonal brass socket with a slotted-port porcelain tip. The dimensions of the port are shown in fig. 3.4. Velocity-traverses were made across the jet and showed a parabolic distribution of flow. The plane of the jet was directed across the sample.

3.5. Calibration of the capillary flowmeter.

Two capillaries were arranged in parallel; one was used at low flow rates and both were used at high flow rates. The pressure drop (ΔPf) across

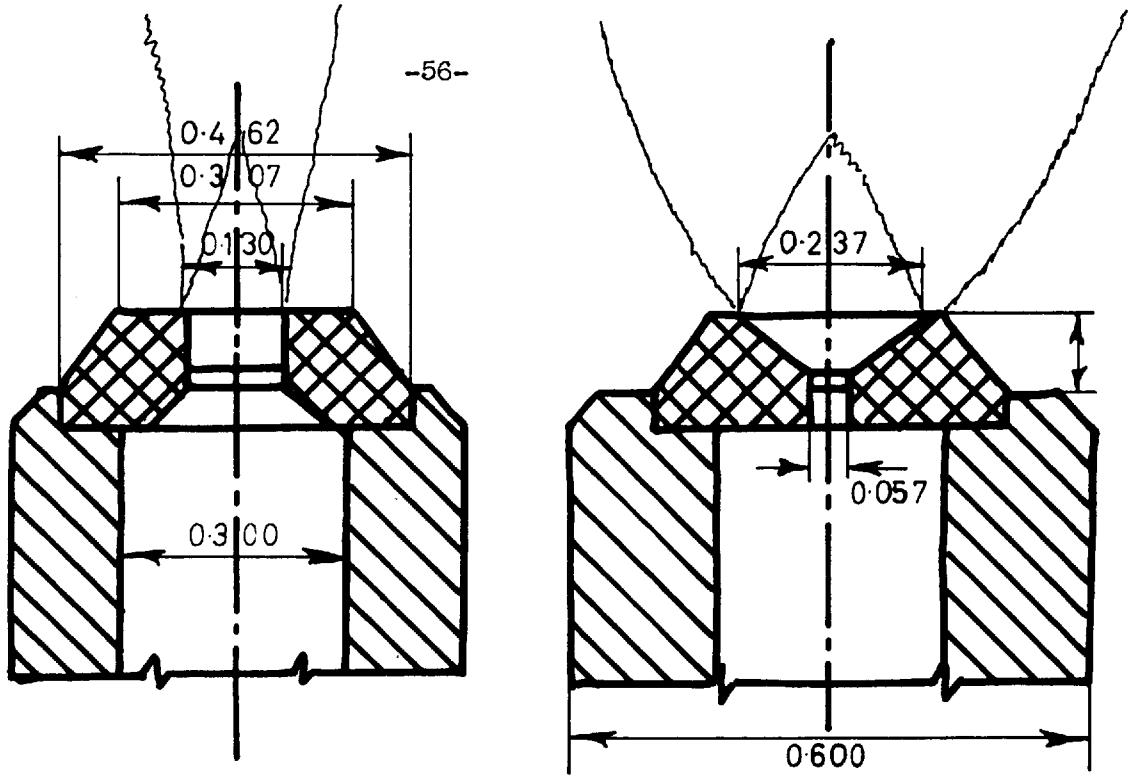

Fig.3.4 Dimensions of Bray burner jet. (no.115N cms)

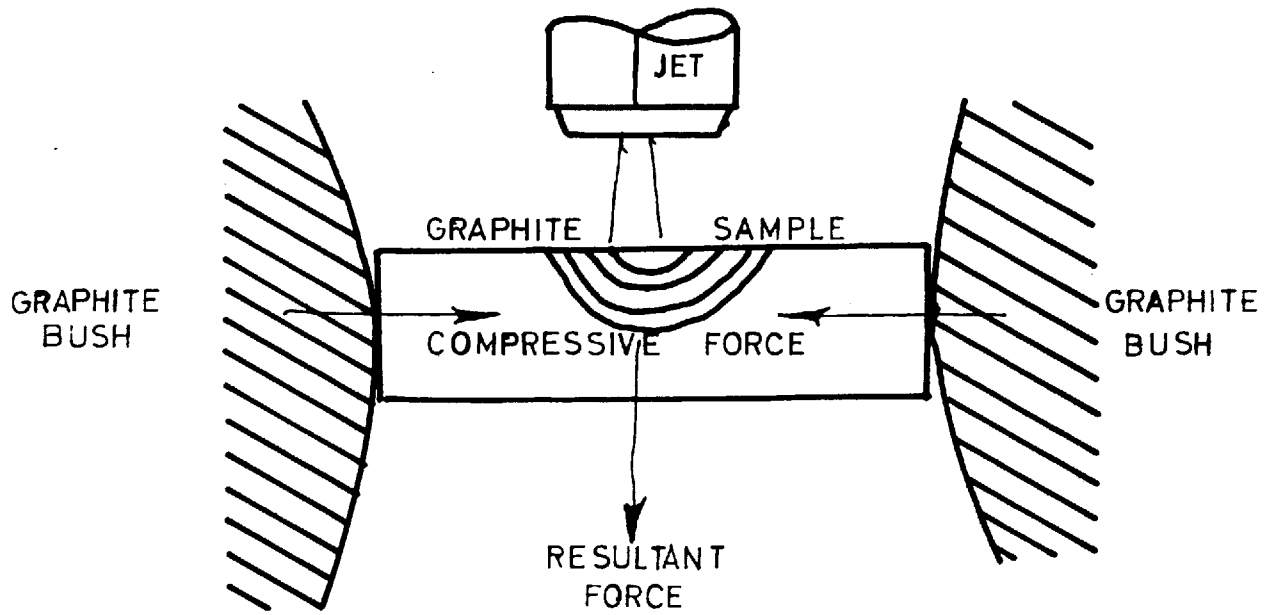

Fig.3.5 Support of graphite sample

the capillaries was measured with a dibutyl phthallate manometer. In addition, the pressure in the capillaries was measured using a mercury manometer and density corrections were made as required.

In the calibration ($\Delta P_f.\bar{P}/760$) was plotted against (Q) measured at S.T.P. When (Q) was plotted against the root of the pressure drop a straight line correlation was produced.

3.6. Velocity of the gas in the jet.

A simple pitot tube made from small-bore, thin-walled, stainless-steel tubing was used to measure the flow velocity. The velocity was dependent upon the ambient gas-pressure, gas flowrate and position of measurement relative to the jet mouth.

The pitot tube was set first of all at a fixed distance from the jet inside the vessel and the gas velocity was measured at different gas flow rates when a straight line calibration was produced; the slope of this calibration line varied directly with the ambient gas pressure. Secondly at one atmosphere pressure, the flowrate-velocity calibration was obtained at several fixed distances (do) mms from the

tip of the jet or (do + 1) mms from the throat of the jet. At distances greater than 3 mms the slope of the calibration was found to vary directly with $(do + 1)^2$. The following calibration was evaluated as characteristic of the jet:-

$$v = \frac{2 \times 10^4 Q}{\bar{P}(do + 1)^2} \qquad 3.1.$$

$do \geq 3$ mm

where (v) is the gas velocity ($cm.sec.^{-1}$) along the axis of the jet, at a distance (do) mms from the tip of the jet, with a gas flowrate (Q) $l.min.^{-1}$ and ambient pressure of ($\bar{P}$) atmospheres.

The above velocity may not be obtained when the free flow of the jet is obstructed by the sample, but the velocity will be characteristic of the conditions appertaining to the flow.

In each experiment a constant pressure was maintained and the jet-sample distance was reproducible from run to run. For this case, the flow-rate (Q), which is directly proportional to velocity (Equation 3.1), can also be used to characterise the flow conditions. Flow-rates could be measured more easily than the flow velocity and so reaction rates were plotted in the

first case as a function of gas flow-rate.

3.7. Surface pressure increase.

A specially constructed dummy sample was used to measure the surface pressure directly. This was made from metal and had a small hole in the leading edge which connected to a copper tube (below the sample): this in turn was connected by PVC tubing to a mercury manometer. When measurements were made under different flow and pressure conditions the following calibration was found to apply:-

$$\Delta P_s = \frac{\Delta P_f}{\bar{P}} \cdot \frac{2.5}{do^2} \qquad 3.2.$$

$do > 3$ mm

Where (ΔP) is the pressure increase; the other symbols have already been described.

In addition to the above experiments the surface pressure was measured at high temperatures (up to 1800°C) in one atmosphere of nitrogen. For this experiment a ceramic tube was inserted into a graphite sample. The temperature of the graphite was found to have no effect upon the surface pressure increase caused by the jet of gas.

3.8. Measurement of the graphite surface retreat.

Rather than continue with a microscope it was decided to project an image of the sample for measurement as the sample itself was incandescent. A magnification up to fifty times was obtained without any noticeable distortion of the image and the retreat could be measured to ± 0.01 mm. (In the travelling microscope a magnification of 3.9 times was obtainable and surface retreats could only be measured to ± 0.1 mm.)

Further improvement was obtained by photographing the projected image with a Bolex (H.16 reflex) ciné-camera, at an exposure rate of 1 frame every 1.94 seconds. Each frame of the ciné-film gave in effect a separate estimate of the rate of combustion, so that a single run was equivalent to several tens of runs using the microscope method of measurement. A check could also be made for steady-state combustion.

The sample silhouette was photographed through a translucent screen made of "Kodatrace" and a reference scale at 1 cm. intervals was drawn upon the screen. This was mounted inside a large rectangular box-frame covered by black cloth and it was possible to see the image clearly even at low temperatures.

FIG.3.6 TWO TYPICAL SILHOUETTES OF A BURNING PYROLYTIC GRAPHITE SAMPLE

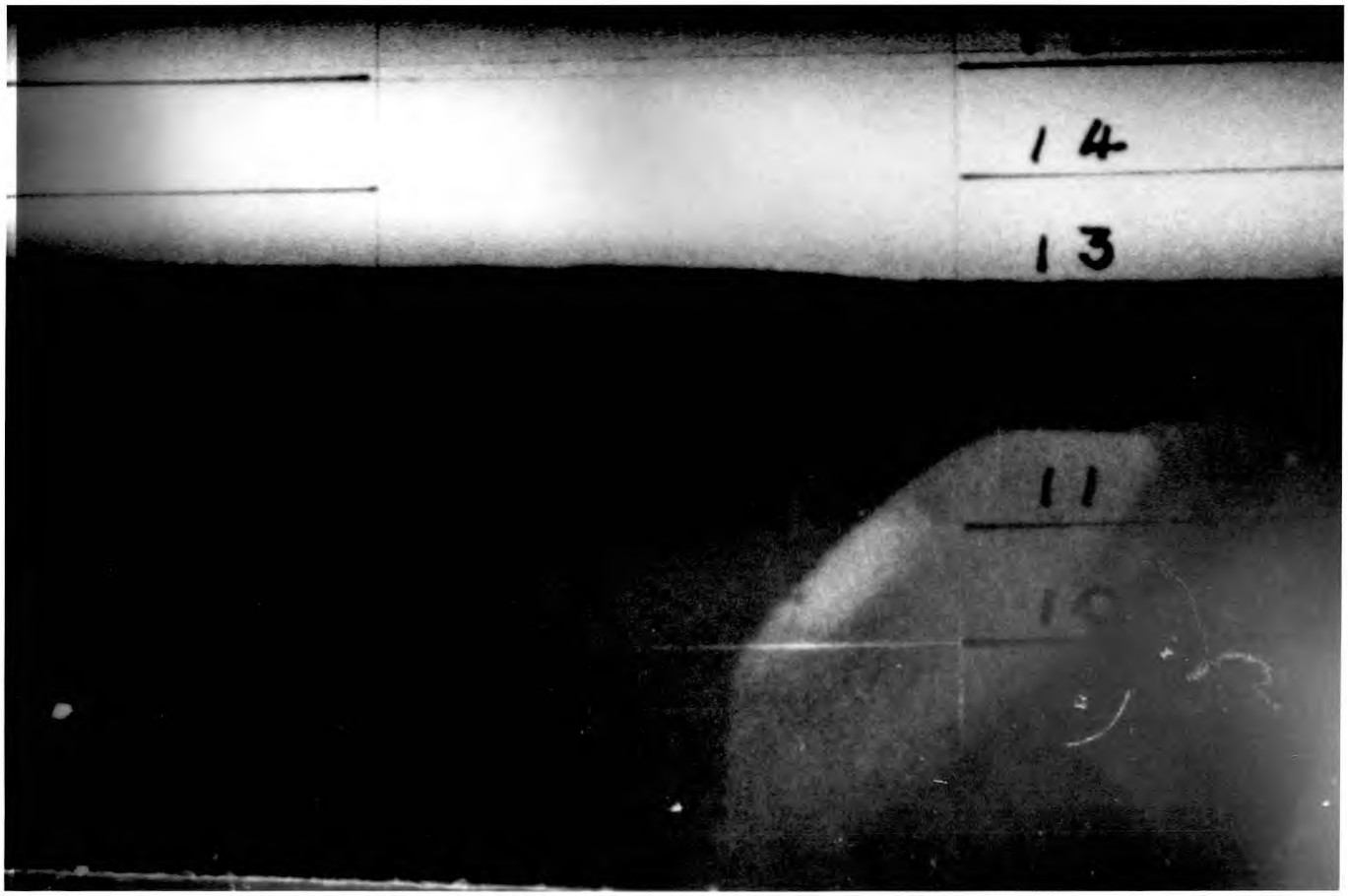
14
13
11

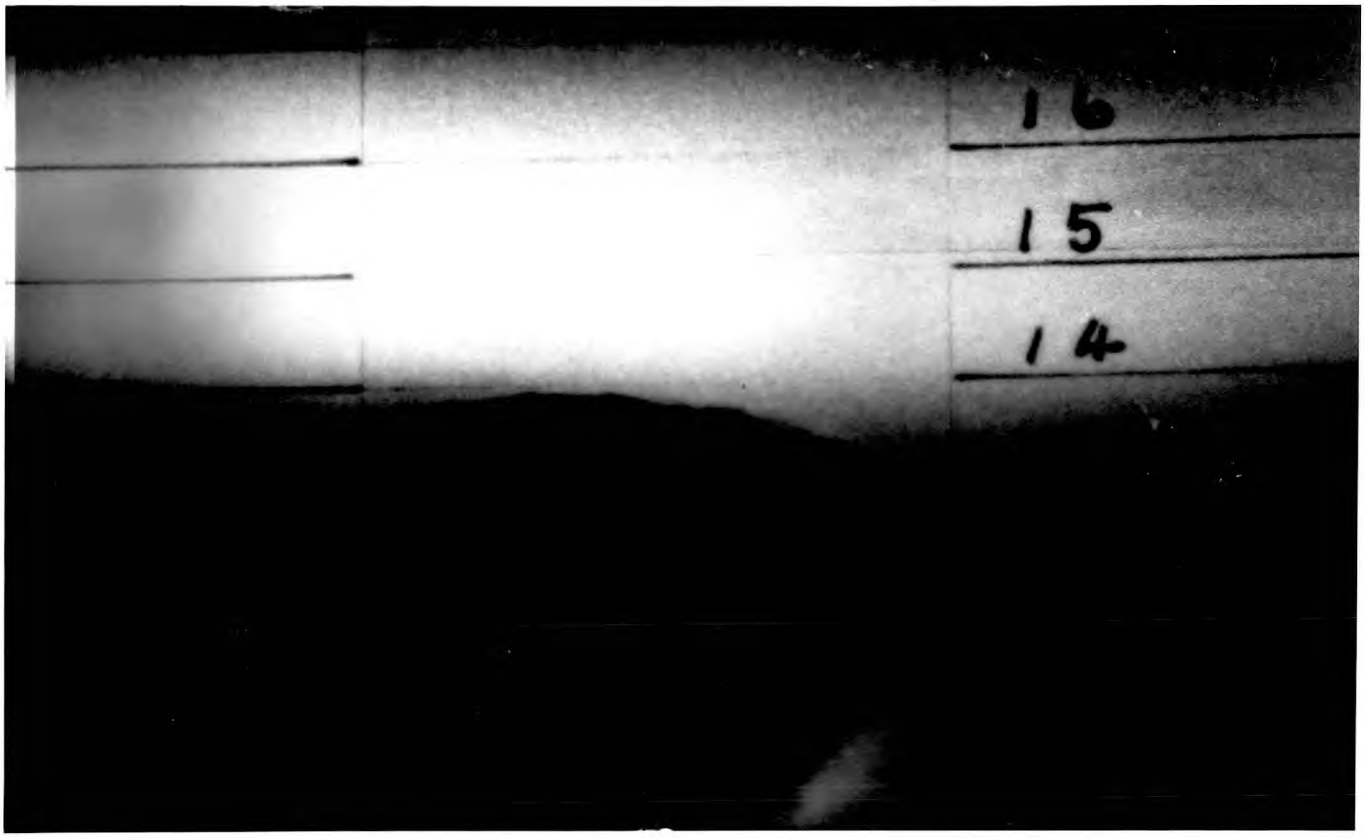
16
15
14

Kodak "plus-X" negative film (64ASA) was used and was sufficiently sensitive for temperatures as low as 1100°C and the resolution of the image at a magnification of thirty-five times was about 0.5 mms.

3.9. Analysis of the ciné-film.

The ciné-film was developed with Kodak D.76 developer. A "Specto" 16 mm. cine-projector was used to project the film, frame by frame, onto a large screen made from "Kodatrace" supported on a sheet of perspex at the rear of the darkened enclosure. The movement of the film was operated by a micro-switch fitted to an extension wire at the screen, and each frame was counted automatically by the projector. The image was viewed through the screen and a tracing of the silhouette was made at each frame interval.

Two typical views of the silhouette are shown in fig. 3.6. The photographs are an enlargement of a piece of film of the oxidation of pyrolytic graphite at 1840°C and are taken from the same film shown in fig.3.7. The two views are separated by 30 frames (equivalent to 58 seconds) and the bite has progressed by about 0.75 mms. An image of the jet can be seen above the sample owing

FIG.3.7 FOUR PIECES OF CINE-FILM OBTAINED WITH DIFFERENT GRAPHITE SAMPLES

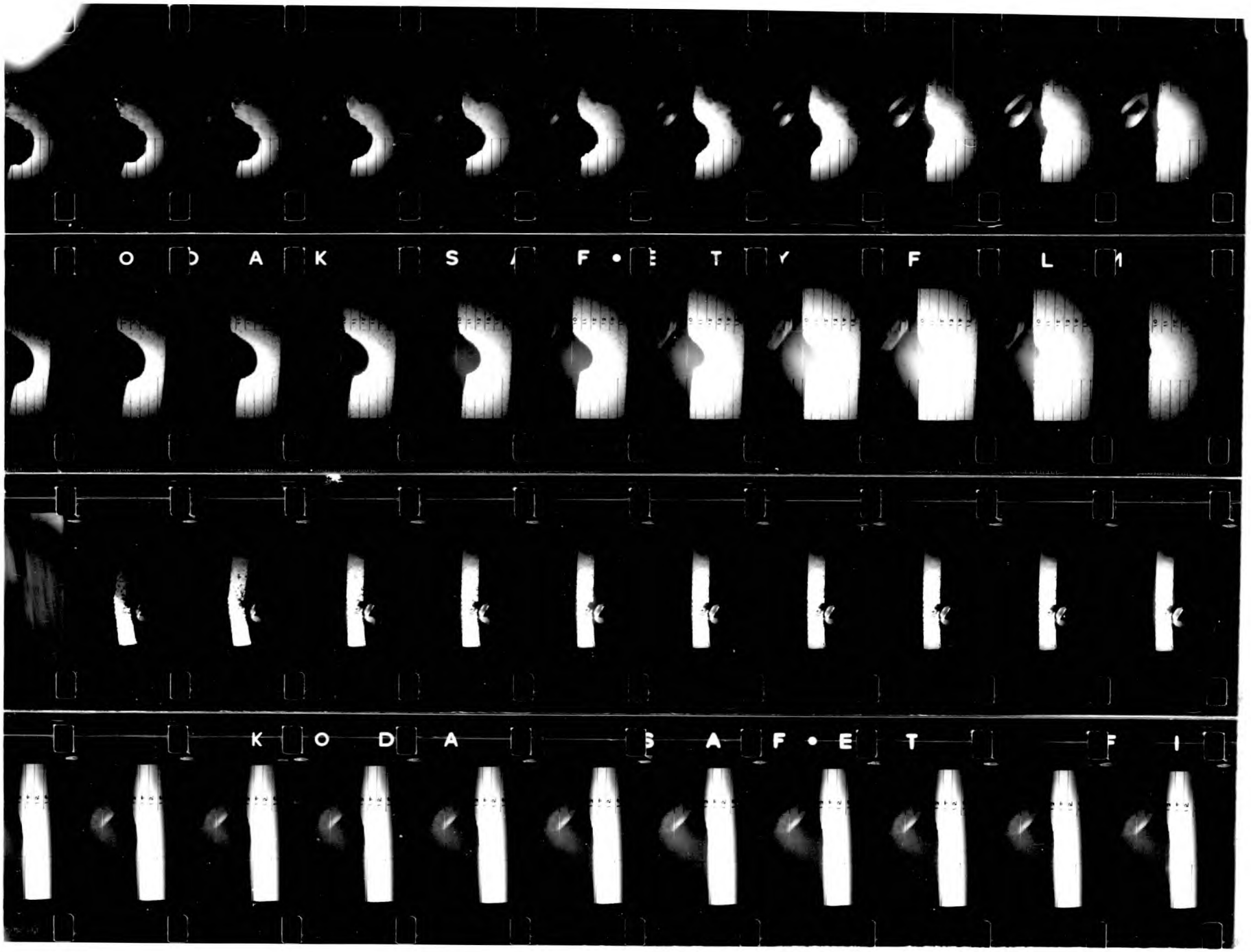
O D A K S A F • E T Y F L M
K O D A K S A F • E T Y F I

to the reflection of light from the white ceramic tip.

Some typical pieces of film are also reproduced in fig. 3.7. On the far right is a film of the oxidation of iron-impregnated reactor graphite at 1400°C. The gas velocity was very high and a reaction rate of 247 x 10^{-5} g.at.cm.$^{-2}$ sec.$^{-1}$ was measured. Centre right is a film of the oxidation of spectroscopic graphite also at 1400°C in a high gas velocity. The reaction rate was 248 x 10^{-5} g.at. cm.$^{-2}$ sec.$^{-1}$. Note how much smoother the silhouette of the sample is for this material. Centre left is a direct view of the sample, obtained in early experimental work. In this strip of film the movement of the sample is clearly visible and shows one of the reasons for the scatter in Nagle's results, since only the initial and final positions of the sample silhouette were recorded. Far left is a film of the oxidation of pyrolytic graphite at 1840°C. Note the much slower reaction rate which was 23.7 x 10^{-5} g.at.cm.$^{-2}$ sec.$^{-1}$.

Each position of the silhouette was plotted against the frame number and from the graph the rate of reaction was determined. The graphs for the three reaction rates described above are reproduced in fig.3.8:

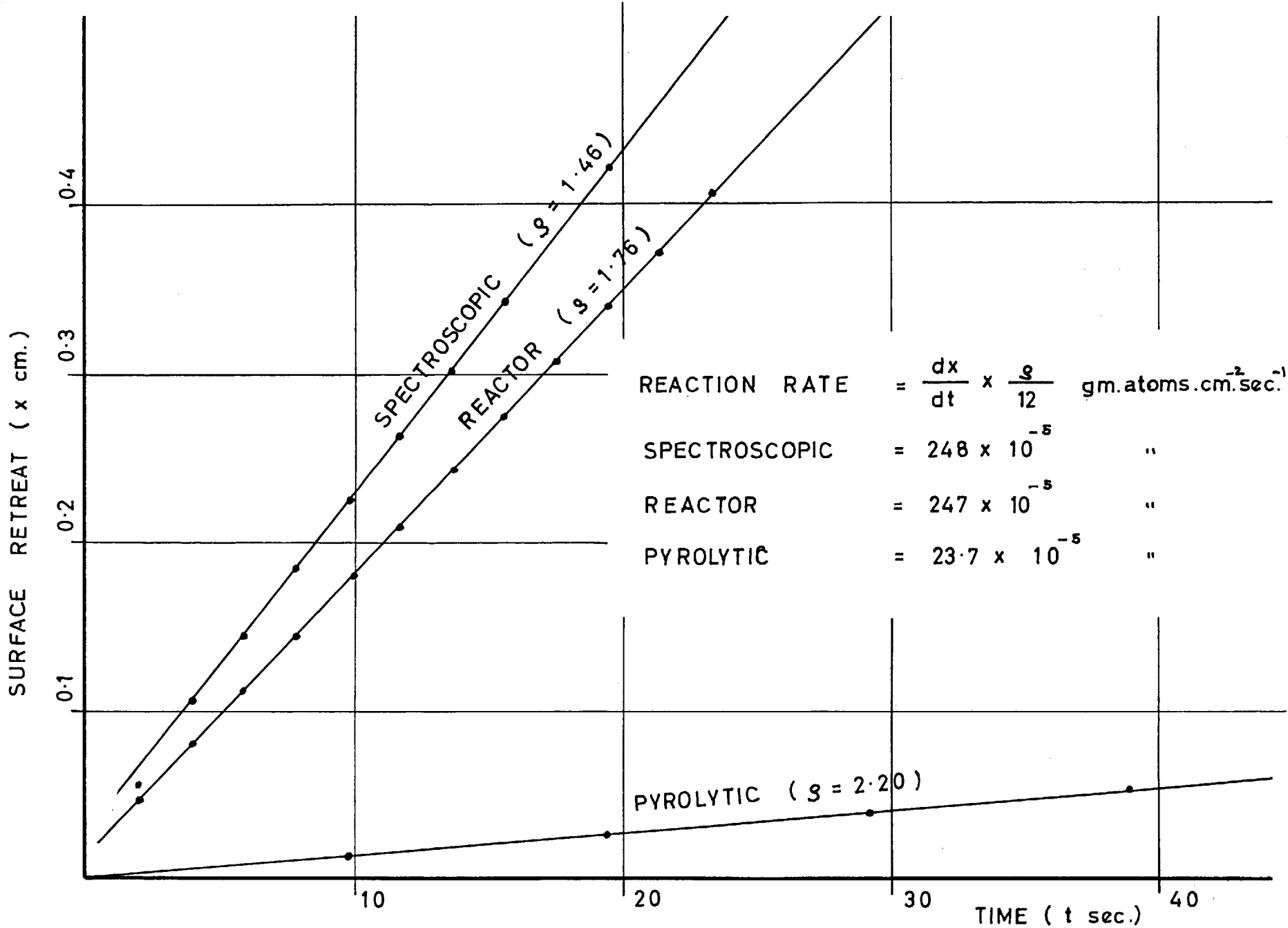

Fig. 3.8 DISTANCE - TIME GRAPHS FROM CINÉFILM

tne actual surface retreat (in cms.) is plotted as the ordinate, and time in seconds is plotted as the abscissa.

3.10. Experimental procedure using the improved experimental method.

1. A graphite sample was prepared and positioned inside the vessel immediately below the tip of the jet. It was possible to view the rod from the top window during this operation.

2. The front cover of the vessel was clamped into position and the vessel evacuated by three rotary vacuum pumps operating in parallel.

3. Atmospheric pressure was recorded and the cartesian manostat adjusted to give the required ambient pressure.

4. The gas flowrate was adjusted to the required level and the manostat reset at the correct ambient pressure.

5. Mains power was switched on and the heating current was increased to give a sample temperature of about 200°C. This was maintained for 15 minutes.

6. In this time the pyrometer was set to the required temperature and a run number photographed by the cine-camera.

7. Immediately before heating the graphite further, the

various pressure measurements were recorded and the camera-lens aperture set. The sample was then brought up to temperature, the camera was started and the enclosure quickly moved forward on its rollers to focus the silhouette of the sample on the screen.

8. Immediately after the run, the various pressure measurements were recorded again and checked for consistency.

3.11. Evaluation of the jet-flow technique.

Previous discussion has shown that when rates of reaction are independent of the degree of turbulence in the gas phase, they are not limited by rates of diffusion to the graphite surface. Therefore when a turbulent gas jet is directed over a carbon surface it is to be expected that a "critical" velocity will be found, above which the rates of reaction are not dependent on further increase in the velocity. The magnitude of the critical velocity can be found from the dependence of the reaction rates on the gas velocity at a constant reaction temperature.

3.11.1. Rate-velocity curves for reactor graphite.

A velocity-independent reaction rate for

reactor graphite was measured at 1400°C and also at 1900°C; but at 1800°C the reaction rate was so high that it was not possible to eliminate boundary-layer mass-transfer control of the reaction. However a maximum was observed in the rate-temperature curve.

In using very high gas velocities in this work it is possible that some "erosion" of the graphite surface could take place: this possibility will now be discussed:-

3.11.2. "Erosion" of the graphite surface.

Several authors[11,k2] have reported that particles of graphite can be detached from a sample without being consumed by the oxidising gas. The reason for this is that as the reaction proceeds in the pores the surface bulk density is progressively reduced until the remaining surface structure eventually disintegrates into a powder. This was observed in the present work for the oxidation of reactor graphite in a stagnant atmosphere of air, when a shower of incandescent particles was continuously emitted. The "erosion" was clearly visible in these circumstances and it is probable that the main reaction was proceeding in the binder (which was only partly graphitised) along the grain

boundaries.

It was expected that the surface erosion would be enhanced in a flow system but when a gas jet was directed over the surface no erosion was observed at all. This difference in behaviour can probably be explained as follows:-

When the oxygen has a uniform and small concentration throughout the porous graphite the bulk density must progressively decrease until the structure eventually crumples as described above. On the other hand with a limited oxygen penetration of the sample the bulk density can decrease only at the surface. From the theory of pore diffusion, the pore profile will then be "Vee"-shaped and not cylindrical, and therefore much stronger. Moreover as the graphite temperature is increased the penetration of the sample progressively decreases; therefore the surface structure during reaction will be stronger at high temperatures. This may explain why no erosion was observed in the flow experiments with reactor graphite.

In the case of pyrolytic graphite the samples are virtually non-porous so erosion of the material is most unlikely to occur. Experimental confirmation can

be sought from the rate-velocity results, presented in the next chapter, because a constant rate was obtained once boundary-layer mass-transfer control had been removed. Therefore despite the increase of skin drag as the gas velocity was increased further, the reaction-rate was still constant, which implies that erosion of the graphite was negligible.

4. The reaction between pyrolytic graphite and oxygen.

4.1. Introduction: As already explained in section 1.7, Nagle observed that at near atmospheric pressures the rate of reaction of oxygen with pyrolytic graphite reached a limiting value at about 1900°C, and appeared to remain constant above this temperature. Two possible explanations for this observation can be entertained, either:-

a) the effect is due to the limiting rates of mass transfer at high temperatures (as already explained in section 1.1.2.) or:-

b) the effect is due to the actual behaviour of the surface reaction kinetics, a suggestion which is strongly supported by the results of the filament experiments (already described in section 1.3.) when a pronounced maximum was obtained in the rate-temperature curve. In these low pressure experiments mass transfer limitations were entirely absent. Some evidence was produced by Nagle that his results were not affected by mass transfer resistance, although this evidence was in no way conclusive. Consequently the flattening-out of the curve at 1700°C might have been due to a mass transfer effect.

It appeared therefore to be a matter of great importance to attempt to obtain results which could be demonstrably shown to be free from any mass transfer effects. With this end in view the technique of Nagle was improved and the measurements rendered much more accurate.

Prior to working with pyrolytic graphite a great deal of work was carried out using reactor graphite. However the results of these experiments proved to be inconclusive for the following reasons:-

a) large rate of reaction: it proved impossible with the present equipment to obtain reaction rates which were independent of the gas velocity between 1600°C and 1900°C. Therefore the chemical rates of reaction could not be determined.

b) high porosity: even the rates that were independent of the gas velocity at other temperatures were shown to be controlled by the rate of in-pore diffusion. Consequently it was very difficult to produce a complete analysis of the rate measurements.

c) impurities: small concentrations of impurities were present in the reactor graphite which may have been catalytic agents for the oxidation of graphite.

For these reasons work was continued with pyrolytic graphite which is of very high purity and has a much smaller reactivity. In addition the material has a very low porosity so that intrinsic reaction rates can be measured. Some further experimental modifications were required to use this new material and they are described in the following section.

4.2. Further experimental modifications.

Unlike reactor graphite in which the micro crystallites are randomly packed, in pyrolytic graphite the crystallites are larger and orientated with their basal planes parallel; consequently the material shows a marked degree of anisotropy. In experimental work it was observed that a sample would striate into hot and cold layers if imperfect electrical contact was made with the sample supports. Moreover the supports were more reactive than the sample and rapidly burnt away.

To solve the latter problem larger supports, 2 inches in length, were cut from a graphite rod one inch in diameter. With the larger thermal capacity, the supports could hold the pryolytic graphite samples

for a longer period of time before the contact was broken. A small hole was drilled and tapped along the axis of the supports which could then be screwed onto the electrical leads: a fresh face could be cut on the support before each experiment, and in this way the pyrolytic graphite was always held firmly between two parallel surfaces.

Attempts to oxidise the sample in the a-direction caused the outer basal-planes (parallel to the direction of the jet) to cool. As a result a pit was formed rather than a saddle depression so that the reaction rate could no longer be measured from the silhouette of the sample.

Oxidation in the c-direction also tended to cause the plane beneath the jet to cool. However in the preparation of the sample (4 x 4 x 25 mm) the ends were slightly inclined to each other so that the top plane facing the jet was in firmer electrical contact with the supports. In this way cooling of the surface was avoided before the bite developed.

A further experimental modifaction was introduced to measure reaction rates below 1300°C when the photographic method was insufficiently sensitive. For

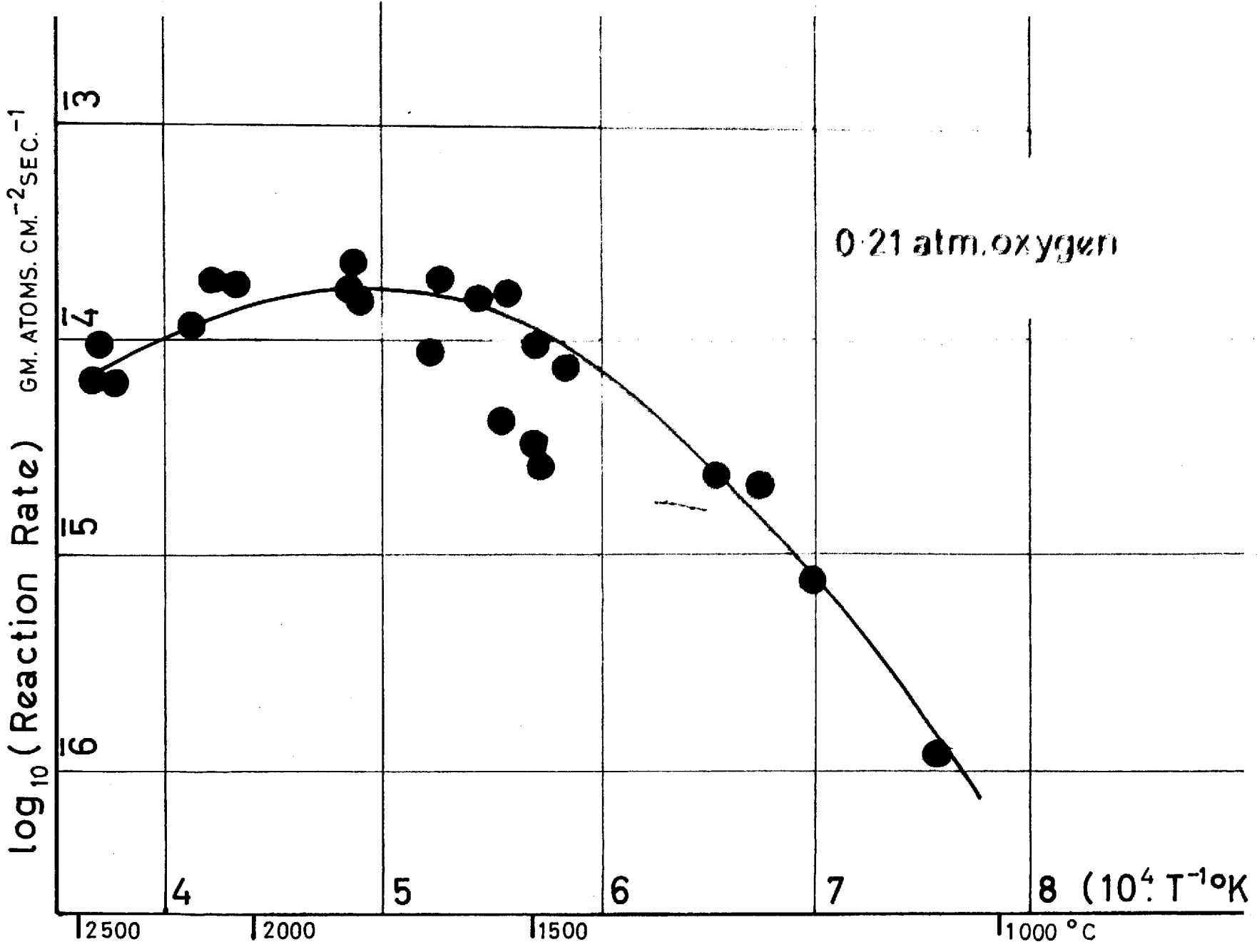

Fig.4.1 OXIDATION OF PYROLYTIC GRAPHITE (HTM)

these comparatively small rates the depression of the surface beneath the jet could be measured by a microscope after the reaction had taken place. In this way the range of experiments with pyrolytic graphite was extended downwards to 900°C.

In more detail - the sample was reacted beneath the gas jet for a fixed time (of approximately five minutes) at a low temperature. When cold the sample was placed on a slide beneath a microscope and observed at a magnification of fifty times, with opaque illumination. A traverse was made across the surface of the sample and the depth of the surface depression at the bite was used to calculate the rate of reaction.

4.3. Rates of reaction with pyrolytic graphite (HTM) using Nagle's technique.

Before starting the work using the improved technique, a set of results was obtained with pyrolytic graphite using Nagle's technique. The sample of pyrolytic graphite was supplied by High Temperature Materials (U.S.A.) and was part of the same material used by Nagle in his experiments. Experimental results

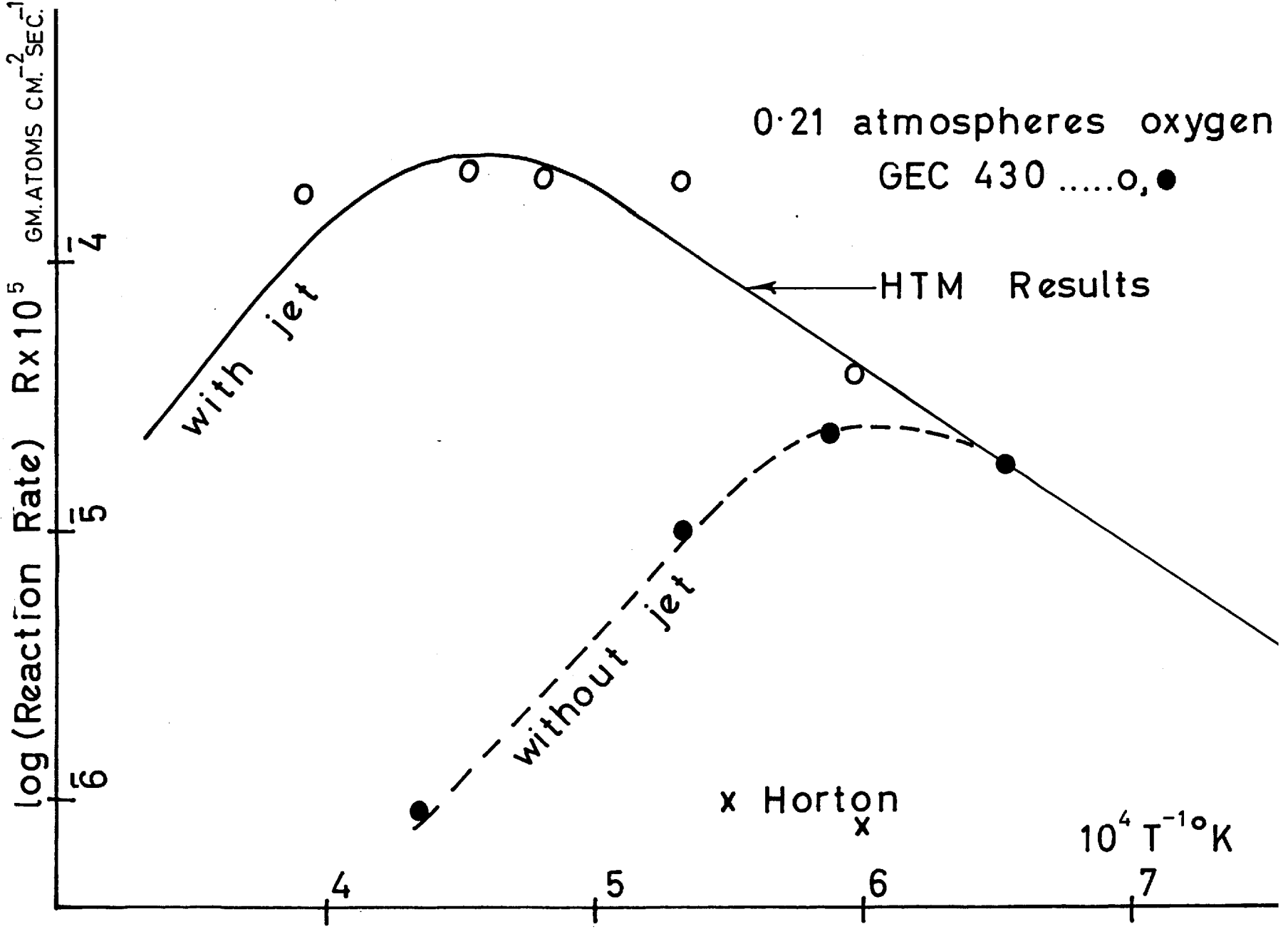

Fig4.2 OXIDATION OF PYROLYTIC GRAPHITE

were obtained for temperatures up to 2500°C and were found to be in substantial agreement with Nagle's work. The results are plotted in fig. 4.1. as the logarithm of the reaction rate ($R_g.at.cm^{-2}.sec^{-1}$) against the reciprocal of the absolute temperature ($10^4/T°K$).

Noticeably the experimental scatter is about the same magnitude as was observed by Nagle. However, when rates were measured above 1800°C they were found to be substantially smaller than those measured at 1800°C; so despite the experimental scatter the occurrence of a maximum and subsequent decrease of rates at higher temperatures was observed. It should be noted that the upper limit of Nagle's temperature range was 1900°C so the above trend was not then apparent.

4.4. Rates of reaction of pyrolytic graphite (G.E.C.).

The remaining quantity of HTM graphite was small so work was continued with material kindly made available by the General Electric Company (U.S.A.). Reaction rates were measured on this material (to be referred to as GEC 430) and were found to have substantially the same reactivity as the HTM sample. In fig. 4.2. the reaction rates of the GEC samples are represented

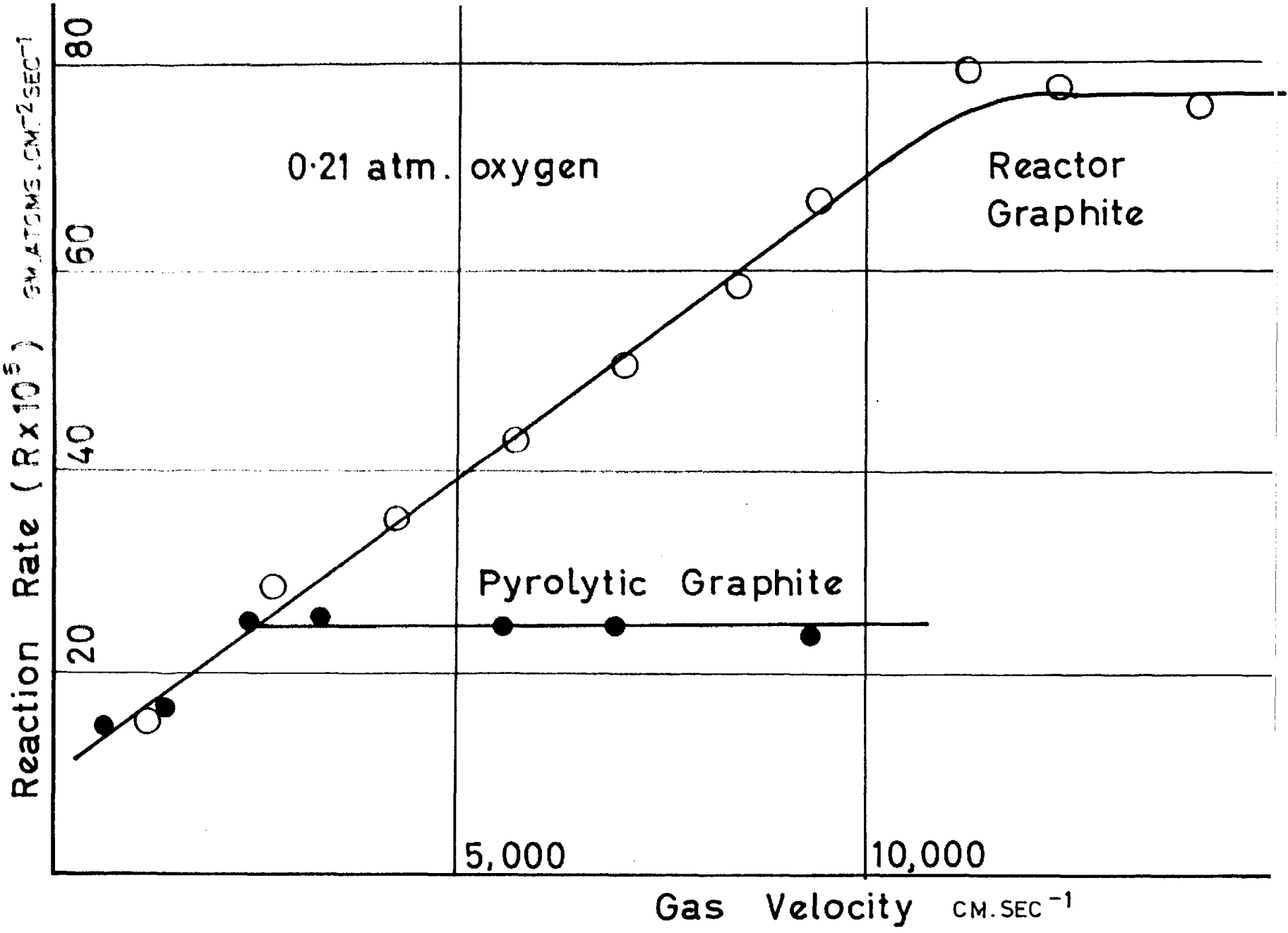

Fig.4.3 REACTION RATE - VELOCITY CURVE AT 1900°C

by circles and are compared with the rate-temperature curve (from fig. 4.1.) obtained with HTH graphite (using Nagle's technique).

4.5. The effect of gas velocity on reaction rates:-

Following this work, the reaction rate was determined as a function of the gas velocity in the jet over a wide range of velocities with (GEC 430) pyrolytic graphite: for comparison an additional curve was obtained with reactor graphite.

4.5.1. Pyrolytic graphite:-

Since the maximum reaction rate for pyrolytic graphite occurs at 1900°C (fig. 4.1.) the rate-velocity experiments were carried out at this temperature, the pressure being 0.21 atmospheres.

The results are given in Appendix 5 and are plotted in fig. 4.3. as the reaction rate $(R.10^5)$ g.at.cm.$^{-2}$ sec.$^{-1}$ against the gas velocity in cm.sec.$^{-1}$. The rates can be seen to be independent of the gas velocity when this exceeds 2500 cm.sec.$^{-1}$. Therefore above a gas velocity of 2500 cm.sec.$^{-1}$, the reaction rates of pyrolytic graphite are not limited by rates of mass transfer at 1900°C or at any other temperature, because

the maximum reaction rate was observed at 1900°C.

These results confirm Nagle's data obtained with pyrolytic graphite where rate measurements at a gas velocity of 1090 cm.sec.$^{-1}$ were not different from rate measurements made at 7000 cm.sec.$^{-1}$.

It is concluded, therefore, that a linear gas velocity of only 2500 cm.sec.$^{-1}$ is required to disperse the gaseous products; above this critical velocity the true chemical kinetics of reaction can be observed.

4.5.2. Reactor graphite:-

Nagle had argued that the system for the oxidation of reactor graphite was geometrically similar to that for pyrolytic graphite, and since the reactor graphite rates were very much higher than those of pyrolytic graphite, the latter could not be controlled by mass transfer.

The rate-velocity curve for reactor graphite was determined experimentally at 1900°C and 0.21 atmospheres of oxygen and was plotted with the pyrolytic graphite results on fig. 4.3. If this curve is compared with that for pyrolytic graphite, the two rates are found to coincide at low gas velocities.

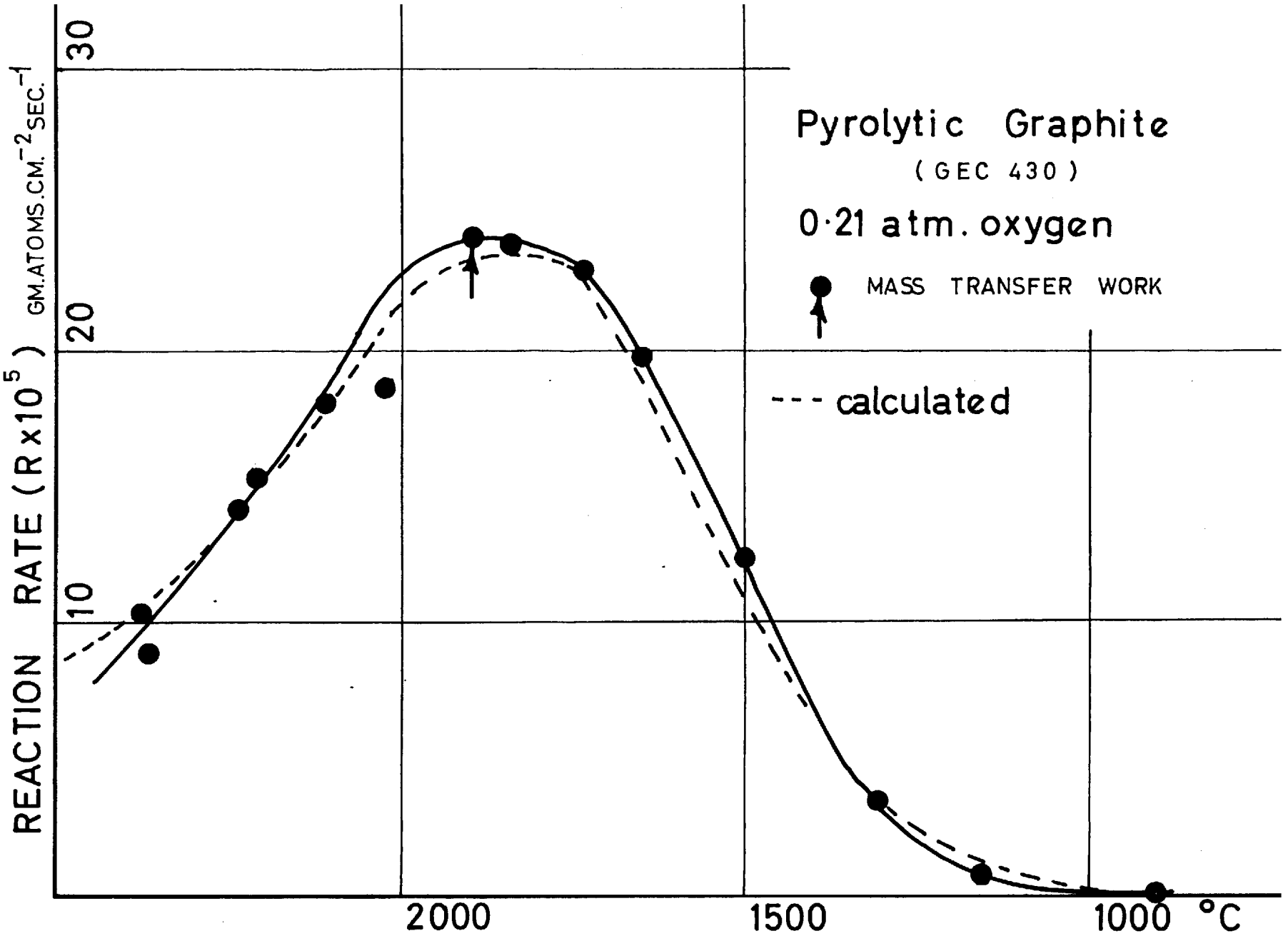

Fig.4.4 REACTION RATE - TEMPERATURE CURVE

However, the reactor graphite rates increase with the rise of gas velocity until the comparatively high velocity of 12,000 cm.sec.$^{-1}$ when a flattening of the curve is apparently obtained.

4.5.3. Conclusion:-

Therefore, in conclusion, the maximum reaction rate of pyrolytic graphite appeared not to be limited by mass transfer rates except at very low gas velocities. If the gas velocity exceeded 2500 cm.sec.$^{-1}$ the constant reaction rate achieved at 1900°C was 24×10^{-5} g.at.cm.$^{-2}$ sec.$^{-1}$.

4.6. Reaction rate temperature curve for pyrolytic graphite (GEC 430).

The above experiments were followed by a series of rate measurements between 1000°C and 2500°C on G.E.C. pyrolytic graphite. In each run the gas velocity was high enough to prevent mass transfer control of the reaction. The scatter in the results was much smaller than in previous work and can be contrasted with Nagle's technique which was used to obtain the results given in fig. 4.1. This comparison

demonstrates the superiority of the photographic technique, and in fact the curve could now be plotted on an arithmetic scale with a considerable degree of accuracy (fig. 4.4.). In this graph, the reaction rate $(R.10^5)$g.at.cm.$^{-2}$sec.$^{-1}$ is plotted against the temperature in ^{o}C. It will be seen that the reaction rate rises to a maximum at 1900^{o}C and falls to less than half the maximum rate when the temperature reaches 2500^{o}C. The reaction rate measured at 1900^{o}C in the experiment described in (section 4.5.) is found to lie at the peak of the curve.

4.7. Summary:-

1. The rate-temperature curve for the reaction of pyrolytic graphite with oxygen at 1/5th atmosphere pressure shows a pronounced maximum at 1900^{o}C.

2. In addition the results demonstrate a marked decrease in the reaction rates for temperatures above 1900^{o}C.

3. Therefore the phenomenon of a maximum reaction rate is not the result of mass transfer limitations; it is a chemical-kinetic effect comparable to that reported at very low pressures on graphite filaments.

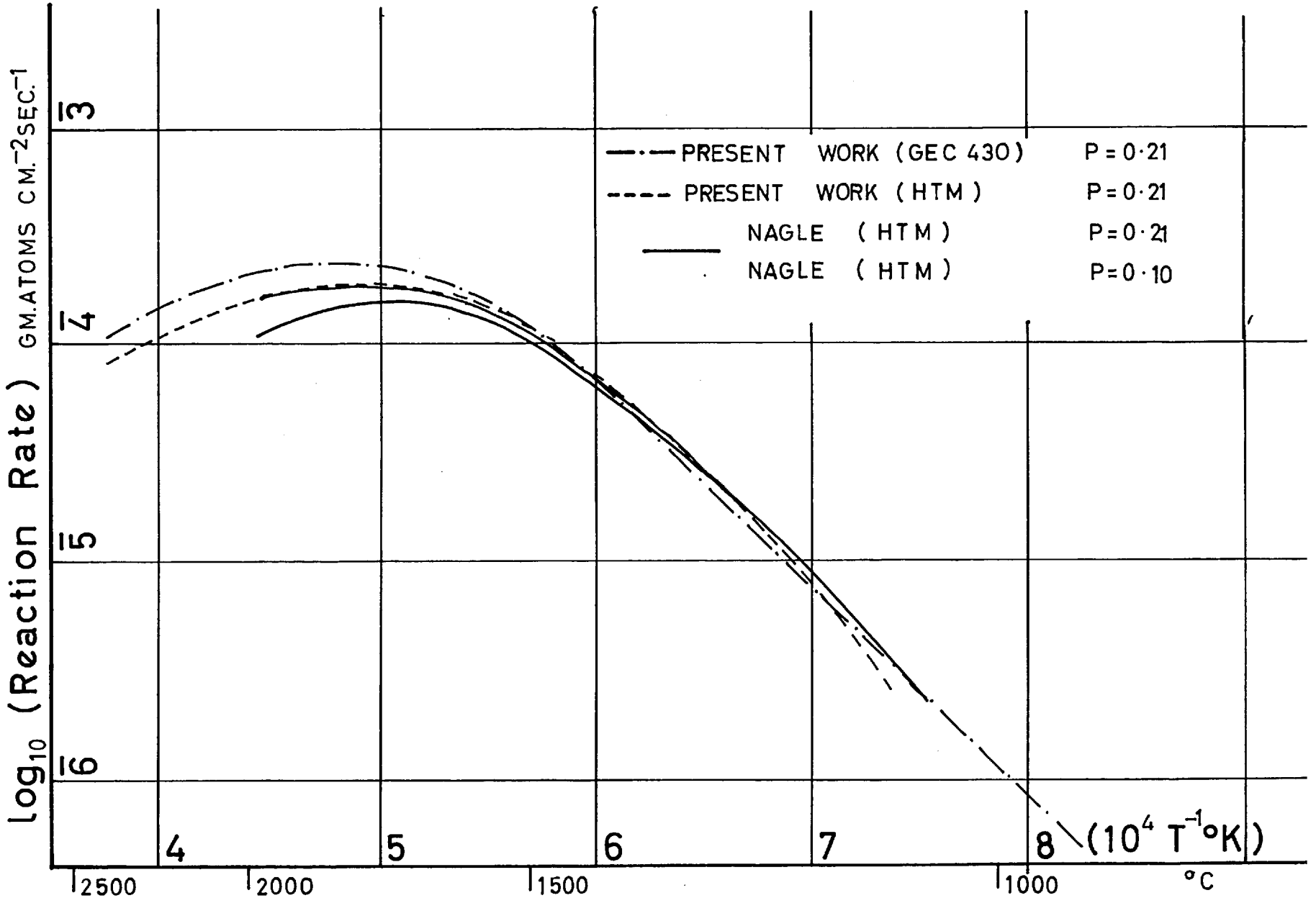

Fig.4.5 OXIDATION OF PYROLYTIC GRAPHITE

4.8.1. Comparison of four different rate-temperature curves obtained with pyrolytic graphite.

In fig. 4.5. four different rate-temperature curves are re-plotted, namely:-

(1) HTM results(Nagle) 0.20 atm at 1090 cm.sec.$^{-1}$.

(2) HTM results (Nagle)0.13 atm at 7000 cm.sec.$^{-1}$.

(3) HTM results (section 4.3) 0.21 atm at 7000 cm.sec.$^{-1}$.

(4) GEC results (section 4.6) 0.21 atm at 3500 cm.sec.$^{-1}$.

The results were obtained with two different pyrolitic graphites at different ambient pressures and gas flowrates by two independent experimenters using different techniques of measurement; but all four curves approximately coincide. This implies, first of all, that the two different experimental techniques are capable of giving the same results; secondly, that the reactivites of pyrolytic graphites from two different sources are the same.

4.8.2. Comparison of the present results with those published by Horton.

Horton has reported much lower reaction rates on H.T.M. graphite than those measured above: these were subsequently interpreted by him using the theory

of pore diffusion. However, as air was used, and not pure oxygen, it is more probable that low rates of gas-phase diffusion are responsible for the low activation energy and the smaller reaction rates.

In order to check this deduction, rate measurements were made in a stationary oxygen atmosphere, to find by how much the rate decreased (in fact the incoming stream of oxygen was directed away from the sample). The results are shown in fig. 4.2. by discs; they are seen to be larger than the rates measured by Horton (shown in fig. 4.2. by small crosses) but smaller than rates measured under flow conditions at all temperatures above 1300°C.

4.9. Overall rate equation:-

The theory of Strickland-Constable and Nagle which was reproduced in section 1.5. was originally proposed to represent the reactivity of all pure carbons at high temperatures. The rate equation can be rearranged to give:-

$$\text{Rate} = \frac{KA.KC.P}{(KA+KC.P)} \times \frac{KB.P}{(KT+KB.P)} + \frac{KB.KT.P}{(KT+KB.P)}$$

An estimate was made by Nagle of the individual rate

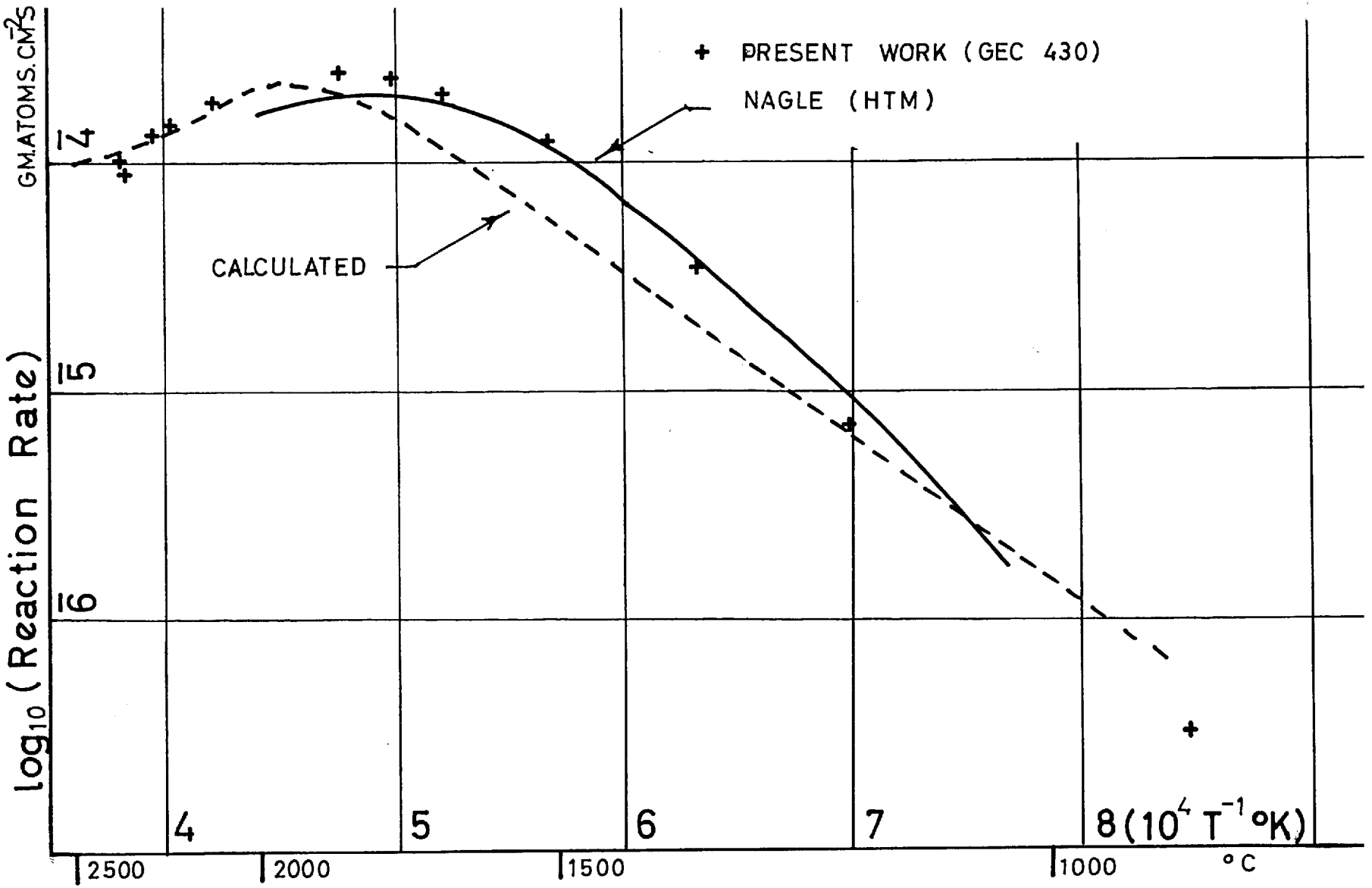

Fig.4.6 OXIDATION OF PYROLYTIC GRAPHITE

constants (KA, KC/KE, KB and KT). Therefore using these estimated values, a reaction-rate temperature curve was calculated at 0.21 atmospheres pressure and compared with the experimental curve for G.E.C. pyrolytic graphite (Table 4.2.) and with Nagle's results (fig. 4.6.) the calculated curve fitted the very high temperature results quite well and correctly predicted the rate decrease at high temperatures: however, it was apparent that the values of the individual rate constants (KA, KC, KE, KT, KB) were in need of correction to fit the more accurate rate-data now available. Consequently, new values of the constants were evaluated by fitting the rate equation to the filament results of Strickland-Constable and to the high pressure results obtained with G.E.C. pyrolitic graphite. The method of calculation is given in detail in Appendix 1.

From the new individual rate constants the reaction rate was calculated at several temperatures and plotted alongside the experimental results in fig.4.4. A close fit was obtained. In addition, the rate-temperature curve was calculated for a gas pressure of 2.5×10^{-5} atmospheres to compare the theoretical value with the published results of Strickland-Constable;

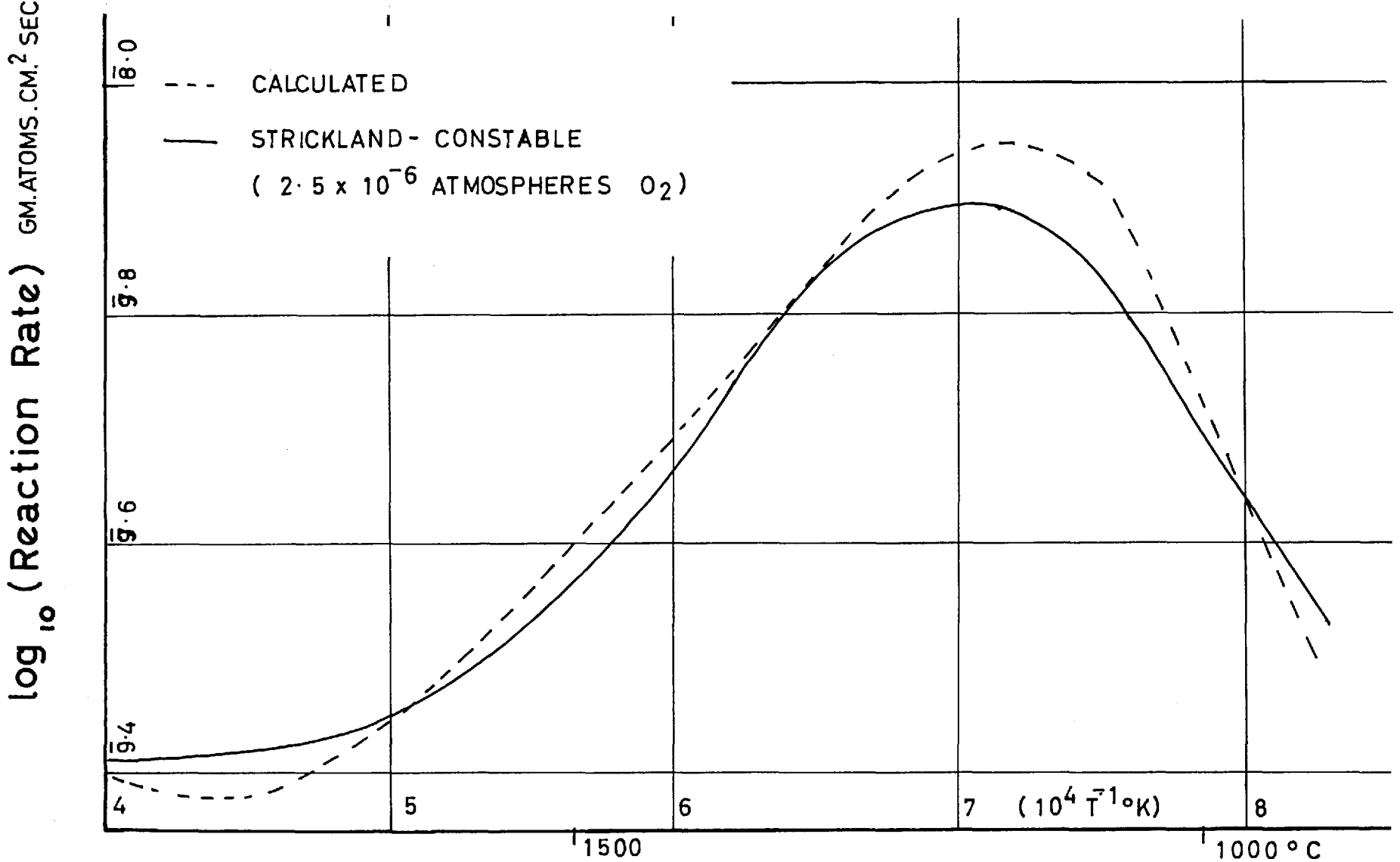

Fig. 4.7 COMPARISON WITH FILAMENT RESULTS

both curves are plotted in figure 4.7. and again the fit is good.

In addition, rates were calculated at several pressures at a constant reaction temperature. Three series of results were calculated in this way in the pressure range (0.1 - 1.0) atmospheres for the temperatures of 1400°C, 1900°C, 2500°K: these are plotted in fig. 4.8. on a logarithmic scale with the rate $(R.10^{-5})$g.at.cm.$^{-2}$sec.$^{-1}$ as a function of the gas pressure in atmospheres.

The slopes of these curves correspond to the reaction order at the particular temperature and pressure range. Hence it can be seen that the reaction is first order above the maximum rate (2,500°K curve); below the maximum the order changes rapidly from first to zero as the reaction pressure approaches one atmosphere (1400°C curve). Thus it is seen that the difference in the rate of reaction is small when measured at 0.21 atmospheres and at 0.13 atmospheres which may explain why the rates measured by Nagle and these two pressures are coincident (see section 4.8.).

4.10. <u>A study of the reaction order at 1900°C</u>.

In the pressure range 0.21 to 1.00 atmospheres

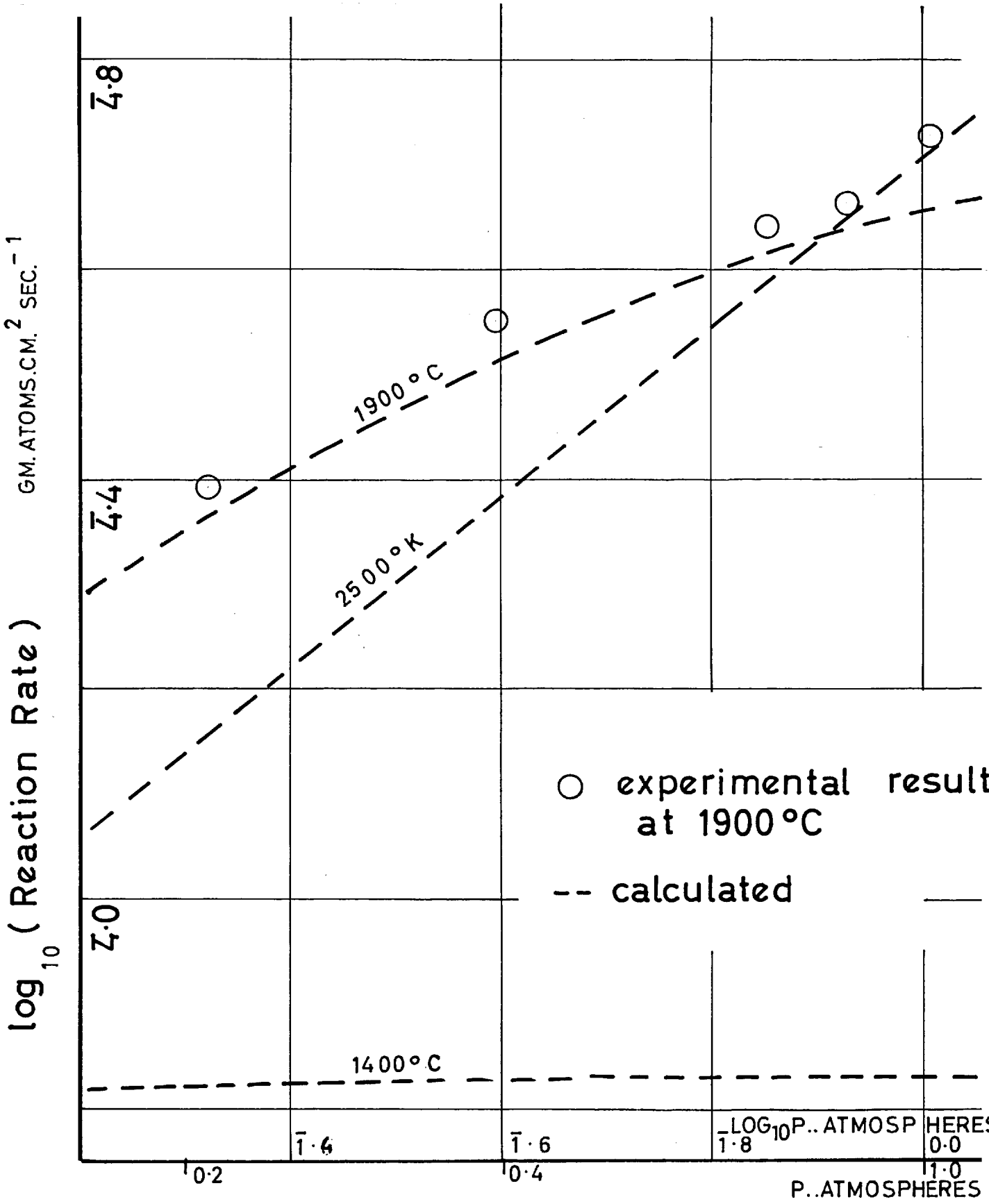

Fig.4.8 CALCULATED $LOG._{10}$ REACTION RATE $LOG._{10}$ PRESSURE CURVES

the order is practically constant at a particular temperature: for instance at 1400°C (1700°K) nearly zero order kinetics would be observed, whilst at 2200°C (2,500 °K) the order would be closer to first. At 1900°C (the temperature at which a maximum rate is measured) the slope of the calculated curve shown in fig. 4.8. is less than one and a fractional order would be expected.

To test this theoretical derivation against experimental evidence, rates of reaction for GEC 430 were measured at 1900°C using a high gas velocity at six oxygen pressures from 0.21 to 1.0 atmospheres. The results are given in Table 4.2. and are also plotted on the log (rate) - log (pressure) graph (Fig. 4.8.) as circles. The points fall close to the calculated curve for 1900°C and the mean slope indicates an "order" of reaction of 0.6 over the pressure range.

4.11. Conclusions:-

1. The rate of reaction of oxygen with pyrolytic graphite rises to a maximum at 1900°C and then falls as the temperature rises further. This fall in rate, which was shown by Nagle to be probably the case with reactor graphite, has now been shown to be quite certainly the

case with pyrolytic graphite.

2. It was shown that under the experimental conditions the rate was not under mass transfer control.

3. The fall in rate is in accordance with the predictions of the Strickland-Constable and Nagle theory for the oxidation of carbon above 1000°C.

4. The order of reaction at 1900°C has also been measured and found to be in accordance with the same theory.

Table 4.1.: Experimental results with G.E.C.430 pyrolytic graphite at 0.21 atmospheres pressure of oxygen.

$R \times 10^5$	$\log_{10} R$	T°K	$10^4/T°K$	Q l.min.$^{-1}$
0.03	$\bar{7}.477$	1180	8.48	2.85
0.69	$\bar{6}.839$	1430	6.99	2.73
3.4	$\bar{5}.532$	1580	6.33	2.80
12.3	$\bar{4}.090$	1770	5.65	2.65
19.7	$\bar{4}.295$	1920	5.21	2.75
22.8	$\bar{4}.358$	2010	4.98	2.86
23.7	$\bar{4}.375$	2110	4.74	2.75
24.2	$\bar{4}.393$	2170	4.61	..

18.5	$\bar{4}$.267	2290	4.37	2.90
18.0	$\bar{4}$.255	2380	4.20	2.90
15.2	$\bar{4}$.182	2480	4.03	2.62
14.0	$\bar{4}$.146	2510	3.98	2.75
8.9	$\bar{5}$.949	2640	3.79	2.70
10.3	$\bar{4}$.013	2650	3.77	2.75

Table 4.2. Experimental results with G.E.C.430 pyrolytic graphite at 1900°C and various pressures.

$Rx10^{-5}$	P(atm)	$Gl.min.^{-1}$	$\log_{10}R$	$\log_{10}P$
53.3	1.019	2.8	$\bar{4}$.727	0.008
46.1	0.851	3.03	$\bar{4}$.664	$\bar{1}$.930
43.6	0.712	2.59	$\bar{4}$.640	$\bar{1}$.853
37.6	0.553		$\bar{4}$.575	$\bar{1}$.743
35.5	0.395		4.550	$\bar{1}$.597

5. Reaction rates of carbon in the present of catalytic materials.

5.1. Introduction: The rate-temperature curve for the reaction between pyrolytic graphite and oxygen at normal pressures can be satisfactorally predicted by the theory of Strickland-Constable and Nagle. Reactor grade graphite gives a similar reaction curve under the same experimental conditions but the rates of reaction are of a much greater magnitude (x10).

The difference can be partially attributed to the higher porosity of the reactor graphite, for, although the reaction is confined to the vicinity of the external surface, limited penetration of the pores must take place. Therefore, although the intrinsic reaction rates may be the same, the extent of reaction in unit volume is greater for the more porous graphite.

Such a direct comparison of the graphites neglects the appreciable difference in the impurity level of the two graphites. Pyrolytic graphite by virtue of its method of preparation is extremely pure. The major requirement of reactor graphite however is mechanical strength and although the preparatory

materials are carefully chosen the impurity level is much higher than in pyrolytic graphite. A purer graphite is available for spectroscopic analysis using the carbon arc. In order to evaluate the possible catalytic effect of impurities at high temperatures the latter two graphites were reacted with oxygen under the same experimental conditions and their rates were compared. A typical analysis of the graphites is summarised below:-

	Spectroscopic Graphite.	Reactor Graphite.	Pyrolytic Graphite.
Ash ppm	1.03	100-300	0.1
Fe ppm	0.3	10	-
Bulk density $g.cm.^{-3}$.	1.46	1.76	2.20

At low reaction temperatures (below 1000°C) the presence of impurities has a marked effect on the reactivity of carbon and graphite as has been shown by many authors; in particular metallic impurities are known to be effective catalysts.

At high reaction temperatures little is known

of the catalytic effect of impurities because rates of mass transfer limit the reaction kinetics. In general it is to be expected that catalytic effects are less marked at high temperatures, for a catalyst provides alternative reaction mechanisms of lower activation energy; the reaction rates on catalysed sites will therefore increase more slowly with a rise in temperature than reaction rates on uncatalysed sites.

5.2. Effect of catalysis at high temperatures.

In contrast to the low temperature range, where many different materials have been found to be effective catalysts for the reaction between graphite and oxygen, at very high temperatures little or no data is available. Pyrolytic graphite, itself, has an extremely high purity level so it is unlikely that catalysis takes place through impurities in this material. However, it was not possible to exclude water vapour completely from the reaction vessel. On the other hand reactor graphite is far less pure: iron is the main impurity. Experiments were therefore arranged to investigate the effects of iron salts added to the graphite and water vapour added to the oxygen.

5.3. Reaction rates in the presence of water vapour.

In view of the apparent effect of water vapour[4.3] on the reaction rate at low temperatures, precautions were taken to dry the reacting gases throughout the experimental investigation. For this purpose the gas passed through a steel tower 8½ cms. in diameter and 70 cms. high, which was packed with silica gel: at a flowrate of 2 litres per minute the residence time was of the order of ten minutes. A small glass tube containing magnesium perchlorate was joined to this tower and both entrances to the drier were connected to smaller guard tubes also containing silica gel. It was estimated that the partial pressure of water vapour was reduced to the order of 0.002 mms.Hg, i.e. 3 ppm, by this technique.

Special experiments were also undertaken in which wet oxygen was used with reactor graphite at 1400°C and at a pressure of 0.21 atmospheres. Retreat measurements were obtained using the travelling microscope technique and the results were compared with those previously obtained with dry oxygen. The saturation was effected by passing the gas stream at atmospheric pressure through a sintered glass disc, which supported a column

of water at 20°C. The partial pressure of water vapour at 20°C is 17.5 mm.Hg, which represents a concentration of 23,000 ppm water in the reacting gases.

Two series of rate measurements were obtained with both wet and dry gas at 1400°C and 0.21 atmospheres of oxygen, as shown in table 5.1. Gas velocities were chosen to prevent mass transfer controlling the overall reaction. There was no significant difference between the means and it is concluded therefore that the presence of water vapour has no significant effect on the reaction rates for concentrations between 3 and 23,000 ppm.

Table 5.1.: Reaction rate of reactor graphite at 1400°C with oxygen, containing different amounts of water vapour.

Run No.	3 ppm H_2O	23,000 ppm H_2O
1	74.6	122.0
2	82.8	88.9
3	79.5	101.0
4	97.9	85.9
5	90.5	115.0
6	90.5	90.5
7	88.0	85.0
8	120.0	97.2
9	83.1	107.0
10	89.5	80.0
11	121.0	117.0
12	94.6	109.0
13	91.0	97.5
14	107.0	107.0
15	93.6	96.2
16	119.0	86.7
17	112.0	-
18	109.0	-
19	99.9	-
20	95.9	-

	3 ppm H_2O	23,000 ppm H_2O
Mean rate	94	95
Standard deviation	9.2	9.4

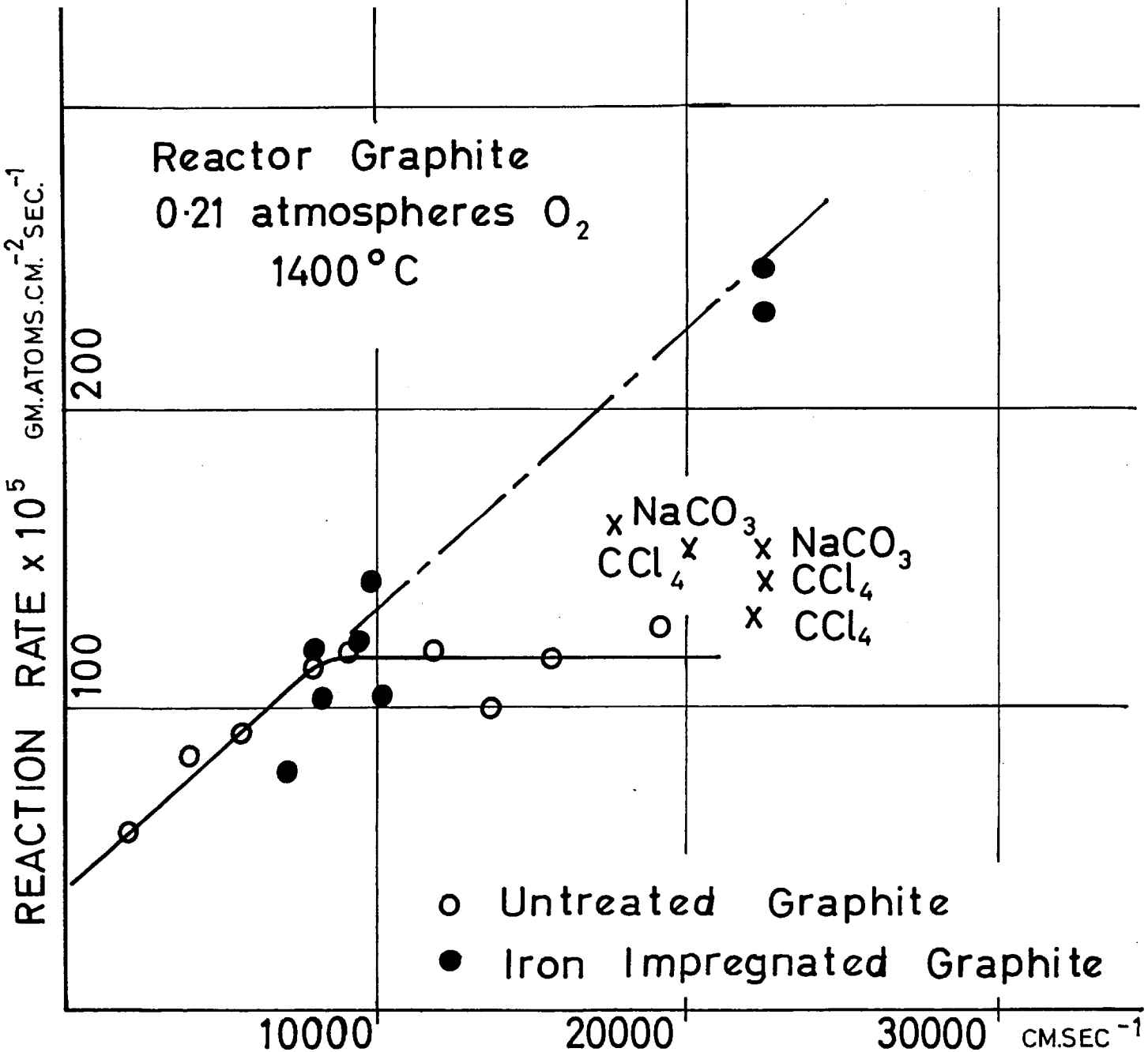

Fig.5.1 REACTION RATE - GAS VELOCITY CURVE

5.4. Reaction rates for reactor graphite impregnated with iron.

The porous graphite was impregnated with ferric nitrate nona-hydrate by heating the salt until a solution was formed (circa 50°C) and then soaking prepared samples of the reactor graphite in this solution for several hours. The samples were dried in an atmospnere of nitrogen and heated to above 1000°C in an electric furnace for several hours: this treatment reduced the salt to metallic iron. It was estimated by weight difference that up to 5% i.e. 50,000 ppm iron was present in the graphite. A section of the graphite was cut and this revealed that iron was evenly distributed throughout the inner pores.

The experimental results are given in Table 5.2. and are plotted on a rate-velocity graph figure 5.1. as the reaction rate $(R.10^5)$ g.at.cm.$^{-2}$sec.$^{-1}$ against the gas flow rate (Q)l min.$^{-1}$ Samples impregnated with iron are represented on the graph by discs, and are compared with results obtained with untreated graphite which are represented by circles. At a gas flowrate of 11.5 l.min.$^{-1}$ (22,500 cm.sec.$^{-1}$) the reaction rate of impregnated samples was twice the rate of untreated

graphite; but at 5.1 $min.^{-1}$ (8000 $cm.sec.^{-1}$) both sets of results are about equal. Therefore the above results indicate that the iron-impregnated graphite reacts faster than untreated graphite, but the full catalytic effect of the iron cannot be assessed because the increased reaction rate was probably limited by rates of mass transfer. Alternatively, so much graphite was used in the reduction of the iron nitrate (deposited in the pores) that the porosity of the reactor graphite was significantly increased: consequently the volumetric reaction rate was increased. A similar effect of porosity was observed in the comparison between reactor and spectroscopic graphite results (see section 5.8).

5.5. Reaction rates for reactor graphite soaked in carbon tetrachloride.

Some reactor graphite was soaked in carbon tetrachloride and immediately oxidised at a high gas flowrate: these results are indicated by small crosses on figure 5.1. However, the above treatment did not appear to affect the reaction rates.

5.6. Reaction rates for reactor graphite impregnated with sodium carbonate.

The graphite samples were covered with sodium carbonate powder and placed in an electric furnace. On heating to 840°C in an atmosphere of nitrogen the salt fused and penetrated into the pores of the graphite. The rates of reaction on this treated graphite, however, did not differ appreciably from raw graphite results. These results are also indicated in fig. 5.1. by small crosses.

Results: Table 5.2.

Slope of graph(s)	cms. frame^{-1}
Magnification	15.3/5 on projection
	10.5/1 on photographing
Framing rate	1.94 sec. frame^{-1}
Molecular weight	12
Density (bulk)	1.76 g.cm.$^{-3}$

$$\therefore \text{Rate} = \frac{S}{1.94} \times \frac{1}{32.15} \times \frac{1.76}{12} = 2.35 \times 10^{-3} S \quad \text{g.at.cm.}^{-2}\text{sec.}^{-1}$$

Slope	R x 10^5	Q l.min.	Impregnated with
0.344	80.0	3.72	Fe
0.520	122	4.16	Fe
0.452	106	4.28	Fe
0.610	143	5.10	Fe
0.514	121	4.85	Fe
0.445	105	5.31	Fe
0.987	232	11.7	Fe
1.051	247	11.7	Fe
0.612	144	11.5	C Cl 4
0.555	130	11.3	C Cl 4
0.655	154	10.5	C Cl 4
0.655	154	11.5	$NaCO_3$
0.690	162	9.3	$NaCO_3$

5.7. Reaction rates for spectroscopically-pure graphite.

The rates of reaction of spectroscopic graphite and reactor-grade graphite were compared. The impurity contents of these materials are as follows:-

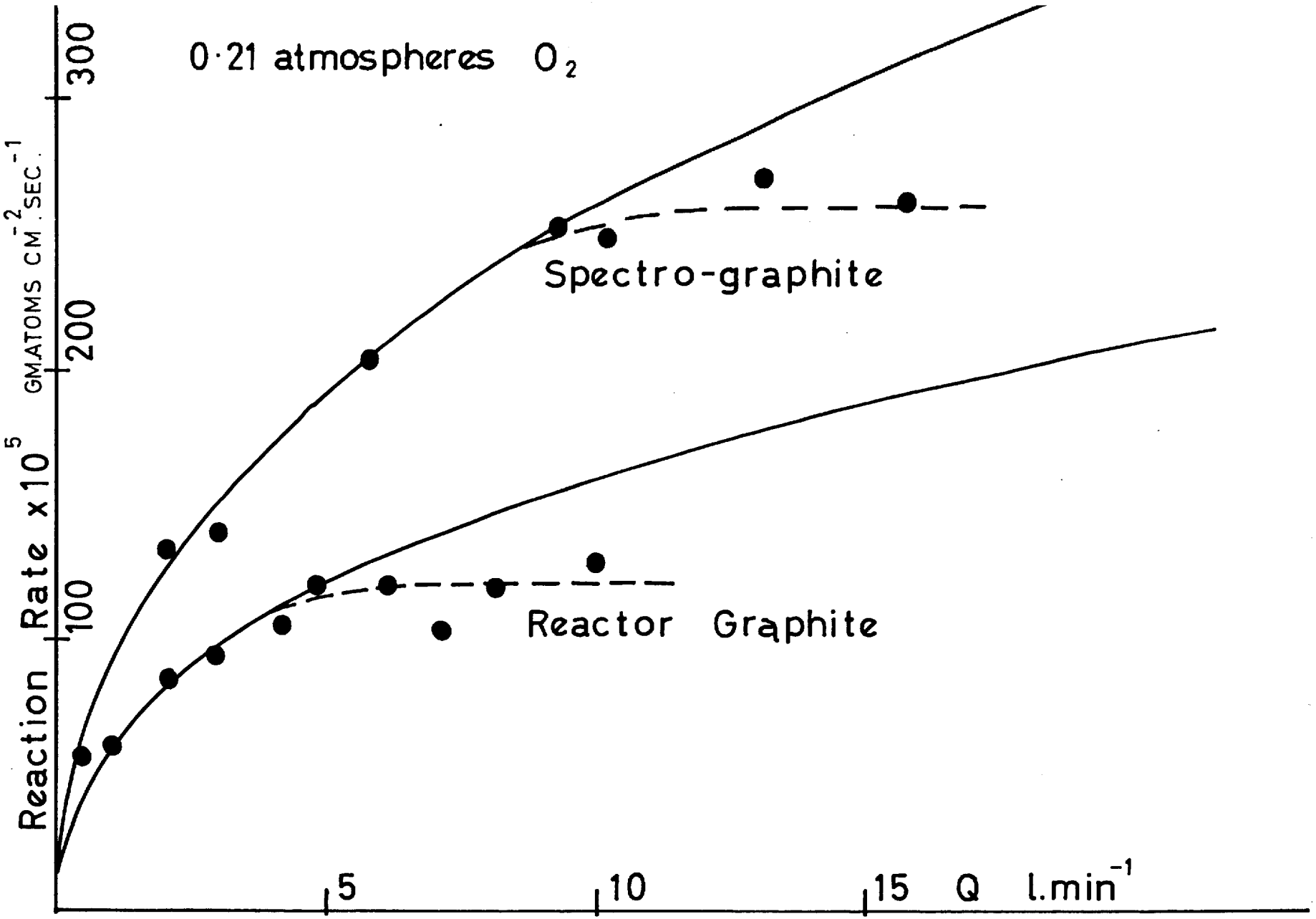

Fig.5.2 REACTION RATE - GAS FLOWRATE CURVES (1400°C)

IMPURITY	SPECTROSCOPIC GRAPHITE.	REACTOR GRAPHITE
Fe ppm	0.3	10
Ca ppm	0.1	15
Sr ppm	0.00	15
Na ppm	0.00	2
V ppm	0.00	10
Si ppm	0.3	-
Al ppm	0.2	< 1
Cu ppm	0.05	< 1
Mg ppm	0.05	< 1
Ti ppm	0.03	< 1
Total ash ppm	1.03	100 - 300

It was anticipated that a significant difference in rate might result from the almost total elimination of inorganic impurities in the case of the spectroscopic graphite. The results were plotted as the reaction rate $(R.10^5)$ gat.cm.$^{-2}$sec.$^{-1}$ against the gas flowrate fig. 5.2. and a table of the results is given below. Contrary to expectations the reactor graphite had only 45% of the reactivity of the purer material. However this

anomolous behaviour can be attributed to the lower porosity of the reactor graphite.

Spectro-graphite		Reactor-Graphite	
Rate x 10^5	Q $l.min.^{-1}$	Rate x 10^5	Q $l.m^{-1}$
55.5	0.5	60	1.04
133	2.04	85	2.08
139	3.0	93	2.94
203	5.8	114	4.18
252	9.3	120	4.79
248	10.2	120	6.12
271	13.1	102	7.12
262	15.75	118	8.12
		128	9.97

5.8. Analysis of the reaction-rate dependence on the gas velocity for spectroscopic and reactor graphites.

A mathematical analysis was sought for both the reactor graphite and spectro-graphite rate-velocity curves obtained at 1400°C. Both sets of results can be analysed simultaneously because the values of (K_g) were identical for both curves so that the differences between them

resulted solely from the different reactivities of the two materials.

If either a first or half-order was assumed for (m) it was shown that the value of (K_G) depended initially on the square root of the gas flowrate (Q). The rate-velocity equations according to this analysis are shown on graph 5.2 by the full lines. However it was not found possible to account analytically for the velocity-independent results shown by broken lines. Therefore it was concluded that the assumptions made in the analysis were probably unjustified and it is suggested that:-

a) (m) must vary appreciably according to the surface oxygen concentration (Ci) as suggested by the Nagle and Strickland-Constable mechanism. Consequently an analytic solution of the rate-velocity curve becomes very difficult to solve in the case of porous graphites, except for a constant first-order reaction. In this special case the mass transfer process is first order, the true reaction order is first and the 'apparent' order under pore diffusion is also first. However, experimental evidence has shown that the order for graphite oxidation is less

than first and will vary therefore according to different conditions of flow.

b) the power of the velocity, on which the value of (K_G) depends, may undergo a change at the critical velocity. For instance it is conceivable that at a critical Reynold's number the boundary layer can suddenly change from laminar into turbulent flow as in the case of a pipe. However, in apparent contradiction it is noted that the critical flow-rate for the spectro-scopic and reactor graphite curves are quite different although the two systems were geometrically similar.

Therefore at this stage of the work the rate-velocity curves for porous graphites could not be interpreted analytically because the progress of the reaction was too complex to be fully understood. All that can be said with certainty is that above the critical velocity the reaction rates are not affected by the rates of boundary-layer diffusion but are controlled by the rate of in-pore diffusion.

6. The reaction of reactor graphite with carbon dioxide at high temperatures.

6.1. Introduction:-

Experiments showing the reaction between graphite and carbon dioxide at low pressures and high temperatures have been described by several authors. As discussed earlier, the reaction-rate temperature curve shows similar characteristics to that for the reaction between oxygen and graphite at high temperatures.

To investigate the carbon dioxide reaction at high temperatures, it is necessary to consider the possible dissociation of the carbon dioxide before the gas reaches the graphite surface:-

$$CO_2 \rightleftharpoons CO + \frac{1}{2} O_2$$

Calculations based upon equilibrium data are given in Appendix 3. A one percent dissociation is given at 1550°C and 10% dissociation at 2150°C.

If appreciable amounts of oxygen are formed in this way, it was anticipated that the reaction rate observed would be at any rate partly that of oxygen and carbon, rather than carbon dioxide and carbon. To avoid this situation, 30% of carbon monoxide was added

to the carbon dioxide which would reduce the percentage of oxygen below 1% for all temperatures below 2150°C.

Calculations on which this estimate is based are given in Appendix 3.

6.2. Experimental:-

A convenient pressure to use was slightly above 1 atmosphere, for this prevented the ingress of air into the vessel. As the rate of reaction was low, rates of mass transfer did not limit the overall reaction rate. A glass mixing chamber was constructed for mixing the gases before they passed to the jet. In addition the backflow of the gases was prevented. Before an experiment was commenced, a rapid flow of gas was passed through the reaction vessel for fifteen minutes: this reduced the residual oxygen concentration in the reaction vessel to a very low level. The flow of the gases was metered on separate capillary flowmeters and adjusted to give a 30% concentration of carbon monoxide in the gas stream.

6.3. Results:-

The experimental results are given in Table 6.1.

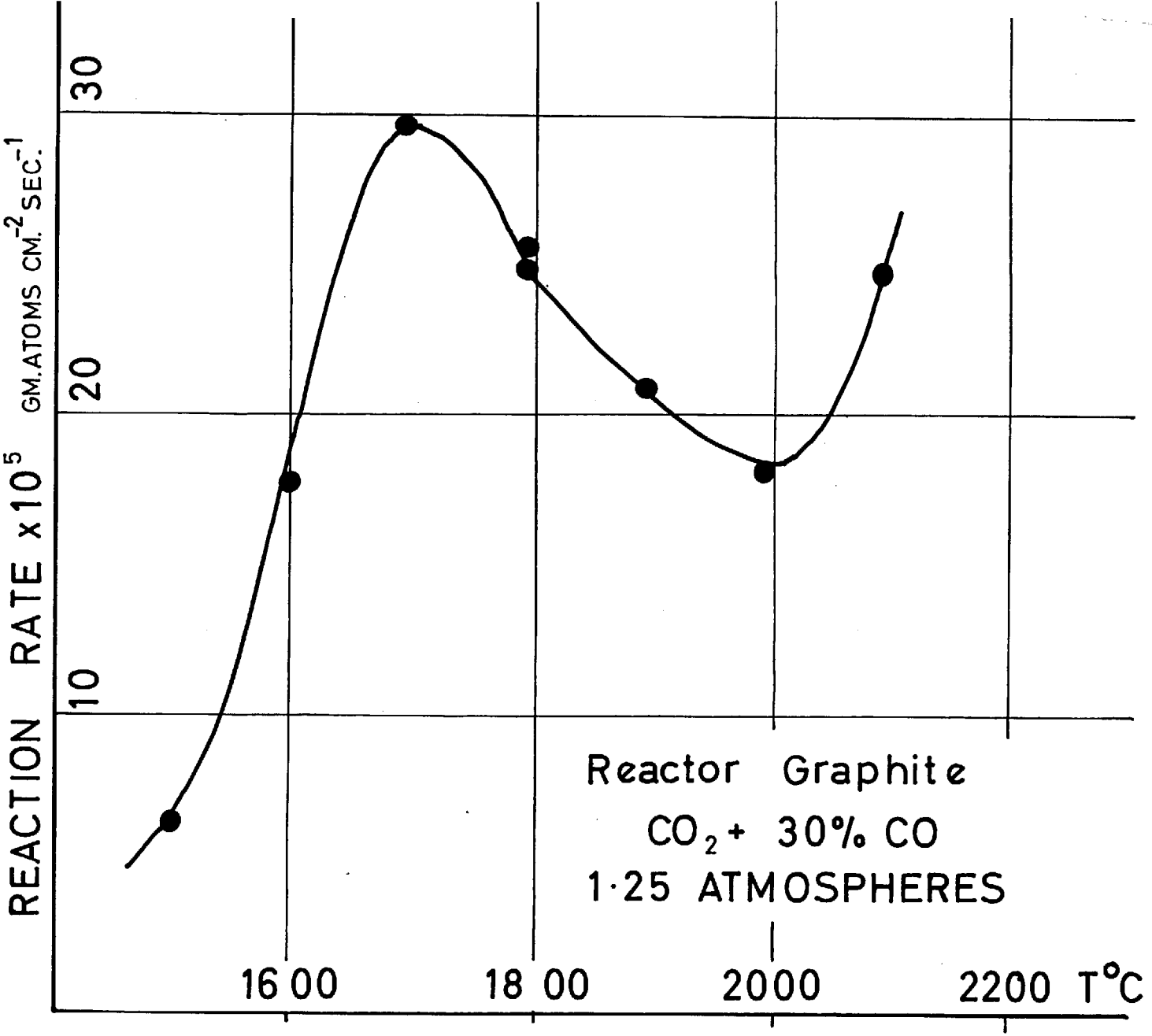

Fig.6.1 REACTION RATE-TEMP. CURVE WITH CO_2

and are plotted in fig. 6.1 as the reaction rate (R g.at.cm.$^{-2}$sec.$^{-1}$ x 10^{-5}) against temperature (^{o}C). A maximum rate of reaction was observed at 1700^{o}C and the similarities with the oxygen results can be clearly seen. One noticeable difference is the further increase of the reaction rate above 2000^{o}C as the temperature increases. This effect was attributed to the partial dissociation of carbon dioxide at this high temperature which now becomes appreciable in spite of the added carbon monoxide.

Two results with pyrolytic graphite gave the much smaller reaction rates of 4.9 x 10^{-5}g.at.cm.$^{-2}$sec.$^{-1}$: these were too small for a complete curve to be satisfactorily obtained using the ciné-technique.

6.4. Reaction of spectroscopically pure graphite at 2100^{o}C. with carbon dioxide in the presence of a varying quantity of carbon monoxide.

In section 6.1. it was shown that the dissociation of carbon dioxide at high temperatures can be suppressed by the presence of carbon monoxide. For this reason, a gas mixture of 30% carbon monoxide to 70% carbon dioxide was used. At 2100^{o}C the reaction rate-temperature

curve showed a positive temperature coefficient as can be seen in fig. 6.1. This was attributed to an increased quantity of oxygen produced by the carbon dioxide dissociation; but this assumption needed a fuller investigation.

Therefore some reaction rates with spectroscopic graphite were measured at a constant pressure (in excess of 1 atmosphere) at a temperature of 2100°C and the CO/CO_2 ratio was varied. Spectroscopic graphite was used in preference to reactor graphite because of its higher reactivity. Results are presented in table 6.2. and it can be seen that the rate of reaction falls with the increase in the CO concentration. However, the rate did not become independent of the carbon monoxide concentration as would be expected from the above discussion.

In view of the complexity of the problem, involving several chemical reactions and in-pore mass transfer effects, no clear interpretation of the results could be formed at this stage.

Table 6.1. Reaction between reactor graphite and carbon dioxide (plus 30% carbon monoxide) at 1.20 atmospheres total pressure.

slope (s)	R x 10^5	T°C
0.1062	24.9	2100
0.0778	18.3	2000
0.0895	21.0	1900
0.1065	25.0	1800
0.1095	25.7	1800
0.1265	29.75	1700
0.0764	17.95	1600
0.0273	6.42	1500

Table 6.2. Reaction between spectro-scopic graphite and carbon dioxide with varying quantities of carbon monoxide at 2100°C.

slope (s)	R x 10^5	pCO/pCO_2	% O_2 equilibrium
0.289	56.3	0	4.5
0.157	30.7	0.632	0.18
0.109	21.3	1.100	0.03
0.319	62.1	0	4.5

7. Discussion.

7.1. Summary of the main experimental results.

1. The rate temperature curve for the reaction of pyrolytic graphite with oxygen (at 1/5th of an atmosphere pressure) was determined for temperatures between 1000 and 2500°C using gas velocities in excess of 2,500 cm.sec.$^{-1}$ The curve rose to a maximum at 1900°C and fell to half the maximum value as the temperature was increased further.

2. The reaction rate of pyrolytic graphite was determined for several gas velocities at 1900°C. Above 2500 cm.sec.$^{-1}$ the reaction rate was found to be independent of the gas velocity: thus it was shown that reaction rates were not under mass transfer control at the curve maximum described above or indeed at any temperature of reaction.

3. Two pyrolytic graphites from different sources gave identical reaction rates.

These results were shown to be in accordance with the theory of Strickland-Constable and Nagle.

The order of reaction was also measured

(at 1900°C) and was found to be in agreement with the same theory.

4. A maximum rate was observed when reactor graphite was oxidised in air but reaction rates were shown to be partly mass transfer controlled. A maximum was also observed in the much slower reaction of reactor graphite with carbon dioxide. Therefore the maximum phenomenon may be a common factor for gaseous reactions with most graphites at high temperatures.

5. In certain experiments water vapour was added to the oxygen and in others the reactor graphite was impregnated with salts (Na_2CO_3 and $Fe(NO_3)_3$); but only the presence of the iron salt caused any appreciable change in the rate of oxidation at 1400°C. (A two-fold rate increase was measured when the gas velocity was very high).

From these experiments catalytic effects seemed to be relatively unimportant when compared to their effects, reported in the literature, at much lower reaction temperatures: for a further comparison

a rate-velocity curve was obtained using spectroscopically pure graphite. Rather suprisingly the reactivity of the spectroscopic graphite was found to be higher than that of reactor graphite, but this was attributed to the different porosities of the two graphites.

7.2. Kinetics of oxidation of carbon at high temperatures: explanations given in the literature for the maximum rate phenomenon.

In the literature dealing with the oxidation kinetics of carbon at high temperatures no comprehensive theory of the reaction kinetics has been universally accepted. This situation reflects upon the complex nature of the reaction mechanism because in recent years the oxidation of graphite has been the subject of an intensive research effort on account of its technological importance.

In the past the inconsistancy of the results obtained with graphite has been attributed to different degrees of:-

a) mass transfer participation in the overall reaction

b) catalytic effects of impurities

c) graphitisation of the carbon.

In the present work graphite of very low porosity and high purity has been used, namely pyrolytic graphite. Catalytic effects were therefore unimportant and it has been shown that rates of mass transfer did not control the reaction kinetics at any temperature under the particular experimental conditions used.

In fact the behaviour of the true surface chemical kinetics was indicated by the experimental rate measurements. Moreover a rate-temperature curve has been experimentally determined at normal pressures with a maximum at 1900°C.

The shape of the curve corresponds with reported results obtained at very low pressures with carbon filaments. Such an unusual result observed at two widely different pressures is strong evidence of a common reaction mechanism which is probably the same for the oxidation of all pure graphites at high temperatures. The reaction theory proposed by Nagle and Strickland-Constable predicted the nature of the curve quite well and was further confirmed by experimental measurement of the reaction order at 1900°C.

Several other explanations have been given in the literature to explain the maximum in the rate-temperature curve of the filament results. Most of these are criticisms of the experimental methods used in the filament work and they will now be reconsidered as a means of explaining the maximum when it is observed at normal gas pressures. As opposed to the criticisms of the experimental technique, two rate mechanisms have

been proposed namely that of Blyholder, Binford and Eyring and that of Strickland-Constable and Nagle.

Finally an attempt to interpret the physical significance of individual constants in the overall rate equation will be made. In addition the equation will be used to predict reaction rates below 1000 ^{o}C, which is outside the experimental temperature range of both the present and the filament results, in order to compare the predicted values with those published for pure graphite specimens.

Criticisms of the experimental methods:

7.2.1. Rate limitations are caused by a limited collision rate.

A gas-solid reaction must be ultimately limited by the number of collisions that a gas molecule makes with the surface, so that a limit in the rate-temperature curve is obtained when the collision rate equals the reaction rate. This ultimate rate $(\hat{R})$ can be calculated from the kinetic theory of gases to give:-

$$\hat{R} = \frac{29.5P}{\sqrt{MT}}$$

where (M) is the molecular weight of the gas, (T) the absolute temperature (^{o}K) and (P) the gas pressure in atmospheres. For oxygen at a temperature of 1900 ^{o}C and a pressure of 0.21 atmospheres:-

$$\hat{R} = 2350 \times 10^{-5} \text{ g.at.cm.}^{-2}\text{sec.}^{-1}$$

The experimental maximum-rate for pyrolytic graphite (at 1900 ^{o}C) was 24×10^{-5} g.at.cm.$^{-2}$sec.$^{-1}$ and therefore only 1% of the theoretical number of collisions need result in chemical reaction.

The theoretical collision rate $(\hat{R})$ is inversely

proportional to the square root of the absolute temperature and so the rate will be expected to decrease above the maximum rate. This effect would produce the maximum phenomenon but the decrease in the experimental reaction rate (R) was much larger than can be predicted by the collision theory:-

$T^{\circ}C$	$R \times 10^5$	$\hat{R} \times 10^5 \sqrt{T/T}$
1900	24	24
2400	10	21.6

Therefore it appears that the reaction is not limited by the number of collisions of oxygen molecules with the surface.

7.2.2. Rate limitations by rates of mass transfer.

When the reaction rate is very rapid the graphite surface is shrouded by gaseous reaction products and the reaction rate is controlled by the speed with which fresh oxygen can penetrate this stagnant boundary layer. In the oxidation of pyrolytic graphite the rate-velocity data obtained at 1900°C showed that the maximum reaction rate was not limited by rates of mass transfer. Consequently, the observed reaction kinetics of pyrolytic

graphite oxidation cannot be accounted for by either of the above physical limitations.

7.2.3. The effect of unheated gas on the reaction rate.

Meyer and Gomar[e.3.] suggest that when a cold gas reacts with a hot filament the thermal accommodation coefficient (α) is less than unity and decreases as the temperature increases. If (t_o) is the gas temperature, (t_i) the filament temperature and (t_r) the desorbed-gas temperature then:-

$$\alpha = \frac{t_r - t_o}{t_i - t_o} = \frac{\text{energy interchange}}{\text{total possible interchange}}.$$

According to this argument the gas will desorb when the energy interchange is large enough to overcome Van der Waal's force (of adsorption): the force is constant and independent of the filament temperature, provided that $(t_i) \geq (t_r)$. Consequently at very high temperatures, the gas molecules will tend to desorb before reaction has taken place and a maximum in the rate-temperature curve will be produced.

The argument is valid at low gas pressures when the gas-phase collisions are rare. However, at normal pressures, multiple gas-phase collisions near to the solid

surface could be expected to raise the temperature of the gas to that of the solid before collision with the surface took place.

Nonetheless it would have been desirable to determine whether or not a pre-heated gas would give an increase in the reaction rate at normal pressures. However very considerable experimental difficulties were foreseen, and the experiment has not been attempted successfully.

Preheating of the gas has been reported by Day and Walker[g.2] to have no effect on the reaction rate: this view was supported also by Kuchta, Kant and Damon[g.3] in their experiments. However it is possible in these cases that mass transfer effects were controlling the reaction rate; preheating of the gas would not then materially affect the overall reaction rate.

In the present work the effect of preheating on the reaction rate can probably be estimated from the rate-velocity data (fig. 4.3). Above the critical velocity, the reaction rate is found to remain approximately constant, despite the fact that with the increase of velocity the gas layer at the surface is cooler. Consequently, it is probable that the rate of reaction

for a given surface temperature is independent of whether the gas is hot or cold.

Perhaps this conclusion is not too difficult to accept because reaction can only take place after the oxygen has been adsorbed by the graphite, by which time thermal accommodation of the molecule with the surface has taken place; this point is discussed later. Moreover as the reaction rate at normal pressures is apparently of zero order over much of the temperature range the rate of adsorption of oxygen onto the graphite is comparatively rapid and would not limit the reaction rate.

7.3. Proposal of a rate mechanism to explain the high temperature reaction kinetics of carbon oxidation.

It is very difficult to explain the high temperature results of carbon oxidation without postulating the existence of two different reactive sites in a graphite surface (for the purpose of this discussion they will be called A- and B-sites.) This proposal was first given by Blyholder, Binford and Eyring[e.2] in order to explain the low pressure filament results (see Appendix 5).

At this time no maximum had been reported at normal gas pressures so Blyholder, Binford and Eyring were led to believe that the reaction of a gas with pure graphite was a B-site reaction which was of zero order with a large activation energy. Otherwise it was proposed that the reaction was catalysed by impurities to give a different reaction rate: this reaction took place on A-sites, was first order, with a much lower activation energy.

Therefore Eyring assumed that the carbon filaments were specimens of impure graphite so that at low temperatures an A-site rate was observed: at higher temperatures the catalytic impurity evaporated from an

A-site which then became a B-site so that for a certain temperature range the overall rate appeared to show a negative temperature coefficient.

However in the present work only pyrolytic graphite samples were used. This is one of the purest forms of carbon available and it seems unlikely that a catalytic A-site reaction is a possibility. Moreover the B-site reaction cannot be considered to be zero order in view of the normal pressure results. Therefore a different mechanism was proposed for the A- and B-site reactions by Nagle and Strickland-Constable as outlined below. This was found to agree with the present results and with those at low pressures.

7.3.1. Annealing of reactive sites: Theory of Nagle and Strickland-Constable.

According to the rate mechanism of Nagle and Strickland-Constable, all carbon atoms in the graphite crystal are regarded as B-sites in the virgin material. However, during the reaction, it is considered that the crystal structure at the surface is disrupted so that a more reactive site is produced (A-site).

At low temperatures of reaction all the surface atoms are A-sites; but at high reaction temperatures the A-site atoms are able to migrate over the surface to more stable lattice positions and become B-sites. By this process of annealing, the reactivity of the graphite decreases and for a certain temperature range the overall rate equation has a negative temperature coefficient (maximum phenomenon).

At a constant temperature a steady reaction rate is achieved when the rate of creation of (A) sites equals the rate of annealing of (A) sites. Consequently the steady-state reaction rate is independent of the previous thermal history of the sample. Thus all graphites are expected to have similar surface reactivities at high temperatures when annealing can take place. In fact in the present work two different pyrolytic graphites were found to have identical reaction rates.

In further support of the Nagle and Strickland-Constable mechanism it can be shown that the maximum in the rate-temperature curve must be dependent on the gas pressure. In the present work a maximum occurred at 1900 ^{o}C but in the reported filament results a maximum was observed at about 1400 ^{o}C.

7.4. Predictions based on the Nagle and Strickland-Constable theory.

The accuracy of each individual reaction constant must be considered in relation to the assumptions made in the curve fitting. By comparing the revised rate constants to Nagle's original constants the variability in magnitude can be seen more clearly. A table of comparison is presented below and a visual comparison can be made on graph A.1.

	K_0	Q	K_0 NAGLE	Q NAGLE
K_B	3.83×10^{-3}	21,000	4.46×10^{-3}	15,000
K_T	2.89×10^{3}	84,000	1.51×10^{5}	97,000
$K_A.K_Z$	8.22×10^{4}	48,900	20	30,000
K_Z	1.17×10^{5}	18,360	21.3	- 4,100
K_A	0.702	30,500	0.939	34,100
	$g.moles.cm.^{-2}sec.^{-1}$	$cal.mole^{-1}.\ ^{o}K^{-1}$	$g.moles.cm.^{-2}sec.^{-1}$	$cal.mole^{-1}.\ ^{o}K^{-1}$

The new rate constant for the A-site reaction (K_A) was calculated from the slope of the rate-temperature curve below 1500°C, (which compares closely with

Nagle's value). From equation 1.16 it can be seen that the reaction rate on an A-site is pressure independent at normal pressures:-

$$R_A = \frac{K_A.P.K_C}{K_E + K_C.P} \longrightarrow \frac{K_A.P.K_C}{K_C.P} \longrightarrow K_A$$

$$\text{if } K_C.P \gg K_E$$

The second assumption is that all reactive sites are (A) sites below 1500°C i.e. x = 1. At normal pressures it is conceivable that the graphite structure at the solid surface is quickly broken up to give only reactive A-sites because of the high reaction rate. The experimental results for two different pyrolytic samples gave evidence of this situation because the rate-temperature curves were coincident in this temperature range.

However at low pressures the reaction rate is very small and would need to proceed for an extended period of time at a fixed temperature before the reactive surface was converted totally to A-sites or an equilibrium value of x was established. Therefore in the low pressure experiments the initial reaction rate would probably depend strongly on the previous thermal history of the samples. This was shown to be true by Strickland-

Constable who observed a 'hysterisis' effect i.e. the rate-temperature curve measured as the filament temperature was progressively increased was different from the curve obtained as the temperature was progressively decreased.

This implies that the potential reaction curve on A-sites must always lie above the experimental curve. In the filament work the initial slope was confined to temperatures below 1100°C (as opposed to 1800°C at normal pressures); very low gas pressures were present so that:-

$$K_E \gg K_C.P$$

$$\therefore \quad R_A = \frac{K_A.K_C.P}{K_E} \qquad \left(= K_A.K_Z.P \right)$$

On graph A.1. the curve for $K_A.K_C/K_E$ is shown to be above the experimental curve.

From the above A-site reaction rates at high and low gas pressures the value of (K_Z) can be deduced. (K_Z) is the ratio of the adsorption rate of oxygen onto A-sites to the desorption rate of the reaction products from A-sites. In Nagle's calculations the activation energy for each of these processes was shown to be approximately equal, with the activation energy for desorption greater than that for adsorption: a physical

process was indicated. However the new constants show that the activation energy for adsorption is very much larger than that for desorption.

This important deduction weakens the Meyer and Gomer arguments for the occurrence of a rate maximum, because if oxygen is chemisorbed as opposed to 'physisorbed' it is unlikely that a chemisorbed oxygen molecule will be released from the surface before reaction has taken place. In fact experimental work has often shown that oxygen is not desorbed from graphite as oxygen gas but only as one of the oxides of carbon.

At normal pressures and very low temperatures $K_E > K_C.P$ because K_C has an appreciable activation energy as opposed to K_E. Consequently the potential A-site reaction will tend asymptotically to the (K_A) curve at high temperatures and to the $K_A.K_C.P/K_E$ line at low temperatures. At an intermediate temperature a change in slope will be observed. In experimental work with porous graphite a change in mechanism as described above has been observed but is usually attributed to pore diffusion effects. If such a change were observed with pyrolytic graphite it is more likely to be caused by the chemical kinetics as opposed to the diffusional effect.

At low pressures and low temperatures the A-site reaction is partly limited by the rate of physical desorption of carbon monoxide from the reactive A-sites. At high pressures and temperatures (K_E) is relatively small despite the fact that the reaction is of zero order. The rate controlling process (on A-sites) is the breakdown of the surface oxide.

The value of (K_T) is smaller than Nagle's constant in both frequency factor and activation energy. Consequently a less sharp peak is given to the calculated rate-temperature curve. (K_T) values were calculated from the peak of the high pressure results when the major part of the reaction is on A-sites. Therefore the calculated values for (K_T) can be considered to be substantially correct.

Note: the negative slope of the low pressure results was assumed to be predominantly an A-site reaction; (x) could be calculated for these temperatures and $K_A \cdot K_C/K_E$ was then determined. Therefore $K_A \cdot K_C/K_E$ was the last fit in a series of three (K_A, K_T, $K_A K_C/K_E$) and subject to the cumulative error.

(K_B) constants were calculated from the low pressure results. Nagle's value was too high to fit

the filament results and was changed to give a better curve fit. The physical difference between a B-site and an A-site can be visualised in that a B-site is more tightly bound than an A-site. Consequently a higher activation energy was expected (but not obtained) for a B-site reaction as opposed to an A-site reaction. The difference in Qo (30%) is not as high as obtained by Nagle (56%) and an equal activation energy could be conceived as neither activation energy was established with very great accuracy. It is not possible to consider a higher activation energy (Qo) for a B-site reaction which is also consistant with both sets of results. However if the $K_A.K_C/K_E$ curve had a smaller activation energy then the value of K_A would also be smaller. In fact a more exact fit might have been obtained from the present data which would have affected the values of (K_A) and (K_B) most.

A computor programme could be devised to fit the different rate functions to the experimental results but to make the effort worthwhile it would have been necessary to repeat the filament results with G.E.C. pyrolytic graphite at several pressures with special care being taken to ensure that steady-state values were

measured at each temperature: then the individual rate constants could be firmly established. However it was not possible to investigate a wider pressure range using the present experimental technique. This could possibly be undertaken at some future stage.

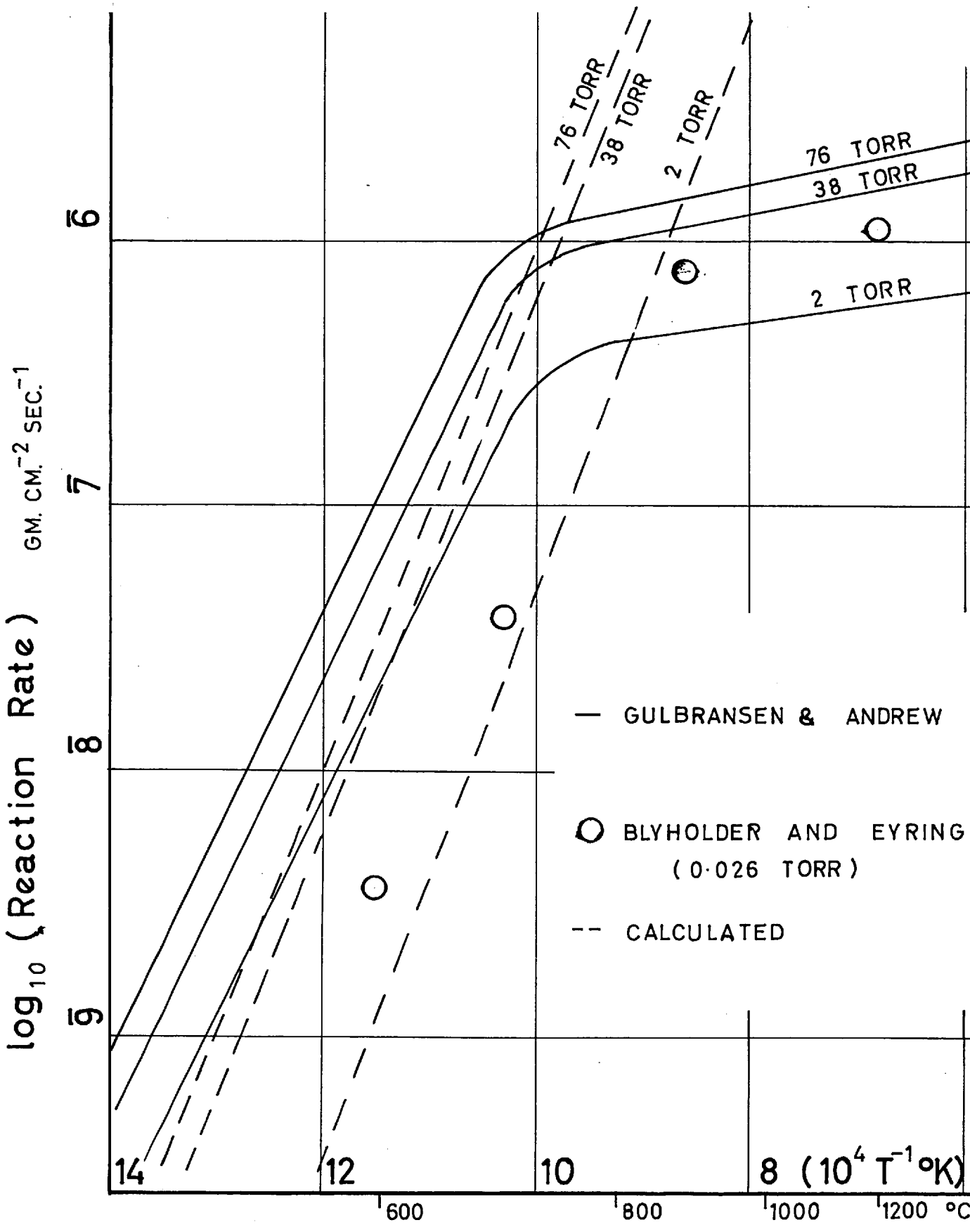

Fig. 7.1 COMPARISON WITH LOW TEMPERATURE RESULTS

7.5. Comparison of data reported at low reaction temperatures with the rates predicted by the overall rate equation.

As already explained there is little published data on the reactivity of graphite in the high temperature range, which is free of mass transfer effects. However a comparison with low temperature data is possible if the pyrolytic graphite results are extrapolated to lower temperatures using the Nagle and Strickland-Constable rate equation. This has been done for reaction pressures of 76, 38 and 2 torr to correspond to the experimental results of Gulbransen, Andrew and Brassart.[j.6.] Both the calculated and experimental rate-temperature curves are given in fig. 7.1. The reaction rate in $g.cm.^{-2}sec.^{-1}$ is plotted as the ordinate; and the reciprocal of the absolute temperature (^{o}K) as the abscissa.

The results described by Gulbransen were obtained with spectroscopically-pure graphite using an electric furnace. To allow for the porosity of the graphite a roughness factor of 350 was used by the authors to

j.6. Gulbransen E.A., Andrew K.F., Brassart F.A.
J. Electro.Chem.Soc. 110 476 (63)

calculate the intrinsic reaction rates. The magnitude of these rates differs from the extrapolated curves by a factor of about 3; however the separation between the curves at 76, 38 and 2 torr corresponds to that of the calculated curves and therefore is in apparent agreement with the Nagle and Strickland-Constable reaction mechanism. (Above 700 °C the "apparent" activation energy of the results described by Gulbransen is 3600 K.cals. which would correspond to the temperature coefficient for the change of diffusivity with temperature. Therefore a mass transfer process probably limits the reaction rate above this temperature).

Blyholder and Eyring's results are indicated on the same graph by circles. The results are again different in magnitude to the calculated values (which are not plotted) although the activation energy corresponds quite closely.

7.6. Summary:

Several theories have been postulated in the literature to explain the maximum in the rate temperature curve. The limited number of oxygen molecular collisions, the limiting effect of rates of mass transfer and the effect of using hot and cold gases have all been examined, but in the light of the present results each has been rejected. A more fruitful source of investigation was Blyholder, Binford and Eyring's theory that there are two different reaction sites A and B in the samples.

In a modification of this theory, Nagle and Strickland-Constable postulated that all virgin material contains B sites only, but that A sites are produced on the solid surface during a reaction. This interpretation of the rate mechanism agreed with the present results for pure graphite.

In addition it was found that the Nagle and Strickland-Constable theory can be used to predict with accuracy the reaction rates over a very large pressure range (10^{-6} to 1 atmosphere) which is quite an unusual achievement. Moreover for temperatures outside the experimental range, the predicted rate values are in approximate agreement with published results.

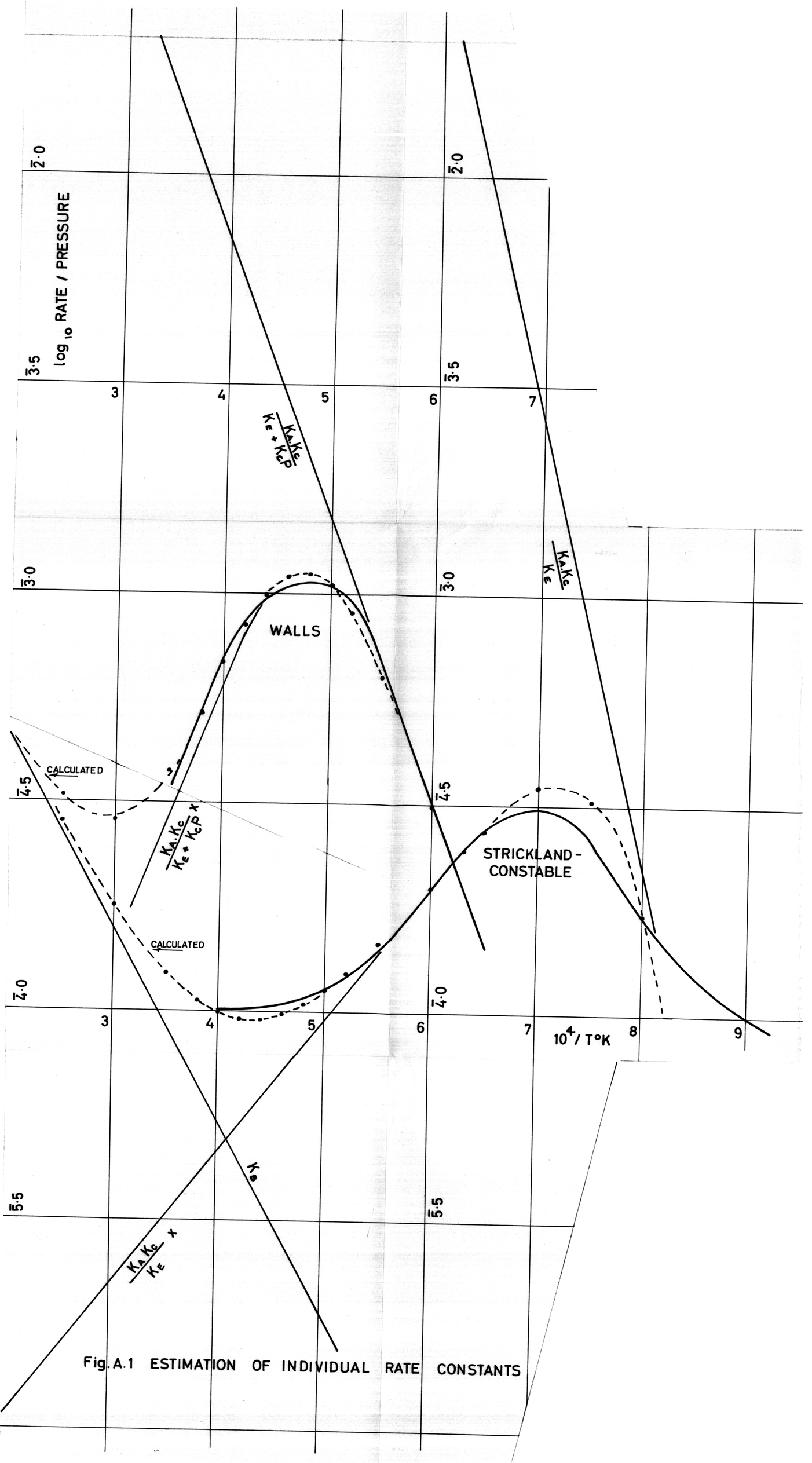

Fig. A.1 ESTIMATION OF INDIVIDUAL RATE CONSTANTS

Appendix 1.

1. Method of calculation of the reaction constants from the experimental data to fit the Nagle and Strickland - Constable theory.

To facilitate the process of curve fitting the two curves Fig. 4.4. and Fig. 4.7. were plotted on the same graph (Fig. A.1) as $\log_{10}$ (rate / pressure) against the reciprocal of the absolute temperature (10^4 / T^{o} K). Statistical curve fitting to the Nagle and Strickland - Constable theory would be extremely complex : consequently the reaction constants were evaluated by means of reasoned approximations.

1.1. Step 1 : The overall rate of reaction can be considered in two parts - the A-site reaction and the B-site reaction, where x is the fraction of reactive sites which are A-sites :-

$$\frac{R}{P} = \frac{K_A \cdot K_C \cdot x}{K_B + K_C \cdot P} + K_B (1 - x) \quad . \quad . \quad . \quad A.1$$

At low temperatures x tends to unity. Therefore the rate at low temperatures is on A-sites :-

$$\frac{R}{P} = \frac{K_A \cdot K_C}{K_B + K_C \cdot P} \quad . \quad . \quad . \quad . \quad . \quad . \quad . \quad . \quad A.2$$

$T \longrightarrow$ low values

In this temperature range, at high pressures:-

$$\frac{R}{P} = \frac{K_A}{P} \quad . \quad . \quad . \quad . \quad . \quad . \quad . \quad . \quad . \quad . \quad A.3$$

In fact Nagle's constants show that this is not true at 0.21 atmospheres but $K_A \cdot K_C / (K_B + K_C \cdot P)$ is approximately a straight line given by the low temperature slope (Fig. A.1). At very low pressures :-

$$\frac{R}{P} = \frac{K_A \cdot K_C}{K_B} \quad . \quad . \quad . \quad . \quad . \quad . \quad . \quad . \quad . \quad . \quad A.4$$

- but the slope for the low pressure curve is not necessarily as given above because x may not be close to unity. (The reaction rate may be too small to convert all reactive sites to A-sites).

1.2. Step 2 : The difference between the experimental curve and potential curve for A-site reactions can be used to find the variation of x with temperature. When this difference is small the contribution to the overall rate from the B-site reaction can still be neglected, therefore :-

$$\log_{10} \frac{R}{P} - \log_{10} \frac{K_A \cdot K_C}{K_B + K_C \cdot P} = \log_{10} x \quad . \quad . \quad A.5$$

But $$x = \frac{K_B \cdot P}{K_T + K_B \cdot P} \quad . \quad . \quad . \quad . \quad . \quad . \quad . \quad . \quad A.6$$

$$\therefore \quad \frac{1}{x} = 1 + \frac{K_T}{K_B \cdot P} \quad . \quad . \quad . \quad . \quad . \quad . \quad . \quad A.7$$

This analysis gives K_T / K_B as a function of T and it was found that:-

$$\log_{10} \frac{K_T}{K_B} = 5 \cdot 878 - 1 \cdot 382 \frac{10^4}{T} \quad . \quad . \quad . \quad A.8$$

1.3. Step 3 : With the derived constants above, x values can be found for the low pressure results. Consequently the variation of $K_A \cdot K_C / K_E$ with temperature can be evaluated.

$$\log_{10} \frac{R}{P} - \log_{10} x = \log_{10} \frac{K_A \cdot K_C}{K_E} \quad . \quad . \quad A.9$$

$$\therefore \log_{10} \frac{K_A \cdot K_C}{K_E} = 4 \cdot 915 - 1 \cdot 072 \frac{10^4}{T} \quad . \quad . \quad A.10$$

1.4. Step 4 : From steps 1 and 3 the rate constants K_A and K_C / K_E can be evaluated :-

$$\frac{P}{R} - \frac{K_E}{K_A \cdot K_C} = \frac{P}{K_A} \quad . \quad . \quad . \quad . \quad . \quad . \quad A.11$$

$$\therefore \log_{10} K_A = \bar{1} \cdot 846 - 0 \cdot 669 \frac{10^4}{T} \quad . \quad . \quad A.12$$

$$\log_{10} \frac{K_C}{K_E} = 5 \cdot 069 - 0 \cdot 403 \frac{10^4}{T} \quad . \quad . \quad A.13$$

1.5. Step 5 : At low pressures the reaction rate curve can now be plotted at all reaction temperatures (fig. A.1). At the highest temperatures the experimental results lie above this calculated

curve on account of the B-site reaction. Therefore the rate constant for B-site reactions can be derived.

$$\frac{R}{P} - \frac{K_A \cdot K_C}{K_E} \cdot \frac{K_B \cdot P}{K_T + K_B \cdot P} = K_B \cdot \frac{K_T}{K_T + K_B \cdot P} \quad \text{A.14}$$

$$\log_{10} K_B = \bar{3} \cdot 583 - 0 \cdot 460 \frac{10^4}{T} \quad \text{A.15}$$

$$\log_{10} K_T = 3 \cdot 461 - 1 \cdot 842 \frac{10^4}{T} \quad \text{A.16}$$

2. Calculation of a reaction - temperature curve.

From equations A.1 and A.6 :-

$$\frac{P}{P} = \frac{K_A \cdot K_C}{K_E + K_C \cdot P} \cdot \frac{K_B \cdot P}{K_T + K_B \cdot P} + \frac{K_B \cdot K_T}{K_T + K_B \cdot P}$$

Put $K_C / K_E = K_Z$,

$$\frac{R}{P} = \frac{K_A \cdot K_Z \cdot K_B \cdot P + K_B \cdot K_T + K_B \cdot K_T \cdot K_Z \cdot P}{K_T + K_T \cdot K_Z \cdot P + K_B \cdot P + K_B \cdot K_Z \cdot P^2}$$

These values can be calculated from equations A.12, A.13, A.15, and A.16, and are presented in table A.1.

It is then a simple matter to calculate the rate - reaction curve at different pressures. See table A.2 for the reaction curve at 0.21 atmospheres (R_2) and for the reaction curve at 2.5×10^{-5} atmospheres (R_1). Calculations were also made for several pressures at temperatures of 2200° K, 1900° C, 1400°C, see table A.3.

TABLE A.1

$\frac{10^4}{T^oK}$	Log $_{10}$ Individual rate constants								
	$K_A.K_Z$	K_B	$K_A.K_Z.K_B$	K_T	$K_B.K_T$	K_Z	$K_B.K_T.K_Z$	$K_T.K_Z$	$K_B.K_Z$
2.5	2.235	$\bar{4}$.433	$\bar{2}$.668	$\bar{2}$.856	$\bar{5}$.289	4.062	$\bar{1}$.350	2.918	0.495
3.0	1.699	$\bar{4}$.205	$\bar{3}$.902	$\bar{3}$.956	$\bar{6}$.138	3.860	$\bar{3}$.998	1.795	0.063
3.5	1.163	$\bar{5}$.973	$\bar{3}$.136	$\bar{3}$.014	$\bar{8}$.987	3.658	$\bar{4}$.646	0.672	$\bar{1}$.631
3.8	0.841	$\bar{5}$.835	$\bar{4}$.676	$\bar{4}$.461	$\bar{8}$.296	3.558	$\bar{5}$.854	$\bar{1}$.999	$\bar{1}$.373
4.0	0.627	$\bar{5}$.745	$\bar{4}$.370	$\bar{4}$.093	$\bar{9}$.836	3.457	$\bar{5}$.293	$\bar{1}$.550	$\bar{1}$.200
4.2	0.413	$\bar{5}$.651	$\bar{4}$.064	$\bar{5}$.725	$\bar{9}$.376	3.376	$\bar{6}$.752	$\bar{1}$.101	$\bar{1}$.027
4.4	0.198	$\bar{5}$.559	$\bar{5}$.757	$\bar{5}$.556	$\bar{10}$.915	3.299	$\bar{6}$.211	$\bar{2}$.652	$\bar{2}$.855
4.6	$\bar{1}$.984	$\bar{5}$.467	$\bar{5}$.451	$\bar{6}$.988	$\bar{10}$.455	3.215	$\bar{7}$.670	$\bar{2}$.203	$\bar{2}$.682
4.8	$\bar{1}$.769	$\bar{5}$.375	$\bar{5}$.144	$\bar{6}$.619	$\bar{11}$.994	3.135	$\bar{7}$.129	$\bar{3}$.754	$\bar{2}$.510
5.0	$\bar{1}$.555	$\bar{5}$.285	$\bar{6}$.858	$\bar{6}$.251	$\bar{11}$.534	3.054	$\bar{8}$.588	$\bar{3}$.305	$\bar{2}$.337
5.2	$\bar{1}$.341	$\bar{5}$.191	$\bar{6}$.532	$\bar{7}$.883	$\bar{11}$.074	2.973	$\bar{8}$.047	$\bar{4}$.856	$\bar{2}$.164
5.5	$\bar{1}$.019	$\bar{5}$.053	$\bar{6}$.072	$\bar{7}$.330	$\bar{12}$.383	2.853	$\bar{9}$.235	$\bar{4}$.183	$\bar{3}$.906
6.0	$\bar{2}$.483	$\bar{5}$.825	$\bar{7}$.306	$\bar{8}$.409	$\bar{13}$.232	2.651	$\bar{11}$.883	$\bar{5}$.060	$\bar{3}$.474
6.5	$\bar{3}$.947	$\bar{6}$.593	$\bar{8}$.540	$\bar{9}$.488	$\bar{14}$.081	2.449	$\bar{12}$.531	$\bar{7}$.937	$\bar{3}$.042
7.0	$\bar{3}$.411	$\bar{6}$.535	$\bar{9}$.774	$\bar{10}$.567	$\bar{16}$.930	2.248	$\bar{13}$.178	$\bar{8}$.815	$\bar{4}$.611
7.5	$\bar{4}$.875	$\bar{6}$.133	$\bar{9}$.008	$\bar{11}$.646	$\bar{17}$.779	2.046	$\bar{15}$.825	$\bar{9}$.695	$\bar{4}$.180
8.0	$\bar{4}$.339	$\bar{7}$.903	$\bar{10}$.242	$\bar{12}$.725	$\bar{18}$.628	1.845	$\bar{16}$.473	$\bar{10}$.570	$\bar{5}$.748

TABLE A.2 : calculated reaction rates at 2.5×10^{-5} and 0.21 atmospheres of oxygen.

$\log_{10}(R_1)$	$R_2 \cdot 10^5$	$\log_{10}(R_2)$	T^oK	$\frac{10^4}{T^oK}$
$\bar{9}.851$	6.87	$\bar{5}.837$	4000	2.5
$\bar{9}.650$	6.02	$\bar{5}.779$	3330	3.0
$\bar{9}.491$	7.94	$\bar{5}.900$	2860	3.5
$\bar{9}.425$	10.88	$\bar{4}.036$	2630	3.8
$\bar{9}.393$	14.38	$\bar{4}.157$	2500	4.0
$\bar{9}.383$	17.75	$\bar{4}.249$	2380	4.2
$\bar{9}.381$	20.5	$\bar{4}.312$	2270	4.4
$\bar{9}.395$	23.1	$\bar{4}.363$	2170	4.6
$\bar{9}.418$	23.4	$\bar{4}.369$	2080	4.8
$\bar{9}.452$	22.1	$\bar{4}.343$	2000	5.0
$\bar{9}.493$	18.9	$\bar{4}.276$	1920	5.2
$\bar{9}.565$	13.4	$\bar{4}.126$	1820	5.5
$\bar{9}.700$	6.60	$\bar{5}.820$	1670	6.0
$\bar{9}.837$	2.75	$\bar{5}.761$	1540	6.5
$\bar{9}.942$	1.42	$\bar{5}.151$	1430	7.0
$\bar{9}.911$	0.645	$\bar{6}.810$	1330	7.5
$\bar{9}.636$	0.293	$\bar{6}.467$	1250	8.0

TABLE A.3 : calculated reaction curves at several pressures and at a fixed temperature.

	PRESSURE (ATM.)				$\frac{10^4}{T^\circ K}$
P	1.0	0.4	0.21	0.1	
$\log_{10} P$	0.000	$\bar{1}.602$	$\bar{1}.322$	$\bar{1}.000$	
R. 10^5	6.74	6.70	6.58	6.40	6.0
$\log_{10} R$	$\bar{5}.829$	$\bar{5}.826$	$\bar{5}.818$	$\bar{5}.806$	
R. 10^5	44.8	32.6	23.1	1.375	4.6
$\log_{10} R$	$\bar{4}.651$	$\bar{4}.513$	$\bar{4}.363$	$\bar{5}.138$	
R. 10^5	49.47	24.3	14.4	6.84	4.0
$\log_{10} R$	$\bar{4}.694$	$\bar{4}.386$	$\bar{4}.157$	$\bar{5}.835$	

Appendix 2.

2.1. Analysis of the experimental results at 1400° C obtained with reactor graphite in air using the microscope technique.

Although the reproducibility of a rate measurement can be best tested at a constant temperature, it was impossible to set or control the rod temperature accurately to a predetermined value using Nagle's technique. So some results were obtained in the temperature range of $1400 \pm 50^{\circ}$ C. Owing to the small variation of rate with temperature these results were all treated as being at the same temperature of 1400° C. Within this range the results did not show a significant dependence on temperature as can be seen from the graph (fig.2.2 - where the group of results are enclosed by a square) so this proce-dure was probably justified.

The seven results in this range are shown below to have a mean value ($\overline{R}$ g.atoms.cm^{-2}.sec^{-1} x 10^5) equal to 21 ·7 with a variance $s^2(R)$ of 24 · 8 : from these figures the reproducibility can be evaluated.

2.2. Statistical analysis of results at 1400° ± 50° C.

(see table overleaf)

$$\overline{R}.\ 10^5 = 20 + \frac{11{\cdot}8}{7} = 21{\cdot}7 \qquad n = 7$$

$$\sum (R - \overline{R})^2 = \sum (R - 20)^2 - \frac{\left[\sum (R - 20)\right]^2}{n}$$

$R \times 10^5$	$(R - 20) . 10^5$	$(R - 20)^2 . 10^{10}$
22.9	2.9	8.41
29.9	9.9	98.01
26.3	6.3	39.69
20.9	0.9	0.81
19.1	- 0.9	0.81
15.5	- 4.5	20.25
19.2	- 0.8	0.64
	18.0 - 6.2	168.62

$$\therefore \quad (R - \bar{R})^2 = 168 \cdot 62 - (11.8)^2 / 7 = 148 \cdot 7$$

$$\therefore \quad s^2(R) = \frac{\Sigma (R - \bar{R})^2}{n - 1} = \frac{148 \cdot 7}{6} = 24 \cdot 8$$

For 6 degrees of freedom at 95% probability :-

$$R . 10^5 = 21 \cdot 7 \pm 2 \cdot 45 \sqrt{24 \cdot 8}$$

$$= 21 \cdot 7 \pm 12 \cdot 2$$

$$\bar{R} . 10^5 = 21 \cdot 7 \pm 12 \cdot 2 / \sqrt{7}$$

$$= 21 \cdot 7 \pm 4 \cdot 61$$

In this analysis R is the expected range for 95 % of the experimental results obtained with the experimental technique at 1400° C. $\bar{R}$ is the range of the arithmetic mean rate about the true reaction rate with a probability of 95 % .

Table A. 4.

h divs	t secs	T° C	R	$\log_{10} R$	$\frac{10^4}{T° K}$
70	115	1420	22.9	1.36	5.90
25	31.5	1445	29.9	1.48	5.83
25	68.2	1305	13.7	1.14	6.34
50	44.5	1480	42.4	1.63	5.71
50	71.7	1380	26.3	1.42	6.05
35	63.1	1380	20.9	1.32	6.05
35	69.1	1450	19.1	1.28	5.80
60	68.5	1640	33.0	1.52	5.23
20	48.8	1400	15.4	1.19	5.98
30	50.6	1260	22.3	1.35	6.52
35	68.8	1410	19.2	1.28	5.94
100 divisions ≡ 0 . 257 cm.					
20	46.4	1935	23.8	1.38	4.53
25	29.3	1790	47.1	1.67	4.85
50	67.7	1755	40.8	1.61	4.93
15	29.5	1830	28.1	1.45	4.75
35	39.4	1910	49.1	1.69	4.58
70	89.1	1830	43.3	1.64	4.75
50	60.2	1800	45.9	1.66	4.83
50	69.4	1840	39.8	1.60	4.74
50	62.5	1665	44.2	1.65	5.17
40	70.3	1815	31.4	1.50	4.79
100 divisions ≡ 0 . 376 cm.					

2.3. Estimate of the instrumental error in the measurement of the rate R, at 1400° C.

The method of rate measurement is given in equation 2.1. :-

$$R = \frac{h}{t} \cdot \frac{1}{12} \cdot \frac{\rho}{M} = \psi \cdot \frac{h}{t}$$

where ψ is constant for a series of runs on the same graphite.

If $\delta^2(R)$ is the total variance in the rate from instrumental error and $\delta^2(i)$ the variance in a measured variable (i), then :-

$$\delta^2(R) = \sum_i \left(\frac{\partial R}{\partial i}\right)^2 \cdot \delta_i^2$$

The two variables are (h) and (t), therefore :-

$$\delta^2(R) = \left\{ \frac{\delta^2.(h)}{t^2} + \frac{h^2}{t^4} \cdot \delta^2(t) \right\} \psi^2$$

The average values of ψ, t and h were calculated from the results presented in table A. 4 and are given below : the probable errors in h and t were known by experience to be :-

$$\delta(h) = \pm 0.5 \text{ divisions}$$

$$\delta(t) = \pm 0.2 \text{ seconds}$$

ρ = 1.76 g. cm^{-3}

M = 100 to 0.257 divs.cm^{-1}

$\therefore \psi = 0.377 \times 10^{-2}$ g.atoms.cm^{-2}.$div.^{-1}$

$\bar{h}$ = 39 divisions

$\bar{t}$ = 67.6 seconds

n = 7

$$\therefore \quad \sigma^2(R) = \frac{0.377^2 . 10^{-4}}{67.2^2} \left\{ (0.5)^2 + \frac{39^2}{67.6^2} \times 0.04 \right\}$$

$$= 0.315 . 10^{-8} (0.25 + 0.013)$$

$$= 8.29 . 10^{-10}$$

$$\sigma(R) = 2.9 . 10^{-5}$$

For 6 degrees of freedom at 95 % probability :-

$$R \times 10^5 = 21 \cdot 7 \pm 2 \cdot 45 \times 2 \cdot 9$$

$$\therefore R \times 10^5 = 21 \cdot 7 \pm 7 \cdot 11$$

In this analysis R is the estimated range for 95 % of the experimental results at 1400° C caused by instrumental error.

The results of the above analysis are summarised in the following table :-

	total variance	standard deviation	95 % confidence limits
Range of the experimental rates	24.8	4.98	± 12.2
Range due to instrumental error	8.29	2.88	± 7.1
Range due to error in h	7.88	2.80	-
Range due to error in t	0.41	0.64	-
Range of $\overline{R}$	-	-	± 4.61
Mean reaction rate = 21 · 7			

2.4. Discussion of the experimental scatter.

2.4.1. The instrumental errors in measuring the reaction rates, arise in the estimation of the reaction time (t) and linear retreat of the surface. From the table given above it can be clearly seen that the error in the measurement of (h) accounted for most of the instrumental error. As a consequence of error from this source 95 % of the experimental results are expected to be in the range of (21.7 ± 7.11) x 10^{-5} g.atoms.cm^{-2}.$sec.^{-1}$

2.4.2. Experimental error : all the experimental results apart from one were inside the range of the instrumental error. However the total experimental variance s^2 (R) was 24.8 as compared with the estimated instrumental variance of 8.29. Therefore it was concluded that other factors outside the error in measurement of the rates made a significant contribution to the overall error.

2.4.3. True reaction rate at 1400° C. By using the Students' t-test on the seven experimental results, it has been shown that 95 % of any further rate measurement at this temperature will be in the range of (21.7 ± 12.2) x 10^{-5} g.atoms.cm^{-2}.sec^{-1}. The arithmetic mean of the results ($\bar{R}$) will approach the true reaction rate (R_{true}) as the number of results (n) tends to infinity,i.e:-

$$\bar{R} = \bar{R}_{true} \pm \frac{t.\ \sigma\ (R)}{n}$$

If a 5 % deviation from the true reaction rate is an acceptable value then :-

$$\frac{t.\ \bar{\epsilon}_i\ (R)}{\sqrt{n}} < \frac{21 \cdot 7}{20}$$

i.e. $n^{\frac{1}{2}} > 0.923 \times 12.2$

$n > 127$

Therefore 127 experimental results are required, with the present experimental technique, to establish the reaction rate with a 5 % degree of accuracy.

2.4.4. Error in temperature : the error in the measurement of the temperature was certainly small, but in the course of a run the temperature of the rod deviated substantially from the mean value. The reaction rate is not strongly temperature dependent, especially near the rate maximum, but even so the temperature deviations could introduce considerable uncertainty into the measurements.

2.4.5. Other experimental errors : later, when the rate of burning was recorded photographically and continuously two sources of error were detected which could not be observed in the microscope technique where only the initial and final positions of the silhouette were recorded:-

a) The initial reaction rate was sometimes found to be quite different from the steady - state value ultimately attained.

b) In addition the sample was sometimes observed to move during the run ; this movement resulted from compressive forces

exerted on the graphite rod, as illustrated in fig. 3.5. The force was required to hold the sample in position but was increased by thermal expansion of the graphite on heating. In the combustion only one face reacted to a large extent so bending moments developed which moved the centre of the sample downwards. The supports did not resist this movement because only point contact was made with the ends of the graphite sample. In fact if the support faces were flat and parallel this movement did not take place . In addition the points of contact were weakened by chemical attack which added to the movement of the sample during oxidation. A piece of ciné-film illustrating this point is reproduced in fig. 3.7.

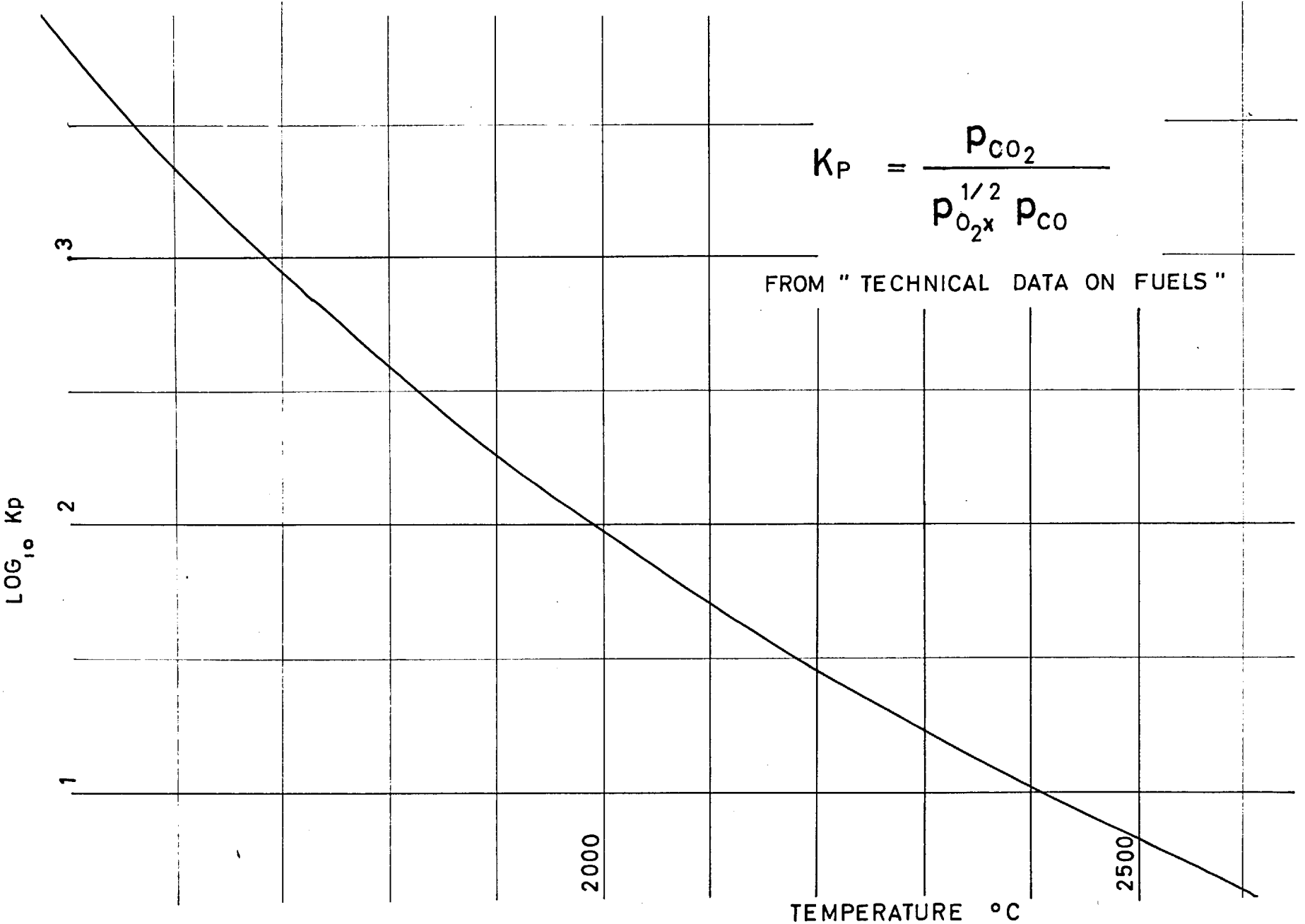

Fig.A.2 DISSOCIATION OF CARBON DIOXIDE

Appendix 3.

Dissociation of CO_2 at high temperatures in excess of CO

$$CO_2 \rightleftharpoons CO + \tfrac{1}{2} O_2$$

The equilibrium data was taken from " Technical data on fuels " and is presented as a graph in fig.A.2.1. $\text{Log}_{10} K_p$ is plotted against temperature in ^{o}C where :-

$$K_p = \frac{p_{CO_2}}{p_{CO} \cdot p_{O_2}^{\frac{1}{2}}}$$

Let $(1 - x)$ moles of CO_2 dissociate.

Initial no. moles		Moles at equilibrium
a	CO_2	$a \cdot x$
b	CO	$b + a (1 - x)$
0	O_2	$\frac{1}{2} a (1 - x)$
	TOTAL =	$\frac{3}{2} a + b - \frac{1}{2} a . x$

$$\therefore \quad K_p = \frac{a \cdot x}{b + a (1 - x)} \sqrt{\frac{\frac{3}{2} a + b - \frac{1}{2} a.x}{(\frac{1}{2} a - \frac{1}{2} a.x) P}}$$

Let the CO / CO_2 ratio , $b / a = q$

$$\therefore \quad K_p = \frac{x}{q + 1 - x} \sqrt{\frac{3 + 2q - x}{(1 - x) P}}$$

$$\therefore \quad \log_{10} K_p = \log_{10} x + \tfrac{1}{2} \log_{10}(3 + 2q - x) - \log_{10} (q + 1 - x) - \tfrac{1}{2} \log_{10} (1 - x) P$$

A value of x, q and P were selected and K_p calculated from the above equation : the corresponding temperature was read from graph A.2.1. In this way a series of equilibrium state values were obtained from which fig. A.2.2. was constructed. The fraction of carbon dioxide dissociated $(1 - x)$ is plotted as the ordinate, temperature ^{o}C as the abscissa and the curve parameter is the CO / CO_2 ratio q : only a constant total pressure of 1 atmosphere is considered.

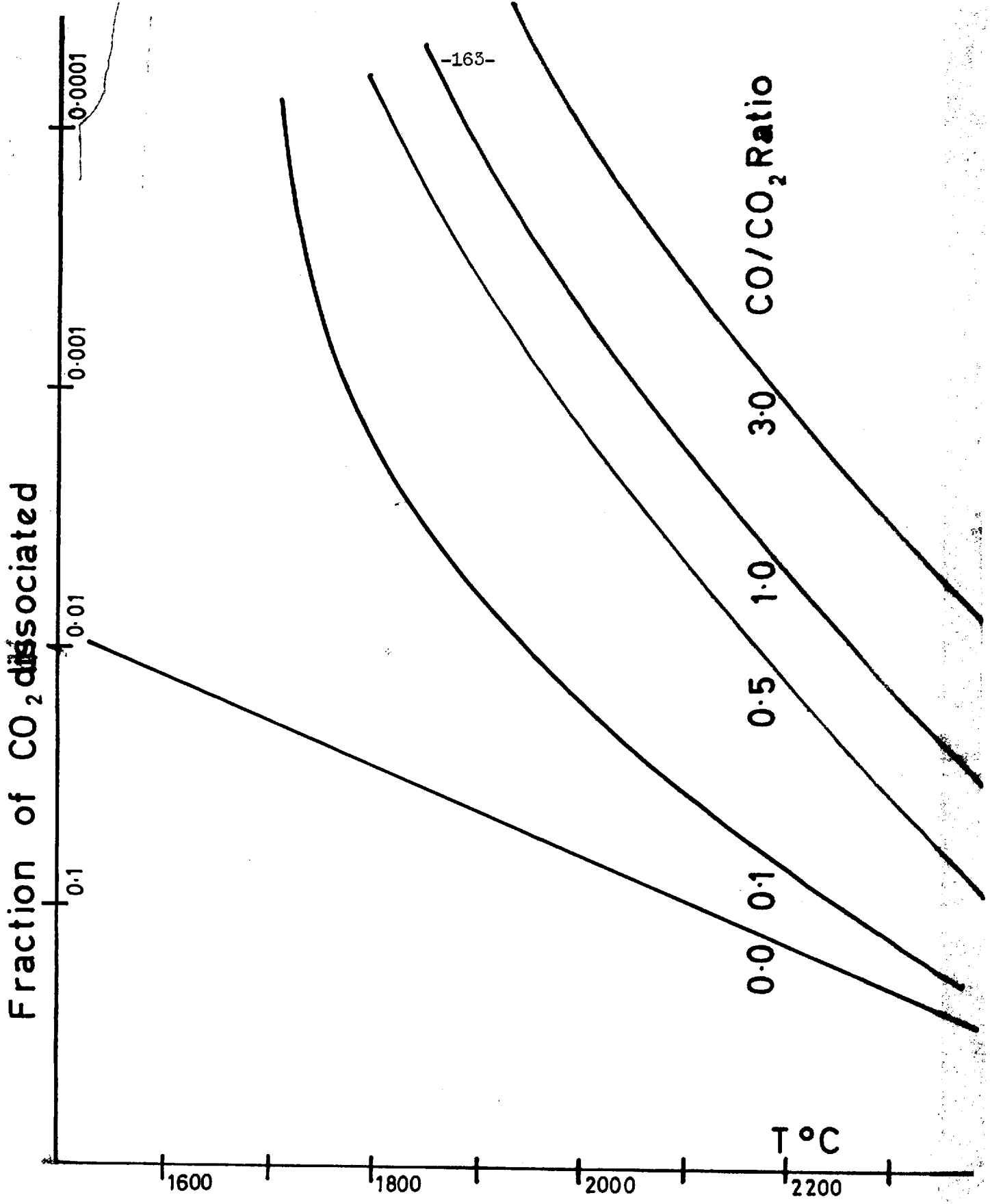

Fig.A.3 Dissociation of CO_2 (CO in excess)

Appendix 4.

Further discussion of the Blyholder and Eyring theory.

4.1. Experimental results of Blyholder and Eyring [1].

Blyholder and Eyring oxidised spectroscopically pure graphite in a heated furnace between 1 and 150 microns and a flow method was used.

Below 800° C an activation energy of 42.5 Kcal.mole^{-1} was observed and the pressure dependence was half order. This activation energy was of a higher value than most other workers had reported in this temperature range, e.g:-

Arthur and Bowing [2] .	23 Kcal	600 - 700° C
Chen [3] . . .	21.5 Kcal	350 - 500° C
Lambert [4] . .	24 Kcal	400 - 500° C
Tsukhanova [5] . .	22 Kcal	400 - 900° C
Wicke [6,7] . .	29 or 58 Kcal	600 - 700° C

---

1. Blyholder and Eyring — A.F.O.S.R. report : technical note O.A. No 20 15 Aug. 1956
2. Arthur and Bowring — J. Chim. Phy. (50) 47 540
3. Chen et al. — J. Phy. Chem. (55) 59 1146
4. Lambert — Trans. Far. Soc. (36) 32 352
5. Tsukhanova — Chem. Abs. (48) 42 3928g
6. Wicke — Z. Electrochem (52) 56 414
7. Wicke — Z. Electrochem (53) 57 636

However Blyholder and Eyring attributed the difference to the very high purity of spectroscopic graphite and compared their activation energy to that obtained by Gulbransen and Andrew[8] (37 Kcal) also working with spectroscopic graphite between 400 and 600° C but at 0.1 to 9.8 mm Hg gas pressure. Furthermore it was shown that the pressure dependence of Gulbransen and Andrew's results could be shown to be half order.

In the published results of Wicke[6,7] it was shown that if powdered rather than compacted graphite was oxidised at atmospheric pressure, the activation energy was increased from 29 to 58 Kcal. Therefore as Blyholder and Eyring's value of 42.3 Kcal (using very pure graphite) was smaller than 58 Kcal, the effect of in-pore diffusion was investigated at their very much lower gas pressures. At 800° C graphite was rubbed onto an "inert" ceramic rod so that only a very thin smear was obtained. The activation energy for the oxidation of these smears was found to be 80 Kcal- almost twice the value obtained with solid graphite (42.3 Kcal), and moreover a zero order reaction was observed. Blyholder and Eyring showed that both sets of results were consistant if explained by the Thiele - Wheeler theory, e,g. from equation 1.12 :-

$$R \propto \frac{\sqrt{D \cdot K_s \cdot c_o^{m+1}}}{\qquad\qquad}$$

8. Gulbransen and Andrew Ind. Eng. Chem. (52) 44 1034

Therefore although the true order (m) is zero, an apparent half order is obtained. (In using the above equation at very low gas pressures the coefficient of diffusion (D) is for Knudsen diffusion and therefore independent of pressure. Whether this is also true for the results of Gulbransen and Andrew at 1 cm Hg pressure is debatable). Moreover half the true activation energy is generally measured according to Blyholder and Eyring, if samples thicker than 0.1 mms are used.

4.2. The proposed rate mechanism to include the carbon filament results.

Blyholder and Eyring developed a theory to explain the filament results based upon two different reactive sites with different mechanisms. This is very similar to the theory presented in section 1.5. so is not re-presented in detail. Site 1 gave a first order reaction and will be called an A - site in the present discussion. Site 2, to be referred to as a B - site, gave a zero order reaction as observed by Blyholder and Eyring, with an activation energy of 80 Kcal.

Commenting on the filament results Blyholder, Binford and Eyring proposed that as the temperatures reached in graphitisation were lower than 3000° C the filament could consist partly of graphite crystals (B - sites), and partly of hydrocarbon material, (A - sites).

A possible reason for this is that impurity atoms prevent the formation of graphite from all the hydrocarbon material. However oxidation can remove the impurity so that the A - sites can then form B - sites.

A rate equation based on the above mechanism is able to predict the general shape of the filament rate - temperature curves and Blyholder and Eyring made the following deductions :-

a) The true reaction between a graphite crystal and oxygen is zero order and has an activation energy of 80 Kcals.

b) Carbon filaments are imperfectly graphitised and contain impurity atoms which disrupt the structure. The filaments are therefore more readily oxidised than pure graphite on account of the impurity atoms.

c) The results reported in different experiments do not agree with each other because of the different quantities of impurities, different degrees of graphitisation, porosity and surface areas of the filaments.

4.3. Discussion of the above deductions in the light of the present results.

a) Pyrolytic graphite is as pure if not purer than that used by Eyring so it is unlikely that a mechanism based on catalysis will explain the observed reaction kinetics. Moreover below 1500° C an activation energy of 44 Kcals was measured which compares well

with the value obtained by Eyring on solid samples. However unlike spectrographite which is prepared from carbonised solids, pyrolytic graphite is slowly formed by the decomposition of a hydrocarbon gas onto a heated carbon former. The resulting material is virtually non-porous and it is unlikely that reaction rates need to be interpreted using the in-pore diffusion equation. Therefore it can be concluded that the reactivity of the graphite smears on the "inert" ceramic gave abnormally high activation energies for oxidation.

b) In the present work with pyrolytic graphite, the rate - temperature curve decreases at a diminishing rate above the maximum and this trend cannot be attributed solely to the A - site reaction. Hence if the B - site reaction is observed at both low and high pressures the reaction could not be of zero order (unless it is accepted that in-pore diffusion makes the B - site reaction pressure dependent).

Appendix 5.

1. Experimental results given in fig. 4.1. (HTM pyrolytic graphite using the microscope technique).

$\log_{10} R$	$R \times 10^5$	$T^\circ C$	$10^4 / T^\circ K$
$\bar{4}.22$	16.7	1570	5.43
$\bar{4}.09$	12.2	2155	4.12
$\bar{4}.24$	17.5	1525	5.57
$\bar{4}.31$	20.2	1630	5.26
$\bar{4}.26$	18.3	1815	4.83
$\bar{5}.93$	8.6	1635	5.24
$\bar{4}.20$	15.7	1770	4.90
$\bar{4}.39$	24.4	1785	4.86
$\bar{4}.01$	10.3	2430	3.70
$\bar{5}.83$	6.7	2390	3.76
$\bar{4}.30$	20.1	2095	4.22
$\bar{5}.85$	7.2	2460	3.66
$\bar{5}.39$	2.4	1260	6.52
$\bar{5}.51$	3.2	1480	5.70
$\bar{5}.63$	4.3	1520	5.56
$\bar{5}.34$	2.2	1210	6.74
$\bar{4}.00$	10.1	1480	5.70
$\bar{5}.41$	2.6	1475	5.72
$\bar{6}.10$	0.1	1050	7.56
$\bar{5}.90$	7.9	1460	5.84
$\bar{6}.90$	0.8	1160	6.98
$\bar{4}.28$	19.2	2043	4.32

2. Experimental results given in fig. 4.2.

a) G.E.C. pyrolytic graphite (preliminary work)				
T^{o} C	$\log_{10}$.R			$10^{4} / T^{o}$ K
1800	$\bar{4}$.32	to	$\bar{4}$.30	4.82
1600	$\bar{4}$.32	to	$\bar{4}$.27	5.34
1400	$\bar{5}$.61	to	$\bar{5}$.52	5.98
1927	$\bar{4}$.36	to	$\bar{4}$.31	4.55
2270	$\bar{4}$.29	to	$\bar{4}$.21	3.93
b) G.E.C. pyrolytic graphite in the absence of a jet.				
1420	$\bar{5}$.378	to	$\bar{5}$.358	5.91
1600	$\bar{5}$.061	to	$\bar{6}$.929	5.34
2010	-	to	$\bar{7}$.955	4.38
1255	$\bar{5}$.415	to	$\bar{5}$.048	6.54

3. Experimental results given in fig. 4.3.

Pyrolytic graphite		Reactor graphite	
R x 10^{5}	v cm.sec.$^{-1}$	R x 10^{5}	v cm.sec.$^{-1}$
23.2	9300	15.1	1100
24.3	6900	29.0	2700
24.2	5500	35.0	4300
25.1	3300	42.2	5700
24.9	2400	50.2	7000
16.5	1400	58.7	8400
14.8	600	66.4	9400
		79.8	11200
		77.5	12300
		75.5	14000

LITERATURE REFERENCES :

a) Carbon filament work

1. Binford, J.S. & Eyring, H — J. Phy. Chem. (56) 60 , 486
2. Euken, A — Z. ang - Chem. (30) 43 , 986
3. Duval, X — J. Chim. Phy. (50) 47 , 339
4. Duval, X — Thèse , Nancy.(54)
5. Meyer, L — Trans. Far. Soc. (38) 34, 1056
6. Sihvonen, V — Trans. Far. Soc. (38) 34, 1062
7. Strickland-Constable, R.F. — Trans. Far. Soc. (44) 40, 333
8. Strickland-Constable, R.F. — Trans. Far. Soc. (47) 43, 769
9. Yates, J.G. — Thesis, London. (62)

b) Pore diffusion

1. Blyholder, G. & Eyring, H. — J. Phy. Chem. (57) 61, 682
2. Blyholder, G. & Eyring, H. — J. Elect. Chem. Soc. (59) 63, 1004
3. Gulbransen, E.A. & Andrew, K.F. — Ind. Eng. Chem. (52) 44, 1034
4. Hedden, K. & Wicke, E — 3rd Carbon Conference (59), 24
5. Kamenetskii, D.A.F. — "Diffusion and heat exchange in Chemical Kinetics" Princeton U.P. (55)
6. Rossberg, M. & Wicke, E. — Chem. Ing. Tech. (56) 28, 181
7. Thiele, E.W. — Ind. Eng. Chem. (39) 31, 916
8. Weisz, P.B. & Prater, C.D. — Adv.in Catalysis (54) 6, 143
9. Wheeler, A. — Adv. in Catalysis (51) 3, 249
10. Wicke, E. — Z. Electrochem. (52) 56, 414

11. Wicke, E. Z. Electrochem. (53) 57, 636

12. Wicke, E. 5th Symposium on Combustion (55) 245

c) High temperatures and pressures with gas flow

1. Nagle, J.F.M. Thesis, London (61)

2. Day, R.J. Thesis, Pennsylvania (49)

3. Horton, W.S. 5th Carbon Conference (63) 2, 233

d) Surface annealing and preferential attack

1. Baker,C. & Kelly, A. Nature (62) 193, 235

2. Dienes, G.J. J.App. Phy. (52) 23, 1194

3. Montet, G.L., Hennig, G.R. & Kurs, A. Nuclear Sci. Eng. (56) 1 33

4. Watt, J.D. & Franklin, R.E. Nature (57) 180, 1190

e) Explanation of rate maximun

1. Nagle, J.F.M. 5th Carbon Conference (61) 154

2. Blyholder, G., Binford, J.S. & Eyring, H.
J. Phy. Chem. (58) 62, 263

3. Meyer, L. & Gomer, R. J. Chem. Phy. (58) 28, 617

4. Meyer, L. & Gomer, R. 3rd Carbon Conference (59) 425

5. Meyer, L. & Gomer, R. 5th Carbon Conference (61) 155

f) Photographic retreat measurement

1. Grayham, J.A., Brown, A.R.G., Hall, A.R. & Watt, W.
Ind. Carbon & Graphite (59) 317

g) Heating of gases

1. Blyholder, G.D. & Eyring, H. J. Phy. Chem. (57) 61, 682

2. Blyholder, G.D. & Eyring, H. J. Phy. Chem. (59) 63, 693

3. Day, R.J., Walker, P.L. & Wright,C.C Ind. Carbon & Graphite (58) 348

4. Kuchta, J.M., Kant, A. & Damon, G.H. Ind. Eng. Chem. (52) 44, 1559

h) Catalysis at low temperatures

1. Earp, F.K. & Hill, M.W. Ind. Carbon & Graphite (57) 320

2. Nebel, G.J. & Cramer, P.L. Ind. Eng. Chem. (55) 47, 2393

3. Nebel, G.J. & Cramer, P.L. Ind. Eng. Chem. (52) 44, 1048

4. Hennig, G 4th Carbon Conference (61) 115

Reviews

1. Walker, P.L., Rusinko, F. & Austin, L.G.
Adv. in Catalysis 11, 133 (59)

2. Culver, R.V. & Watts, H. Rev. Pure & Applied Chem. (Australia)
(60) 10, 95

Low temperature oxidation range

1. Tsukhanova, O.A. Chem. Abs. (48) 42,3928g

2. Lambert, J.D. Trans. Far. Soc. (36) 32, 352

3. Chen, M.C et alia J. Phy. Chem. (55) 59, 1146

4. Arthur, J.R. & Bowring, J.R. J.Chim. Phy. (50) 47, 540

5. Blyholder, G.D. & Eyring, H. A. F. O. S. R. report
O. A. No. 20 Aug. 15th 1956

6. Gulbransen, E.A., Andrew, K.F., & Brassert, F.
J.Electrochem. Soc. (63) 110, 476

k) Other references

1. "Technical Data on Fuels" Ed. Spears 1963

2. Rao, V.V. & Trass, O. Can. J. Chem. Eng. (64) 42, 95